ADVANCES IN GAS CHROMATOGRAPHY AND VACUUM UV SPECTROSCOPY: APPLICATIONS TO FIRE DEBRIS ANALYSIS & DRUGS OF ABUSE
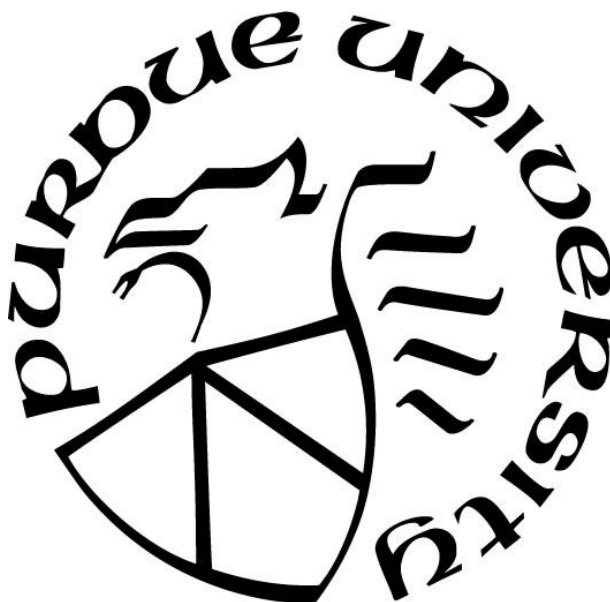
by

Zackery Ray Roberson

A Dissertation

Submitted to the Faculty of Purdue University

In Partial Fulfillment of the Requirements for the degree of

Doctor of Philosophy

Department of Chemistry and Chemical Biology at IUPUI

Indianapolis, Indiana

December 2020

THE PURDUE UNIVERSITY GRADUATE SCHOOL
STATEMENT OF COMMITTEE APPROVAL

Dr. John V. Goodpaster, Chair

Department of Chemistry and Chemical Biology

Dr. Nicholas E. Manicke

Department of Chemistry and Chemical Biology

Dr. Sébastien Laulhé

Department of Chemistry and Chemical Biology

Dr. Ian K. Webb

Department of Chemistry and Chemical Biology

Approved by:

Dr. Eric Long

Dedicated to El Roi and my Ohana

ACKNOWLEDGMENTS

Many thanks to the many wonderful people who have been a part of this journey. John Goodpaster for being a great mentor and being patient with me. Donna Roskowski for her experience, wisdom, and support. Amy Maidi for being an awesome undergraduate advisor. Nick Manicke, Sébastien Laulhé, and Ian Webb for being great committee members. The entire faculty of the Forensic and Investigative Sciences program for being awesome people. Logan Hickey, Jordan Ash, Jacqueline Ruchti, and Kymeri Davis for being great coworkers. Ashur Rael, Christine Skaggs, and Courtney Cruse for being my friends and fellow sufferers on the path of the PhD. And Heather Gordon, my junior and former undergraduate mentee, for her diligence and hard work on derivatization that produced Chapter 5 and other work that went into Chapter 3.

I am ever grateful to my ohana, my family, for their unending support and love. My Mom and Dad who gave me a love for learning and a desire to seek truth, among so many other things. My cousins for being my friends and confidants. Deanna, for her support, patience, and being my companion. Emalyn, for just being my daughter. And, most of all, I am thankful to God for being my fortress, my lamp, my teacher, and my LORD.

TABLE OF CONTENTS

LIST OF TABLES

LIST OF FIGURES

ABSTRACT

In forensic chemistry, a quicker and more accurate analysis of a sample is always being pursued. Speedy analyses allow the analyst to provide quick turn-around times and potentially decrease back-logs that are known to be a problem in the field. Accurate analyses are paramount with the futures and lives of the accused potentially on the line. One of the most common methods of analysis in forensic chemistry laboratories is gas chromatography, chosen for the relative speed and efficiency afforded by this method. Two major routes were attempted to further improve on gas chromatography applications in forensic chemistry.

The first route was to decrease separation times for analysis of ignitable liquid residues by using micro-bore wall coated open-tubular columns. Micro-bore columns are much shorter and have higher separation efficiencies than the standard columns used in forensic chemistry, allowing for faster analysis times while maintaining the expected peak separation. Typical separation times for fire debris samples are between thirty minutes and one hour, the micro-bore columns were able to achieve equivalent performance in three minutes. The reduction in analysis time was demonstrated by analysis of ignitable liquid residues from simulated fire debris exemplars.

The second route looked at a relatively new detector for gas chromatography known as a vacuum ultraviolet (VUV) spectrophotometer. The VUV detector uses traditional UV and far-ultraviolet light to probe the pi and sigma bonds of the gas phase analytes as well as Rydberg traditions to produce spectra that are nearly unique to a compound. Thus far, the only spectra that were not discernable were from enantiomers, otherwise even diastereomers have been differentiated. The specificity attained with the VUV detector has achieved differentiation of compounds that mass spectrometry, the most common detection method for chromatography in forensic chemistry labs, has difficulty distinguishing. This specificity has been demonstrated herein by analyzing various classes of drugs of abuse and applicability to "real world" samples has been demonstrated by analysis of de-identified seized samples.

CHAPTER 1. PREPARATION AND CHARACTERIZATION OF MICRO-BORE WALL-COATED OPEN-TUBULAR CAPILLARIES WITH LOW PHASE RATIOS FOR FAST-GAS-CHROMATOGRAPHY-MASS SPECTROMETRY: APPLICATION TO IGNITABLE LIQUIDS AND FIRE DEBRIS

1.1 Introduction

Since Gas Chromatography (GC) has been in common use, there have been many studies on how to shorten analysis time and improve resolution [1,2]. Current practice in capillary GC is the use of open tubular columns with inner diameters of 0.25 - 0.53 mm while "fast" GC typically uses columns with inner diameters of 0.10 - 0.18 mm [3]. Typically, capillary GC achieves separations within one hour with peak widths at half height greater than 3 seconds [3]. "Fast" GC is a title given to analyses that achieve separation within minutes with peak widths at half height of 1-3 seconds [1,3]. "Very fast" GC is classified as having analysis times measured in seconds with peak widths at half height of 30-200 ms [3]. Through the years many different techniques and methods have been used to achieve "very fast" or faster GC analysis times [1,4,5]. Some examples include low pressure Gas Chromatography (LP-GC), narrow-bore (NB) GC, and micro-bore (MB) GC [1,2,6,4,7,8,9].

One of the common arguments against NB and MB GC has been the decreased sample capacity that occurs with decreased column diameter [6,7,10]. Other limitations include the instrumental constraints due to high pressure requirements, detector sampling rates being too slow, and wide sample peak width from the injector [3,4,11,12]. The limitation of sample capacity is not as problematic for trace analysis such as is used in forensic analysis of samples such as ignitable liquid residues on fire debris, post-blast residues of explosives or toxicological analysis of drugs in bodily fluids. While the chromatographic performance may decrease slightly, sample capacity is known to increase with stationary phase film thickness [13]. The thick films assist in overcoming the limitations of MB columns. While very thick films have been used in past GC columns, [13,14] the MB application of thick films to fire debris analysis has yet to have been accomplished.

This study focuses on investigating the practicality of preparing MB GC columns coupled to a vacuum-outlet to produce "very fast" GC analyses. In-house prepared columns of 50 micrometer inner diameter were tested for suitability and efficiency. The application of interest for this technique is the analysis of ignitable liquid residues in fire debris. "Fast" or "very-fast" GC is

advantageous in fire debris analysis due to the traditionally long run times, commonly upwards of 20 minutes [15,16]. Micro-bore GC columns can achieve similar performance in one fifth of the time. Decreased analysis time could also decrease case back-log in forensic laboratories.

1.1.1   Theory

As per the Purnell equation, chromatographic resolution (Rs) is dependent upon column efficiency (N), retention (capacity factor, k_2) and selectivity ($\alpha = k_2/k_1$).

Equation 1: Purnell

$$R_s = \frac{\sqrt{N}}{4}\left(\frac{\alpha - 1}{\alpha}\right)\left(\frac{k_2}{1 + k_2}\right)$$

Of the three variables, increasing column efficiency offers potentially unlimited increases in resolution. Chromatographic efficiency is characterized by the height equivalent of a theoretical plate (H) or by the number of theoretical plates (N) for a column of certain length (L) [17]. H and N are related by Equation 2:

Equation 2: Plate Numbers

$$N = \frac{L}{H}$$

For open-tubular columns, H depends upon physical factors such as column radius (r) and the thickness of the stationary phase film (d_f). In addition, H depends upon chemical factors such as the capacity factor of a retained peak (k_2), and the diffusivity of the analyte in the mobile phase (D_G, and stationary phase (D_S).

The dependence of H on these variables as well as the linear velocity of the mobile phase (*u*) is given by the expanded Golay equation below [18].

Equation 3: Expanded Giddings-Golay

$$H = \frac{2D_G}{u} + r^2 u \frac{1 + 6k_2 + 11k_2^2}{24(1 + k_2)^2 D_M} + u\frac{2k_2 d_f^2}{3(1 + k_2)^2 D_S}$$

The phase ratio (β) is the ratio of the total empty volume of the capillary to the volume of stationary phase. β is also given as the ratio of the partition coefficient (K) to the capacity factor

(k). Given a known column inner radius and film thickness, phase ratio can be calculated using Equation 4.

Equation 4: Phase Ratio

$$\beta = \frac{(r - d_f)^2}{2rd_f} = \frac{K}{k}$$

The minimum plate height that will result in maximum efficiency is directly proportional to column radius, as given by Equation 5.

Equation 5: Minimum Height Equivalent of a Theoretical Plate

$$H_{min} = 2r \sqrt{\frac{1 + 6k + 11k^2}{12(1 + k)^2} + \frac{k}{3(1 + k)^2 \beta^2 \left(\frac{D_S}{D_M}\right)}}$$

The other implication of this equation is that minimum plate height decreases with increasing phase ratio (β), which manifests as a loss of column efficiency with increasing film thickness.

As an example, Figure 1.1 displays a variety of commercially available WCOT columns as a function of their inner diameter and film thickness. As can be seen in this graph, most columns have phase ratios between 62.5 and 250. Other columns reported in the literature are also included, which clearly deviate from the norm. These columns and the columns described in this paper operate in a drastically different region.
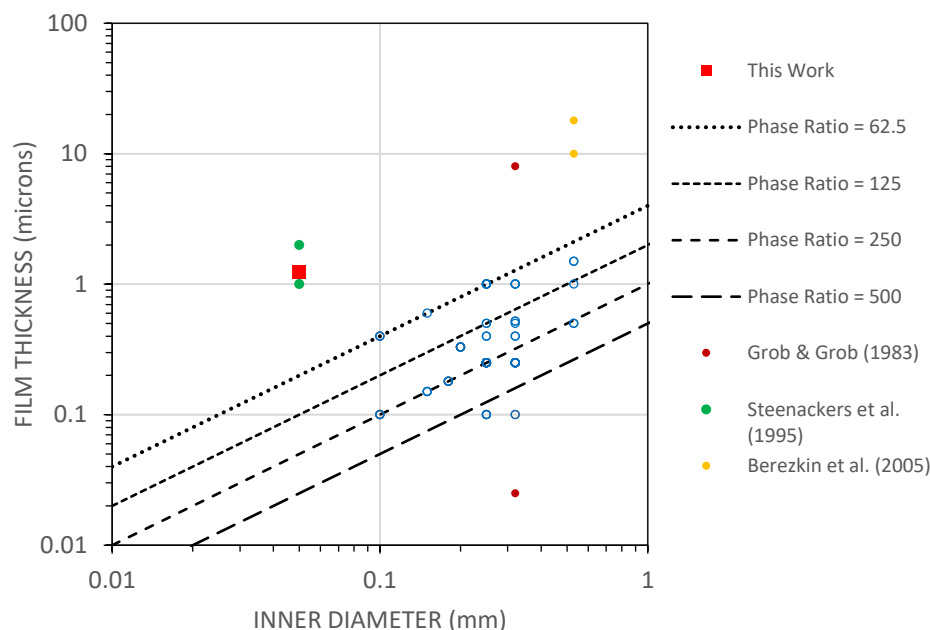
Figure 1.1 Commercially available WCOT GC columns with a 100% PDMS stationary phase plotted according to their inner diameter and stationary phase film thickness. Columns reported in the literature are also included, as well as the columns described in this paper (β = 10).

The mass of an analyte that can be loaded onto a column is related to the film thickness; a thin film column suffers from low loadability when compared to a thick film column of the same inner diameter. As shown in Equation 6, the relation between film thickness and plate height does mean that thicker films will have worse separation efficiency than thin films. Though the maximum separation efficiency is less for thick film columns, the maximum separation may not be necessary. For most applications, the separation efficiency of a thin film 0.25 mm or 0.18 mm inner diameter columns is enough. However, the time required for those analyses can be dramatically reduced using a thick film MB column.

An important limitation of micro-bore capillary columns is high inlet pressures and extra column broadening from the injector [3, 4, 11, 12]. The high head pressure requirements can be offset to some extent by using a low-pressure or vacuum outlet such as with a mass spectrometer detector. The impact of a vacuum outlet on column head pressure is well known and can be seen in the Poiseuille equation for the flow of compressible fluids given as Equation 6. Where P_i is the column head pressure, r is the column inner radius, L is column length, F is the volumetric flow rate, η is carrier gas viscosity, Po is the column outlet pressure, and T is temperature.

Equation 6: Poiseuille equation rearranged for inlet pressure.

$$P_i = \sqrt{P_o^2 + \frac{F * L * P_o * \eta}{3.75 * \pi * r^4}}$$

For example, at low flow rates, changing from an atmospheric pressure outlet (~15 psi) to a vacuum outlet ($< 10^{-6}$ psi) can increase flow rates by ~10%. Extra-column broadening from the injector can be countered via the use of either high split ratios to reduce sample volume or retention gaps to aid in the separation of solutes from the solvent vapor [19].

1.2   Materials/Methods

1.2.1   Materials

All capillary tubing was purchased from Polymicro Technologies (Phoenix, AZ). Polydimethylsiloxane (PDMS) with a viscosity of 100 centistokes was purchased from Acros (Bridgewater, NJ). Pentane (pesticide grade) was purchased from Fisher Chemical (Fair Lawn, NJ) and used in all dilutions. Hexadecane (ReagentPlus) was purchased from Sigma-Aldrich (Milwaukee, WI).

1.2.2   Instrumentation

An Agilent 7890A gas chromatograph (GC) with 7693 autosampler connected to an Agilent 5975C mass spectrometer was used to obtain chromatographic data of prepared capillary columns. All liquid injection vials and caps were purchased from Fisher Scientific (Hanover Park, IL).

1.2.3   Column Preparation

Several capillary columns were prepared using a static coating procedure. The static coating process was performed by filling the capillary with PDMS solution then allowing it to dry with one end capped for 16 hours. Helium gas was used to purge excess liquid before heating the column in a GC oven at 200 ºC for 4 hours. Filling of the columns was achieved using a Nanobaume apparatus (Western Fluids Engineering & Mfg, LLC, Wildomar, CA) where PDMS solution had been substituted for the typical packing slurry. A vial with 0.5 mL of solution was

placed in the apparatus, the capillary was affixed to rest just above the bottom of the vial, 80 psi of pressure was applied to the apparatus until liquid was observed at the end of the capillary.

The film thicknesses of the prepared columns were calculated using the Equation 6 [20].

Equation 6: Film Thickness

$$d_f = \frac{d_c \times C}{400}$$

Where d_f is film thickness, d_c is capillary diameter, and C is the volume percent of PDMS in the coating solution. Based upon this equation the columns prepared for this study had a film thickness of 1.25 microns.

1.2.4   Column Testing

Columns were tested with either pentane or hexadecane in pentane under isothermal and ramped conditions with different head pressures. Testing was done to confirm effective column production and to determine the most successful head pressure for each column.

A 1 meter long 50 micrometer column was tested for efficiency versus pressure measurements with pentane as the analyte. Hexadecane was analyzed under varying isothermal conditions where the capacity factor was calculated. An Agilent 6890N GC with FID was used to obtain the results.

A 5 meter length 50 micrometer column was tested with pentane and hexadecane using the 7890A instrument at head pressures from 5 to 50 psi, split 200, inlet 280 °C, transfer line 280 °C, oven isothermal and varied at 85, 90, 92, 95, 97, and 100 °C. Testing continued with separations of an *n*-alkanes mixture, a sample of E85 fuel, and an ASTM e1618 test mixture for fast-GC analyses.

1.2.5   Preparation of Fire Debris Samples

A sample of carpet was cut into 4 squares 3 inches long, each piece was then placed in a clean metal can. One was burnt without an accelerant, one with 1.0 mL of 87 octane gasoline, one with 10.0 mL gasoline, and one with 5.0 mL of charcoal lighter fluid. Samples with accelerant burned until they self-extinguished. Samples were sealed with the metal lid then sat for 42 hours at room temperature. An activated charcoal strip was hung in each can then resealed and placed in

an oven for 23 hours at 65 °C. Strips were placed in 2.0 mL of pentane and vortexed for 10 seconds each. 250 μL of sample was then placed into GC vials and analyzed with GC-MS.

1.3   Results/Discussion

As a proof of concept, a 50-micrometer inner diameter, 1-meter long column was prepared with a 1.25 micrometer film thickness. This column was tested using a non-retained solute (pentane) to determine the dependence of H upon inlet pressure. As pressure is directly proportional to the mobile phase velocity, this allows us to produce a Van Deemter curve. An Agilent 6890N GC with FID was used to obtain the results. The results of the separation efficiency versus calculated velocity can be found in Figure 1.2. The data was fit to the Van Deemter equation.
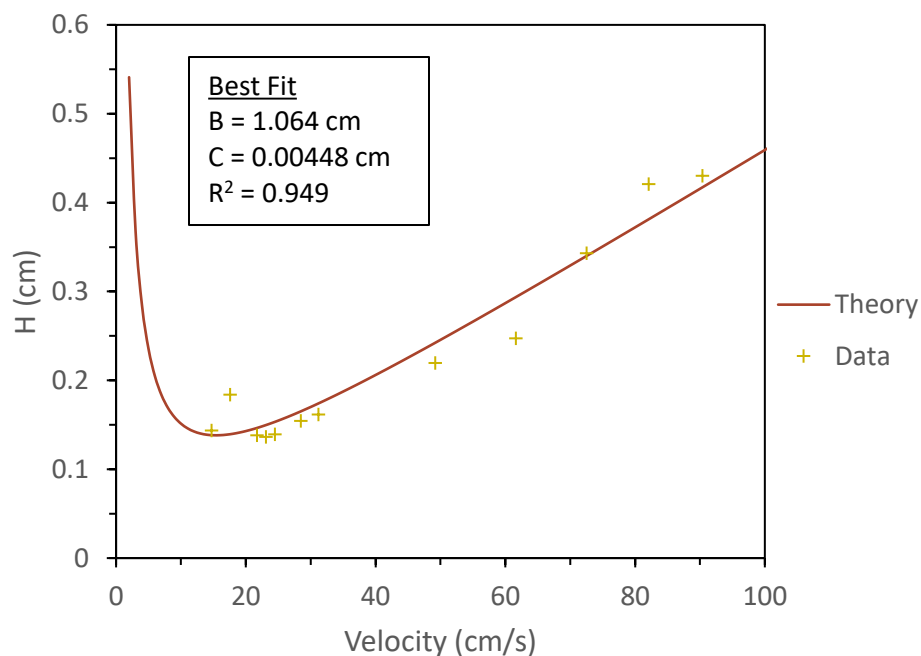
Figure 1.2 The Height Equivalent of a Theoretical Plate (H) for a non-retained solute (pentane, k < 0.05) is plotted against the mobile phase velocity at which the chromatograms were produced.

A solution of hexadecane in pentane was analyzed isothermally at various temperatures. From the isothermal data, capacity factors (k) were calculated. The natural logarithm of k was plotted against the inverse of the temperature in Figure 1.3. As expected, the natural logarithm of k plotted vs. the inverse of temperature is linear, as its slope is directly related to the enthalpy (ΔH) of the separation [21,22,23].

y = 515.960x - 2.719
R² = 0.956
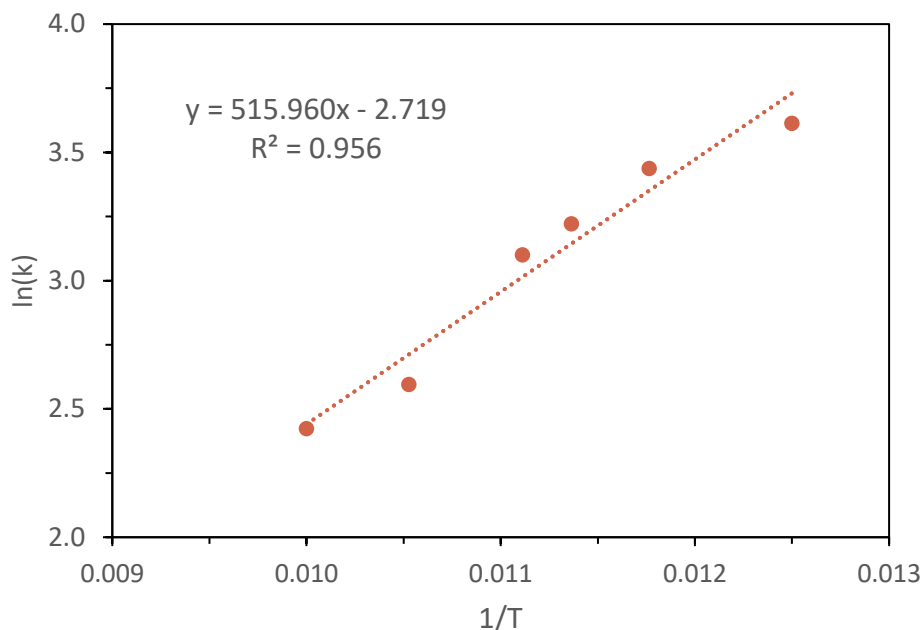
Figure 1.3 The natural log of the calculated capacity factor (k) for hexadecane plotted against the inverse of temperature to produce a curve for the 50 μm i.d. 1-meter capillary column.

A longer 5-meter column was prepared to generate additional theoretical plates and evaluated. Then, a solution of *n*-alkanes was analyzed using an isothermal method at 120 °C under constant pressure of 75 psi. The alkanes are well-resolved in under 3.1 minutes. As expected, due to the isothermal conditions, later-eluting straight-chain alkanes are noticeable broadened (see Figure 1.4).
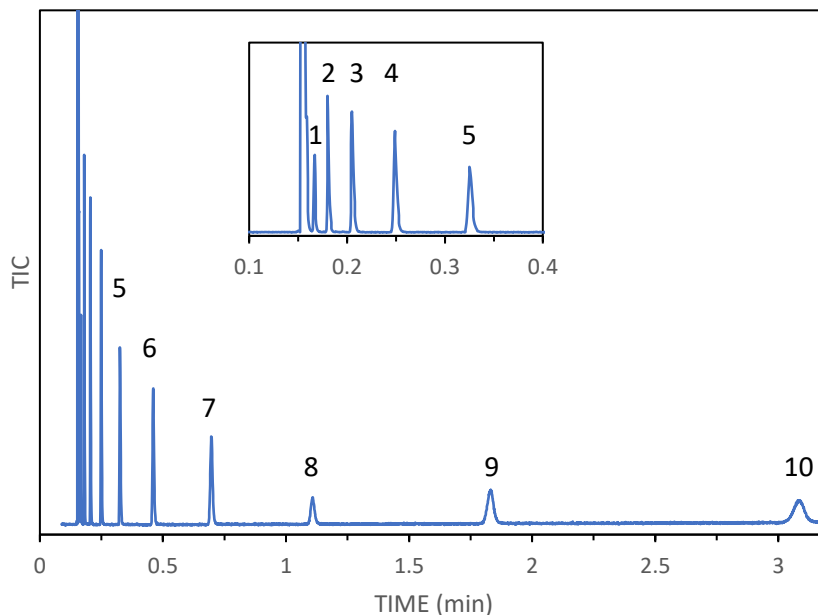
Figure 1.4 An isothermal separation of an *n*-alkanes sample at 120 ºC and constant 75 psi. Peaks: 1. heptane, 2. octane, 3. nonane, 4. decane, 5. undecane, 6. dodecane, 7. tridecane, 8. tetradecane, 9. pentadecane, 10. hexadecane.

Four compounds in the alkane mixture were analyzed for the efficiency of the column, the data is provided in Table 1.1 below. The lowest height equivalent of a theoretical plate (H) was found to be 0.110 mm, this is comparable to previous literature that used manufactured columns with thin films [9].

Table 1.1 Chromatographic efficiency for four *n*-alkanes on a 5 meter long 50 μm i.d. column with a 1.25 micron stationary phase.

Compound	t_r	W	N	N/m	H (mm)
Heptane	0.167	0.002	38000	7700	0.12
Octane	0.181	0.002	45000	9000	0.11
Nonane	0.206	0.003	26000	5200	0.19
Decane	0.249	0.004	21000	4200	0.23

The alkane mixture was analyzed at various temperatures and the capacity factors for heptane, octane, nonane, and decane were calculated. The natural logarithm of k was plotted against the carbon number as shown in Figure 1.5 below.
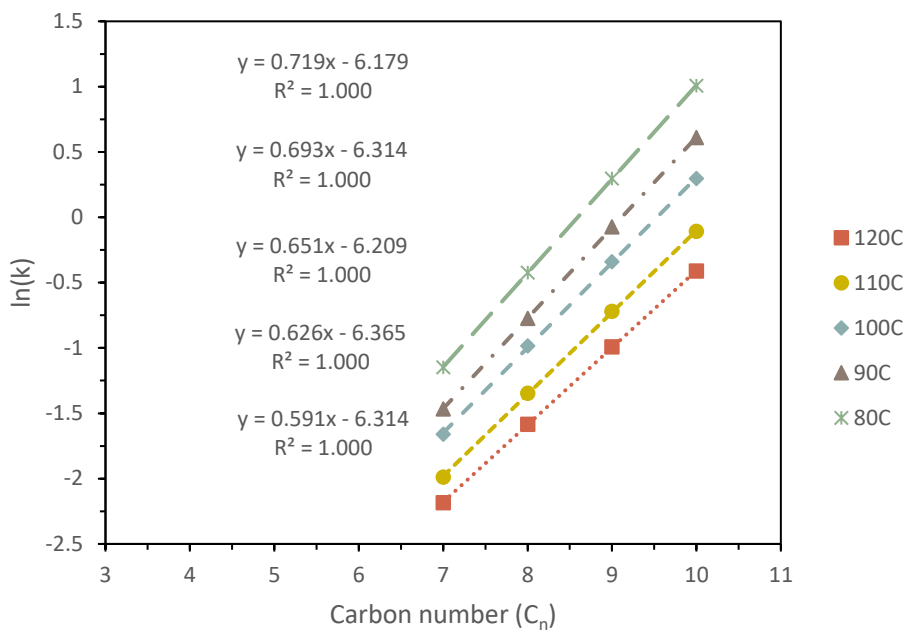
Figure 1.5 The natural logarithm of the capacity factors for heptane, octane, nonane, and decane plotted over the carbon number at various temperatures.

A sample of the ASTM mixture was analyzed on a 5-meter, 50 micrometer i.d. column with a 1.25 μm film to determine the shortest analysis time while maintaining baseline resolution. The chromatograms show full separation of all 13 components and undecane. A constant flow of 0.3 mL/min was used with a program starting at 50 $^{\circ}$C and increasing to 200 $^{\circ}$C at 75 $^{\circ}$C/min where it would hold final temperature for 1.5 min (see Figure 1.6).
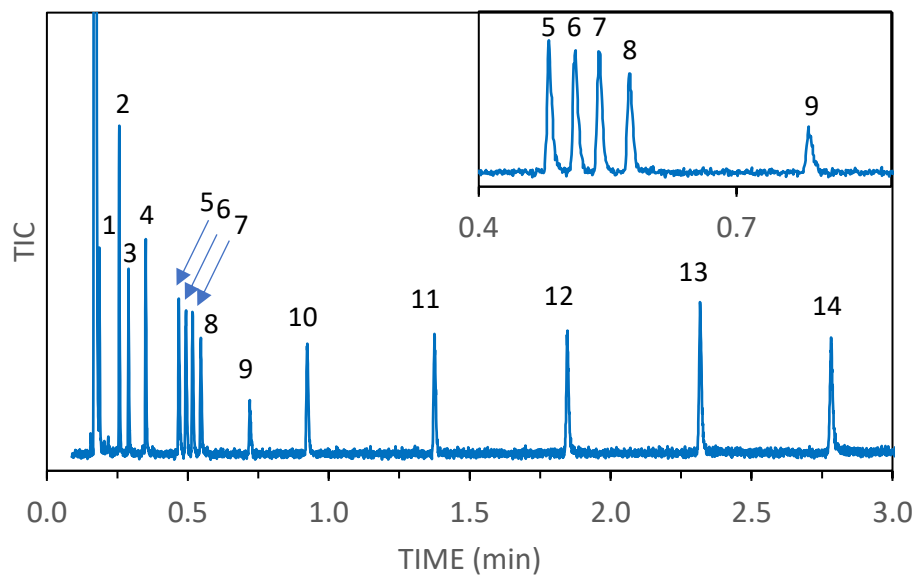
Figure 1.6 Chromatogram of the ASTM E1618 mixture ramped at 75 ºC/min with constant flow. Peaks: 1. hexane, 2. toluene, 3. octane, 4. *p*-xylene, 5. 2-ethyltoluene, 6. 3-ethyltoluene, 7. 1,2,4-trimethylbenzene, 8. decane, 9. undecane, 10. dodecane, 11. tetradecane, 12. hexadecane, 13. octadecane, 14. Eicosane

The analysis of the ASTM mixture showed no significant improvement in time with an increased ramp, which reflects the upper practical limit of the GC to ramp temperature. The time could also have been improved with an increased flow rate, though separation efficiency would have decreased slightly. Another restriction on increasing the flow rate was that the pressure required for 0.3 mL/min at the final temperature was the 100 psi (the maximum for the installed inlet).

Then, a sample of E85 gasoline was analyzed to confirm the ability of the method to separate and characterize such a complex sample. The sample was analyzed using a constant flow of 0.3 mL/min and a ramp of 15 ºC/min from 35 ºC to 200 ºC (see Figure 1.7).
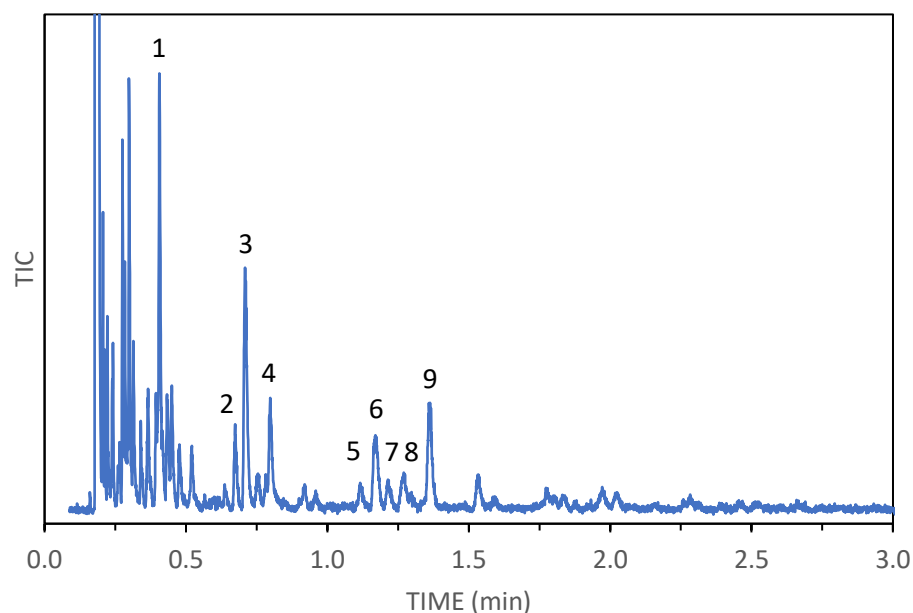
Figure 1.7 Chromatogram of an E85 fuel sample analyzed at constant flow 0.3 mL/min with a ramp of 15 ºC/min. Peaks: 1. toluene, 2. ethylbenzene, 3. *m*- and *p*-xylene, 4. *o*-xylene, 5. *n*-propylbenzene, 6. ethyltoluene, 7. 1,3,5-trimethylbenzene, 8. 2-ethyltoluene, 9. 1,2,4-trimethylbenzene

Gasoline is a common accelerant used in arson,[15] E85 is also used. E85, being a complex mixture with lower concentrations of traditional gasoline compounds, was used as a representative sample for neat accelerants. The method was able to separate the mixture enough for clear determination of toluene, xylenes, and C3-alkylbenzenes. While a ramp of 15 ºC/min is much slower than the 75 ºC/min shown in the analysis of the ASTM standard, more complex samples were analyzed at slower ramp rates to limit coelution of peaks. If a higher ramp were used the analysis time would be shorter, but the risk of coelution would negate any gains in analysis time. Results are shown in Figure 1.8.
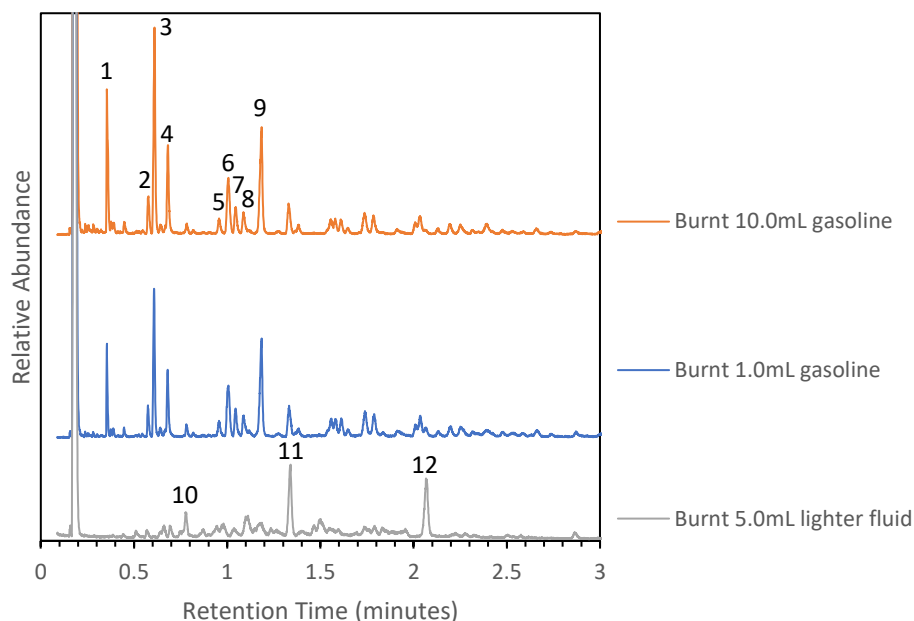
Figure 1.8 Analysis of ignitable liquid residues from test burns. Oven 35 °C to 200 °C at 15 °C/min, constant flow 0.3 mL/min, split 200, inlet 280 °C, 50 μm i.d. column 4.99 m long with a 1.25 μm thick PDMS film. Chromatograms were normalized to 350,000 abundance. Peaks: 1. toluene, 2. ethylbenzene, 3. *m-* and *p*-xylene, 4. *o*-xylene, 5. *n*-propylbenzene, 6. ethyltoluene, 7. 1,3,5-trimethylbenzene, 8. 2-ethyltoluene, 9. 1,2,4-trimethylbenzene , 10. nonane, 11. decane, 12. undecane.

The chromatograms in Figure 1.8 show that the column was adequate to separate and classify the ignitable liquids at a fraction of the traditional analysis time.

1.4 Conclusions

An in-house process for static coating glass capillaries was shown to be effective, as demonstrated by retention and efficiency data. The usefulness of the prepared columns was shown towards fire-debris analysis based upon the separations of the ASTM E1618 test mix and E85 fuel samples as well as the burnt sample exemplars. The ability to conduct fast-gas chromatographic analyses, bordering "very fast", with the 50 micrometer micro-bore column was demonstrated. This approach was successful in analyzing ignitable liquids and their residues in simulated fire debris.

CHAPTER 2.   DIFFERENTIATION OF STRUCTURALLY SIMILAR PHENETHYLAMINES VIA GAS CHROMATOGRAPHY–VACUUM ULTRAVIOLET SPECTROSCOPY (GC–VUV)

2.1   Introduction

Vacuum Ultraviolet (VUV) spectrophotometry coupled to gas chromatography is a relatively new "hyphenated technique" with the ability to differentiate structural isomers and diastereomers. While VUV absorption spectroscopy has been around for many years, the ability to couple VUV spectrophotometry to a separation technique is a recent development [24]. The region of the electromagnetic spectrum known as the vacuum ultraviolet extends to wavelengths shorter than 200 nm where the electronic transitions of sigma and high energy pi bonds lie. The detector used for this study has a spectral range of 125-430 nm, where all but the smallest molecule (H_2) absorbs. With nearly every molecule absorbing in this region, the question arises as to just how differentiable these spectra are? This study seeks to determine the discriminating power of this technique through chemometrics.

Chemometrics is multivariate statistics applied to chemistry to extract valuable information from a data set [25-28]. Of the many statistical methods available, Principal Component Analysis (PCA) and Discriminant Analysis (DA) were used for this study. PCA was chosen for its ability to show correlations in a data set as an unsupervised technique. DA was used for its ability to separate the different groups within the data set as a supervised technique. Using PCA and DA, the spectra of the phenethylamines were analyzed and determined to be sufficiently differentiable from one another.

In forensic chemistry, several phenethylamines are commonly found in seized drug exhibits (see Figure 2.1). Five seized drug casework samples, de-identified from the Indiana State Police, were analyzed as "street" samples for his work. In general, phenethylamines when analyzed by GC-MS, while distinguishable by gas chromatography and retention time, give fragments with the same mass to charge ratio and in similar ratios of fragments as other phenethylamines. Methamphetamine's fragmentation has been studied in detail, [29] but is also known to be sufficiently similar to its stereoisomers and regioisomers to make definitive identification difficult with fragment ions at *m/z* 58 and *m/z* 91 being predominant [30]. GC-IRD (infrared detector) has been proposed as a possible complimentary technique to differentiate these isomers [30]. Though the

spectra can be more visually distinct with an IRD, VUV is more sensitive and allows for easier quantitation [31]. Having the same functional groups, the seven phenethylamines studied in this work would have similar spectra in both the IR and VUV regions. Where IR detection relies on vibrational modes of the functional groups on a molecule, VUV is dependent on the electronic transitions of the molecule. Both techniques are affected by vibronic coupling that allows for spectra to be potentially unique to each molecule. The phenethylamines in this study, though similar in spectra, produce individual spectra that allow for the identification of one apart from another.
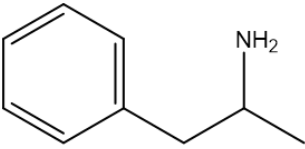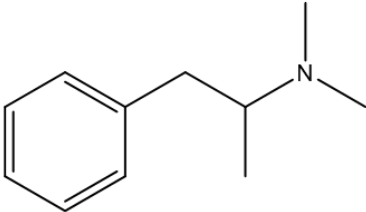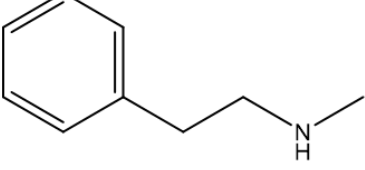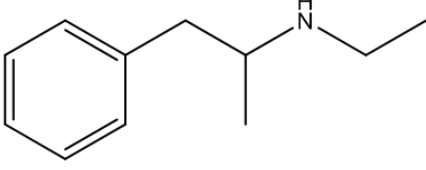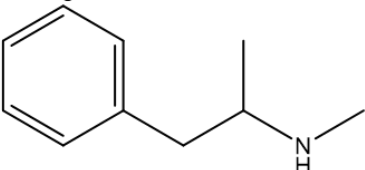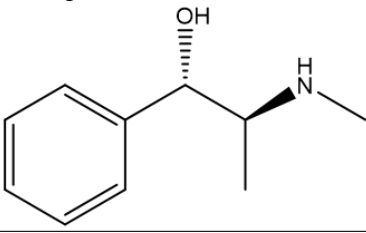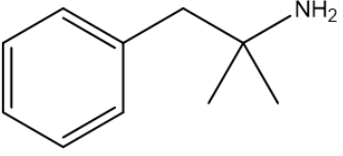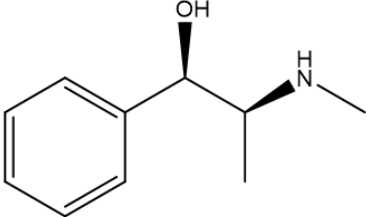
Figure 2.1 Structures and molar masses of the phenylethylamines discussed in this work.

VUV's specificity has been increasingly demonstrated since its availability on the market beginning in 2014. VUV has also been used in tandem with MS [32]. VUV has shown the ability to differentiate fatty acid methyl esters, pesticides, fuels, and more [24, 33-41]. VUV has been demonstrated to be able to differentiate 67 designer drugs [33, 42-44].

One of the exciting advantages of VUV is the ability to easily quantify as well as characterize an analyte. VUV is reliant on the Beer-Lambert Law for quantification and has been considered as a pseudo-absolute quantitation method [45]. With the reliance on Beer's Law, VUV is a concentration dependent detector, though mass dependent characteristics such as increased sensitivity with an increased flow rate through the instrument are observed [46].

2.2   Materials/Methods

2.2.1   Materials

Methylene chloride was purchased from Fisher Scientific (Fairlawn, NJ) for solution preparation and dilution. All vials and caps were purchased from Fisher Scientific as well. D-amphetamine, *N,N*-DMA (dimethylamphetamine), and ethylamphetamine were purchased from Cayman Chemical (Ann Arbor, MI). Phentermine HCl was obtained from USP (Rockville, MD). Methamphetamine, ephedrine, and *S,S*-pseudoephedrine were purchased from Sigma-Aldrich (St Louis, MO). *N*-Methylphenethylamine (MPEA) was obtained from Acros Organics (China).

2.2.2   Instrumentation

An Agilent 7890A gas chromatograph with 7693 autosampler was connected to a VUV Analytics VGA-101 Vacuum Ultraviolet spectrophotometer. This instrument was used to obtain all chromatographic and spectrophotometric data. All liquid injection vials and caps were purchased from Fisher Scientific (Hanover Park, IL).

2.2.3   Gas Chromatography Method for drug analysis

A flow of 1.8 mL/min of hydrogen was used for the carrier gas, inlet temperature 250 °C, injection volume 1 μL (splitless), oven ramped from 50 °C to 250 °C at a rate of 20 °C/min with a final oven temperature hold of 2.50 minutes. The VGA-101 transfer line and flow cell were set to

a temperature of 275 ºC and a makeup gas pressure of 0.35 psi of nitrogen. The VGA-101 was set to a sampling rate of 6 Hz.

2.2.4   Chemometric Analysis

The phenethylamine spectra were baseline subtracted and the absorbance was normalized to the square root of sum of squares of all wavelengths. The software used for the multivariate analyses was JMP 13 by SAS Institute.

2.2.5   Determination of Figures of Merit

Accuracy and precision determined by analysis of five calibrants and a separate challenge sample, all TFAA derivatized MPEA in triplicate. Calibrants were prepared at 180, 150, 100, 50, and 25 µg/mL, the challenge samples were prepared at 75 µg/mL in a manner identical to the calibrants from a separate stock. LOD and linearity were determined with triplicate calibrants spanning the range from 10 µg/mL to 1000 µg/mL.

2.3   Results/Discussion

2.3.1   GC/VUV Analysis

Solutions of seven phenethylamines (methamphetamine, amphetamine, methylphenethylamine, phentermine, dimethylamphetamine, ethylamphetamine, and pseudoephedrine) were prepared at 0.5 mg/mL and a solution of ephedrine was prepared at 1.4 mg/mL. All standard solutions were analyzed by GC-VUV.

The separation of seven phenethylamines can be seen in the chromatogram in Figure 2.2. Ephedrine was excluded because it could not be well resolved from pseudoephedrine. Tailing of peaks is common for underivatized phenethylamines on a column with a silicone stationary phase due to the basic nature of the molecules.
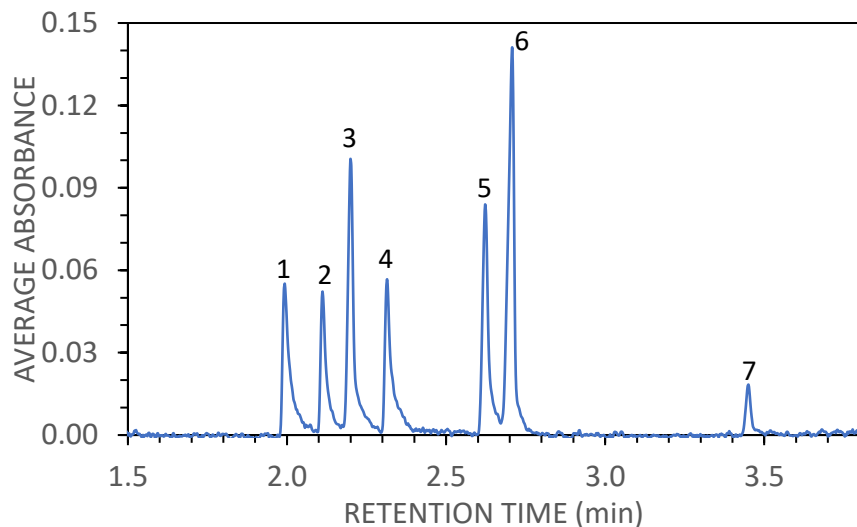
Figure 2.2 Chromatogram of seven phenethylamines. Peaks: 1) amphetamine, 2), MPEA, 3) phentermine, 4) methamphetamine, 5) ethylamphetamine, 6) DMA, 7) pseudoephedrine.

The normalized and overlaid spectra are shown in Figure 2.3. The spectra are rather similar with all having a decreasing "slope" of absorbance from < 125 nm, absorbance maxima around 185 nm, and a "shoulder" around 210 nm.
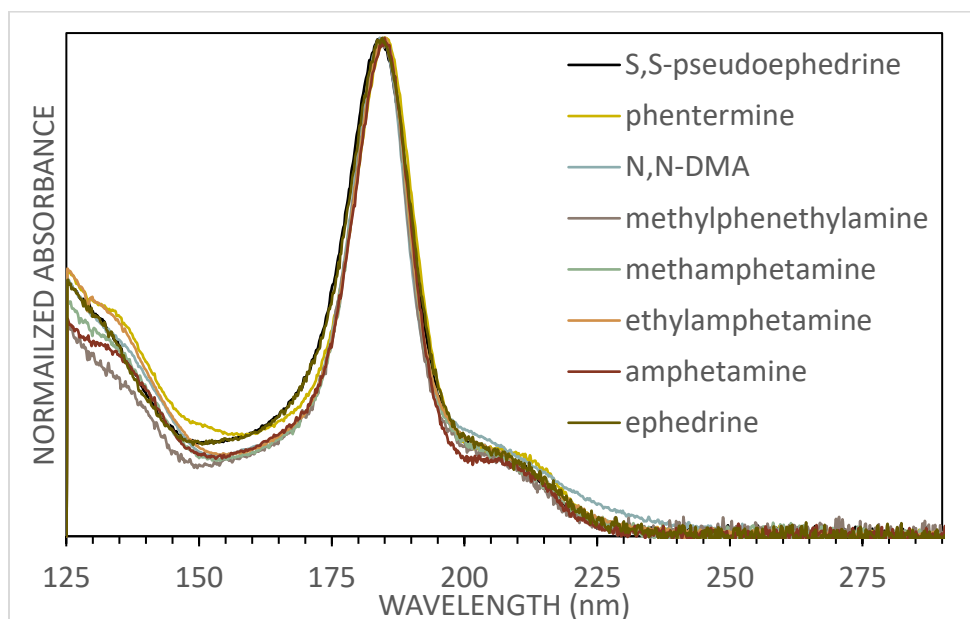
Figure 2.3 Overlaid spectra of *S,S*-pseudoephedrine, phentermine, dimethylamphetamine (*N,N*-DMA), methylphenethylamine, methamphetamine, ethylamphetamine, amphetamine, and ephedrine. The spectra were truncated at 275 nm because no sample absorbed at longer wavelengths.

2.3.2 Assessing Similarity/Dissimilarity of Spectra

The average correlation coefficients and sums of square residuals provide numeric values for the similarity of the spectra as seen in Table 2.1

Table 2.1 Matrix of correlation coefficients (COR) and sums of square residuals (SSR) for the phenethylamines pseudoephedrine (PE), ephedrine (Eph), amphetamine (amph), MPEA, methamphetamine (Meth), phentermine (Phen), DMA, and ethylamphetamine (EA). Sums of square residuals are given in red whereas correlation coefficients are given in blue. Averages taken from three by three matrices of triplicates.

SSR / COR	PE	Eph	Amph	MPEA	Meth	Phen	DMA	EA
PE	0.0377 / 0.9997	0.3734	1.3324	1.8717	1.0488	1.1414	1.1167	1.0869
Eph	0.9973	0.0152 / 0.9999	1.5427	2.1568	1.2495	1.1249	1.3806	1.2569
Amph	0.9944	0.9936	0.1000 / 0.9992	0.5404	0.2650	1.3978	0.9721	0.8669
MPEA	0.9933	0.9921	0.9960	0.1329 / 0.9989	0.6764	2.9698	1.4793	1.8467
Meth	0.9947	0.9938	0.9979	0.9960	0.0650 / 0.9995	1.1701	0.4607	0.4349
Phen	0.9916	0.9916	0.9945	0.9865	0.9949	0.0256 / 0.9998	1.2290	0.5798
DMA	0.9932	0.9914	0.9942	0.9927	0.9975	0.9924	0.0330 / 0.9997	0.3414
EA	0.9923	0.9913	0.9951	0.9902	0.9977	0.9966	0.9976	0.0282 / 0.9998

To the extent that SSR for two analytes approaches zero or r approaches unity, deconvolution of a chromatographic peak containing the two analytes becomes increasingly difficult. Given that SSR is a continuous variable with a lower limit of 0 and no upper limit, it can vary significantly within a group of compounds. In general, pairs of co-eluting compounds with SSR > 1 can be deconvoluted using the VUV software. Classes of compounds from previous publications using GC/VUV are summarized in Table 2.2 with a comparison to the SSR results from this study.

Table 2.2 Comparison of the sums of square residuals (SSR) for various compound classes as compared to this work. The SSR of a compound spectrum compared to itself is zero.

Analytes	n	SSR range	Ref.
Designer Drugs (methcathinones)	43	1 - 227	[33]
Dimethylnaphthalene isomers	8	0.60 – 42.65	[31]
Benzene isotopologes	10	0.0158 – 1.70	[47]
Phenylethylamines	8	0.158 – 3.225	This Work

The use of multi-variate statistical methods applied to chemical data (chemometrics) were also explored. After normalization, the spectral data was analyzed by Principal Components Analysis (PCA). The PCA results are shown in Figure 2.4. The spectra of the phenethylamines produced distinct groups with little variation between replicates. Two outliers can be seen in the score plot, one being a replicate of DMA and one a replicate of ephedrine.
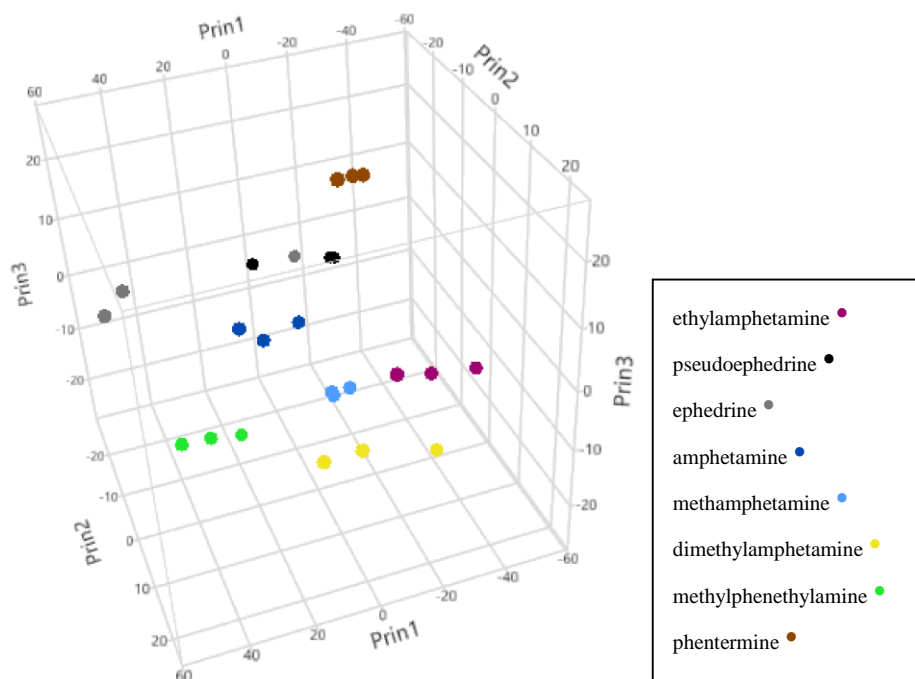
Figure 2.4 3-dimensional PCA scores plot of Principle Components (Prin1, Prin2, and Prin3) showing the distribution of the phenethylamines based on their VUV spectra

The first 4 principal components, representing 91.8% of the cumulative variance, were subjected to DA with the categories being the seven phenethylamines. Clear distinction was

observed between six of the eight phenethylamines. Ephedrine and pseudoephedrine clustered close together but are still distinguishable. The DA results are shown in Figure 2.5.
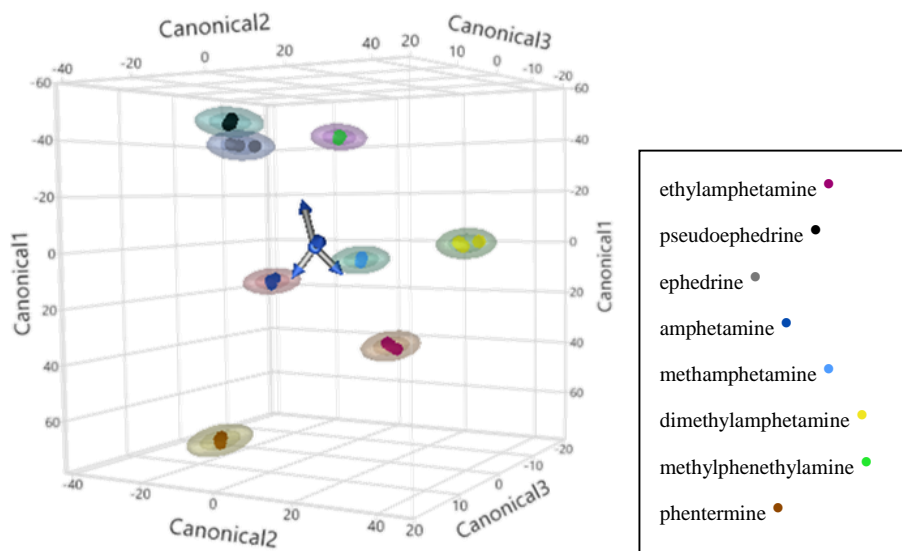
Figure 2.5 Three-dimensional canonical plot illustrating the clustering of the phenethylamines. The ellipsoids indicate the 95% confidence interval for each compound class. The first four principle components were used as inputs for the DA.

2.3.3   Differentiating Ephedrine and Pseudoephedrine

Given their nearly identical structure, the diastereomers Ephedrine and Pseudoephedrine were analyzed in greater detail. In particular, the correlation coefficients for the ephedrine and pseudoephedrine replicates (see Table 2.1) were Fisher transformed and found to be statistically significant via the "student's T-test" at a 95% confidence interval.

Seven replicates of pseudoephedrine and ephedrine were analyzed to determine if the diastereomers were reliably differentiable. Visual spectral comparison is given in Figure 2.6 with a magnified view of the maxima. A very slight blue shift in the pseudoephedrine spectra can be observed at both ends of the maximum. Both compounds overlap at the 184 nm maxima, in the "valley" between 150-155 nm, and approaching 125 nm.
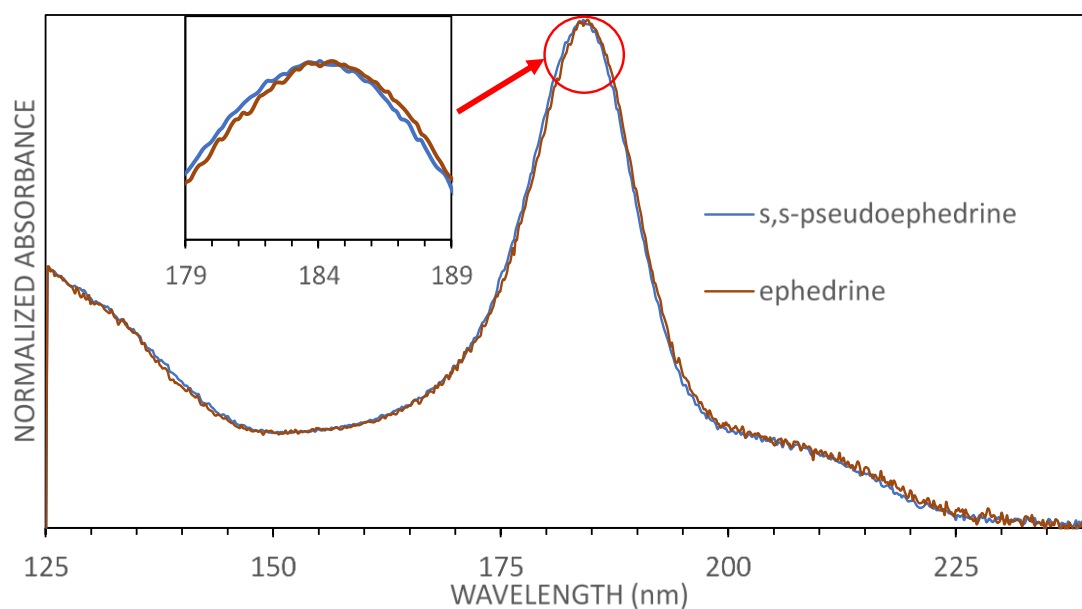
Figure 2.6 Overlaid spectra of *S,S*-pseudoephedrine and ephedrine, spectra were truncated at 240 nm as neither absorbed at longer wavelengths. Window magnifying the region between 179 and 189 nm highlighting the blue shift of the pseudoephedrine.

The normalized diastereomer data was analyzed by PCA which separated the ephedrine and pseudoephedrine samples along Component 2. The two-dimensional PCA is given in Figure 2.7A. The first 4 principle components were then analyzed by DA resulting in Figure 2.7B. For the DA, 4 replicates of each compound were used for the training set and 3 replicates were used as the training set, the classification accuracy was found to be 100%.
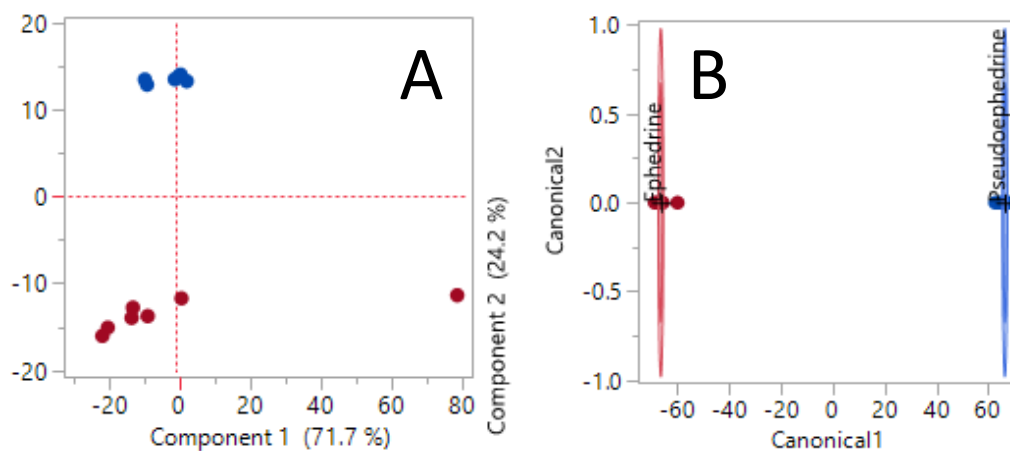
Figure 2.7 A) 2-dimensional score plot showing the distribution of ephedrine and pseudoephedrine along Component 2 B) 2-dimensional canonical plot showing the classification and 95% confidence interval around ephedrine and pseudoephedrine. The first four principle components were inputs for the DA.

Based on the spectral differences and chemometric differentiation, diastereomers such as ephedrine and pseudoephedrine are differentiable by VUV Spectrophotometry. Differentiation diastereomers is impossible by Mass Spectrometry, though chromatography can be used to separate and distinguish diastereomers.

2.3.4   Figures of Merit and Comparison to GC/MS

The phenethylamines were also analyzed by GC-MS using a method that is in common use by forensic chemists. The three most abundant m/z fragments for each compound are tabulated in Table 2.3 with relative abundances. Relative abundances will vary slightly from instrument to instrument, limiting the ability to make determinations based on relative abundances. [48] Ephedrine was excluded as it is a diastereomer of pseudoephedrine and would give the same mass spectrum despite having a slightly different retention time and VUV spectrum.

Table 2.3 The three most abundant fragment ions for amphetamine (Amph), MPEA, phentermine (Phen), methamphetamine (Meth), pseudoephedrine (PE), ethylamphetamine (EA), and DMA with the relative abundance to the base peak in the corresponding mass spectrum.

	Amph	MPEA	Phen	Meth	PE	EA	DMA
Base Peak (m/z)	44 (100%)	44 (100%)	58 (100%)	58 (100%)	58 (100%)	72 (100%)	72 (100%)
2nd (m/z)	91 (55%)	91 (42%)	91 (33%)	91 (29%)	77 (22%)	91 (28%)	91 (16%)
3rd (m/z)	65 (16%)	65 (13%)	134 (20%)	134 (7%)	105 (17%)	44 (9%)	65 (5%)

A GC/VUV LOD study using MPEA as a phenethylamine exemplar determined the LOD to be 10 ng on column. The method for determining LOD used peak height from a spectral filter summing the absorbance from 184 nm to 185 nm. Peak area results from the LOD analyses indicated a lower limit of linearity of 25 ng on column and an upper limit of linearity around 1 μg on column with an R^2 of 0.9971 for the mentioned range. It is possible that with further method development the LOD could reach 1 ng on column or lower. The linearity and LOD determinations were compared to that of an MSD in "scan" mode, the values obtained from the extracted ion

chromatograms for the base peak at *m/z* 44 produced similar LOD results to the VUV. If the MSD had been operated in the "SIM" mode, the LOD and linearity limits would decrease by at least an order of magnitude.

An accuracy and precision study using the derivatized form of MPEA was conducted at concentrations ranging from 180 to 25 μg/ml, the derivative was used to improve precision from one analysis to another. The spectra of MPEA and the TFAA derivative of MPEA are shown in Figure 2.8. An obtained average percent error of -0.26% and relative standard deviation of 0.62% were determined from calculating the concentration of a challenge sample prepared in identical manner to the calibration samples but from a separate stock and at a concentration bracketed by, but separate from, the calibrants. It is suspected that the derivatized form would lower LODs below 10 ng on column. Pre-concentration techniques or more sensitive methods are recommended for future work.
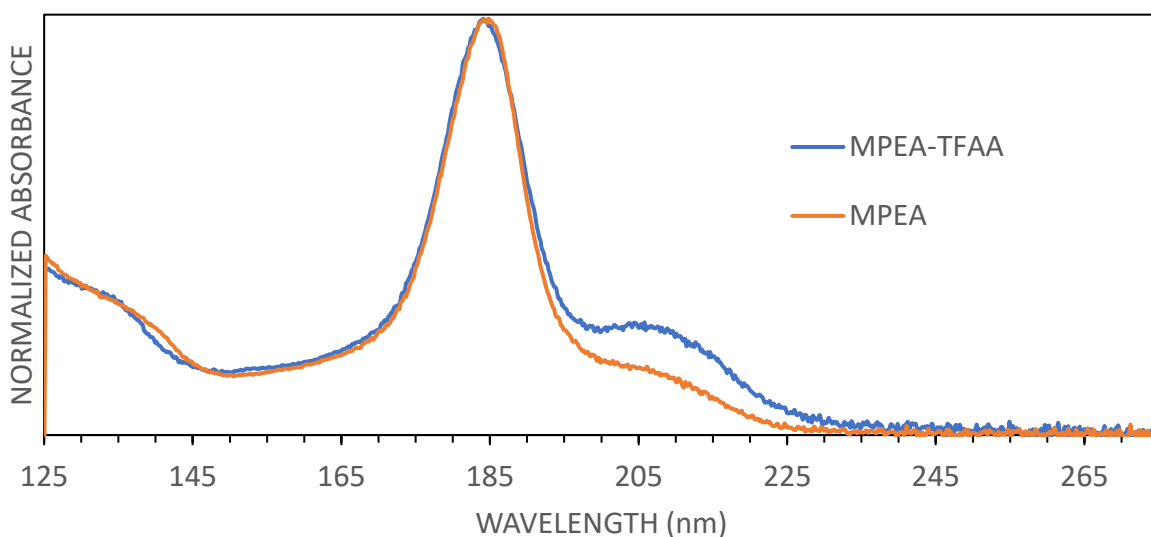
Figure 2.8 Overlaid spectra of MPEA non-derivatized and MPEA-TFAA derivative.

Upon derivatization the absorbance spectrum alters from the non-derivatized form by shifting in the sigma bond region from 125-150 nm, an observed hypsochromic shift in the maximum, and a larger absorbance band is seen from 190-235 nm in the pi bond region.

2.3.5 "Real World" Samples

Five "street" samples of seized phenethylamine exhibits were analyzed by GC-VUV. GC-MS analysis performed for comparison. The chromatograms from the GC-VUV analyses are in Figure 2.9.
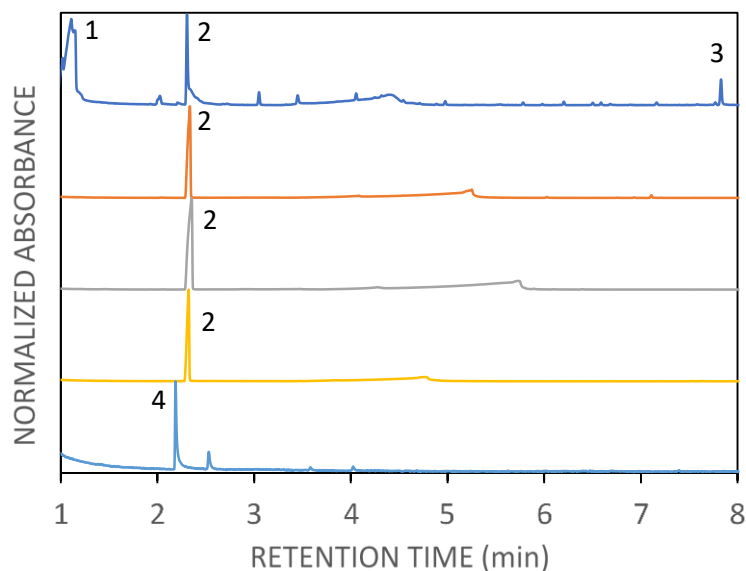
Figure 2.9 Seized "street" samples of phenethylamines. Peaks: 1) dimethyl sulfone, 2) methamphetamine, 3) cocaine, 4) phentermine

The peaks labeled in Figure 2.9 were consistent with the standards analyzed. There are unidentified peaks in the top trace for which the limited library could not identify and was not consistent with any standards analyzed in this work. Future work is needed to expand on the available VUV spectra of compounds to contribute to a spectral library that can be used for reference.

2.4 Conclusions

Several forensically important phenethylamines were analyzed by GC-VUV and found to be distinguishable from one another. The diastereomers ephedrine and pseudoephedrine are distinguishable by VUV spectrophotometry. The specificity of the VUV absorbance spectra was further supported by chemometric analyses. A limit of detection of 10 ng on-column was determined for methylphenethylamine and is representative of the eight phenethylamines. Though GC-MS analysis gives results that can be ambiguous for certain phenethylamines, GC-VUV with

chemometrics shows unambiguous discrimination for these compounds. Ephedrine and pseudoephedrine can also be discriminated despite being diastereomers. We consider GC-VUV to be an excellent complimentary technique to GC-MS and would do well in forensic labs.

2.5 Acknowledgements

CHAPTER 3.   INSTRUMENTAL AND CHEMOMETRIC ANALYSIS OF OPIATES VIA GAS CHROMATOGRAPHY – VACUUM ULTRAVIOLET SPECTROPHOTOMETRY (GC – VUV)

3.1   Introduction

The use of Vacuum Ultraviolet Spectrophotometer (VUV) as a benchtop detection method for Gas Chromatography (GC) has grown in popularity since its introduction in 2014 [24, 31]. GC/VUV has applicability to analytes such as fuels, pesticides, fatty acid methyl esters, and drugs [24, 33-44, 49, 50]. In addition, GC-VUV combined with chemometric techniques can differentiate structural isomers and even diastereomers such as ephedrine and pseudoephedrine [42-44, 49, 50]. As it is non-destructive, VUV can be used in parallel or in series with mass spectrometry [32, 44]. There is also a dearth of published spectra of controlled substances. This study strives to obtain spectra of compounds common in illegal street drugs and prove the specificity of VUV via pattern recognition techniques.

Calculating the similarity/dissimilarity of VUV spectra can be expressed using statistical quantities such as the correlation coefficient and/or the sum of square residuals. Multivariate statistics (i.e., chemometrics) can also extract information from complex data sets [25-28]. Chemometrics can be used in part to optimize methods through response surface methodology. For the purposes of this study, data analysis was conducted using principal component analysis (PCA) and discriminant analysis (DA), both of which have been used to show analyte differentiability, deconvolution capability, and classification accuracy of GC-VUV [33, 34, 39, 41, 47, 50, 51].

Opiates such as morphine and codeine are naturally occurring and are a product of the opium poppy (*Papaver somniferum*) [52]. The semi-synthetic opiate heroin is derived from these naturally occurring alkaloids, and it is of great interest to forensic science laboratories as a public health threat [52, 53]. Synthetic opioids such as meperidine and fentanyl target the opioid receptors but are not directly derived from opium [54, 55]. The structures of the opioids analyzed for this work are shown in Figure 3.1.

Morphine	Heroin
3-acetylmorphine	6-acetylmorphine
Codeine	Oxycodone
Hydrocodone	Hydromorphone
Fentanyl	
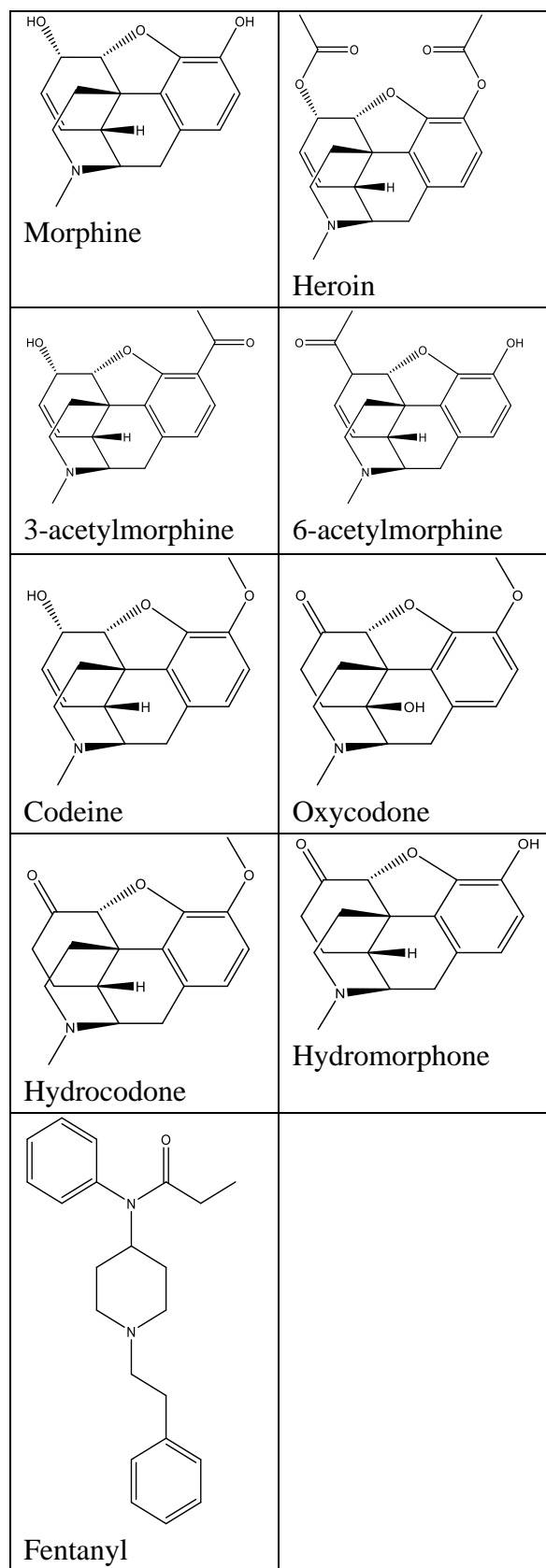
Figure 3.1 Structures of opioids discussed in this work.

Drugs of abuse are rarely pure, often containing a variety of additives used as diluents and adulterants as well as impurities and by-products from production [56-58]. Caffeine, procaine, and quinine are a few of the many additives commonly found in seized heroin exhibits [56, 57]. Eight adulterants, known to be found in heroin exhibits, were chosen for analysis as a part of this work.

To date, for natural and semi-synthetic opiates, only the VUV absorption spectra of morphine and codeine have been published [44, 47]. GC-VUV analysis of synthetic fentanyl opioids have been reported by Lurie [44]. This article aims to present the previously unreported VUV spectra of several opiates, by-products of heroin production, common heroin impurities, and additives, conduct chemometric analysis, and to demonstrate "real world" performance through the analysis of three seized heroin samples.

3.2   Materials/Methods

3.2.1   Instrumentation

An Agilent 7890A gas chromatograph with 7693 liquid autosampler and 30 m x 0.25 mm x 0.25 μm Agilent HP-5MS UI column was connected to a VUV Analytics VGA-101 Vacuum Ultraviolet spectrophotometer for all data collection unless specified otherwise. A Thermo Nicolet iN10 FTIR with an ATR Germanium crystal was used for preliminary IR analysis of "real world" heroin samples. Chemical structures were generated in ChemDraw Professional 18 by PerkinElmer Inc. (Waltham, MA).

3.2.2   Materials

All vials, caps, acetonitrile (HPLC grade), and methylene chloride (HPLC grade) were purchased from Fisher Scientific (Fairlawn, NJ). Heroin (≥98% neat solid), 3-acetylmorphine (≥98% neat solid), and hydromorphone (≥98% neat solid) were purchased from Cayman Chemical (Ann Arbor, MI) under a DEA license maintained by IUPUI. Oxycodone (analytical standard), hydrocodone, and methanol (ACS reagent grade) were purchased from Sigma-Aldrich (St Louis, MO). Single component solutions of morphine, codeine, fentanyl, and 6-acetylmorphine

were purchased from Cerilliant Corporation (Round Rock, TX) at 1 mg/mL in methanol (codeine, fentanyl, and morphine) and acetonitrile (6-acetylmorphine).

3.2.3   GC-VUV Method

The GC inlet temperature was 250 $^{\circ}$C with a 10:1 split ratio, 1 µL injection volume, 4 mL/min hydrogen carrier gas (85 cm/sec linear velocity), initial oven temperature of 45 $^{\circ}$C held for 1.0 minute, ramped at 20 $^{\circ}$C/min to 255 $^{\circ}$C with a final temperature hold of 5 minutes. The VUV scan rate was 6 Hz with a flow cell temperature of 275 $^{\circ}$C, and nitrogen make-up gas pressure of 0.35 psi. All analyses were performed under these conditions unless specified otherwise. A mixture of nine opiates was analyzed using a splitless method with inlet temperature 265 $^{\circ}$C, 1 mL/min carrier gas, initial oven temperature of 150 $^{\circ}$C held for 1 minute, ramped at 20 $^{\circ}$C/min to 280 $^{\circ}$C with a final temperature hold of 5.5 minutes, VUV flowcell 300 $^{\circ}$C, and a make-up gas pressure of 0.13 psi.

3.2.4   Chemometrics

JMP 13 by SAS Institute was used for multivariate analysis. All spectra were baseline subtracted and normalized to the square root of sum of squares of all wavelengths prior to chemometric analysis. For PCA, spectra were truncated at 350 nm. Linear discriminant analysis performed using the first five principal components from the PCA.

3.3   Results/Discussion

3.3.1   Opiate Spectra, SSR's, and Correlation Coefficients

Standard solutions of nine opiates (3-acetylmorphine, 6-acetylmorphine, codeine, heroin, hydrocodone, hydromorphone, morphine, oxycodone, and fentanyl) were prepared individually at a concentration of 1 mg/mL and analyzed by GC-VUV in triplicate. The spectra obtained were normalized and are shown stacked in Figure 3.2. The spectra feature maxima below the shortest recorded wavelength and a secondary main absorbance between 200-210 nm. The spectra of morphine, 3-acetylmorphine (3-MAM), 6-acetylmorphine (6-MAM), and heroin are interesting in that the addition of acetyl groups appears to "flatten" the absorbance region from 180-215 nm.
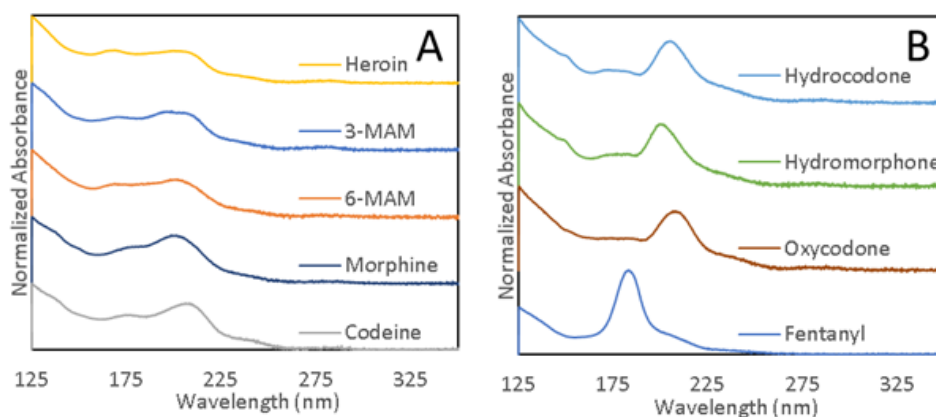
Figure 3.2 Normalized and stacked spectra of A) heroin, 3-acetylmorphine (3-MAM), 6-acetylmorphine (6-MAM), morphine, and codeine. B) hydrocodone, hydromorphone, oxycodone, and fentanyl. Spectra were truncated at 350 nm.

Fentanyl being deemed significantly different from the other eight opiates and having been reported prior, was excluded from statistical analysis [44]. The correlation coefficients and sum of squares residuals were calculated for triplicates of the eight opiate spectra and the averages are displayed in Table 3.1. To get meaningful values for the similarity of each compound's spectra with itself, the averages of the triplicate values were reported here.

Table 3.1 Matrix of average correlation coefficients (COR) and sums of square residuals (SSR) for Morphine, 3-MAM, 6-MAM, Heroin, Codeine, Oxycodone (OC), Hydrocodone (HC), and Hydromorphone (HM). Averages taken from three by three matrices of triplicates. COR are shown in blue to the left whereas SSR are shown in red to the right.

SSR / COR	Morphine	3-MAM	6-MAM	Heroin	Codeine	OC	HC	HM
Morphine	0.0109 / 0.9882	0.0187	0.0206	0.0644	0.0251	0.0347	0.0329	0.0325
3-MAM	0.9795	0.0074 / 0.9915	0.0158	0.0406	0.0184	0.0303	0.0295	0.0370
6-MAM	0.9787	0.9870	0.0144 / 0.9924	0.0363	0.0245	0.0409	0.0388	0.0432
Heroin	0.9748	0.9898	0.9910	0.0013 / 0.9989	0.0359	0.0750	0.0681	0.1087
Codeine	0.9809	0.9811	0.9802	0.9777	0.0056 / 0.9949	0.0248	0.0214	0.0519
OC	0.9555	0.9583	0.9556	0.9563	0.9746	0.0114 / 0.9854	0.0156	0.0390
HC	0.9603	0.9602	0.9596	0.9581	0.9765	0.9789	0.0084 / 0.9906	0.0354
HM	0.9610	0.9580	0.9562	0.9537	0.9608	0.9517	0.9641	0.0187 / 0.9768

Note that the monoacetylmorphines can be resolved by chromatography. Their VUV spectra are also distinguishable visually and statistically by correlation coefficients and sums of squares residuals. Differentiation of the acetylmorphines is not unexpected, as prior work has shown differentiation of diastereomers and positional isomers [44, 50].

To show chromatographic performance of the opiates, a mixture of the nine compounds at 100 µg/mL in methanol was analyzed by GC-VUV to produce the chromatogram in Figure 3.3. Morphine and hydrocodone overlap but are still easily distinguishable.
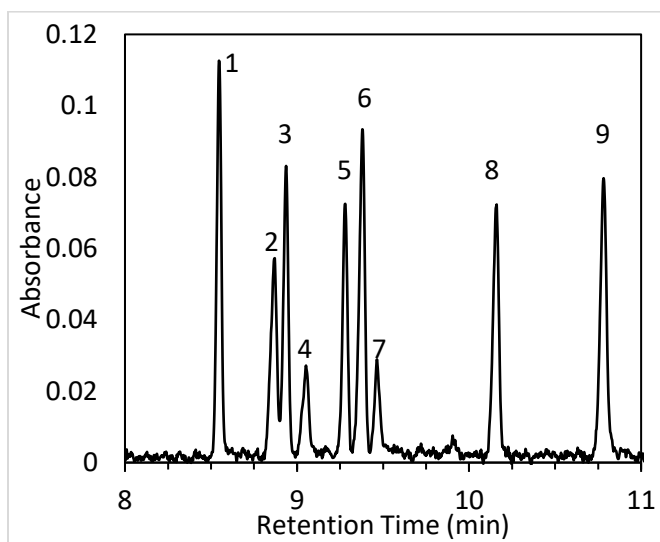
Figure 3.3 Chromatogram of the opioid standards. Peaks: 1) codeine, 2) morphine, 3) hydrocodone, 4) hydromorphone, 5) 3-acetylmorphine, 6) 6-acetylmorphine, 7) oxycodone, 8) heroin, and 9) fentanyl.

3.3.2   Trends in PCA and Differentiation by DA

The triplicate spectra of the eight opioids were background subtracted, then normalized to the square root of the sum of squares of the spectra. The two-dimensional scores plot from PCA is shown in Figure 3.4. The scores plot shows a structure that sorts the compounds nicely by chemically structure. For example, the naturally occurring morphine, acetylated morphine and heroin cluster along a line (in that order) from the top of the upper right quadrant to the lower left quadrant, which would indicate that they share some spectral similarities as can be seen in Figure 3.2A. The remaining opiates (codeine, hydrocodone, hydromorphone, and oxycodone) lie parallel to this group and each other yet occupy distinct regions of the PCA space.
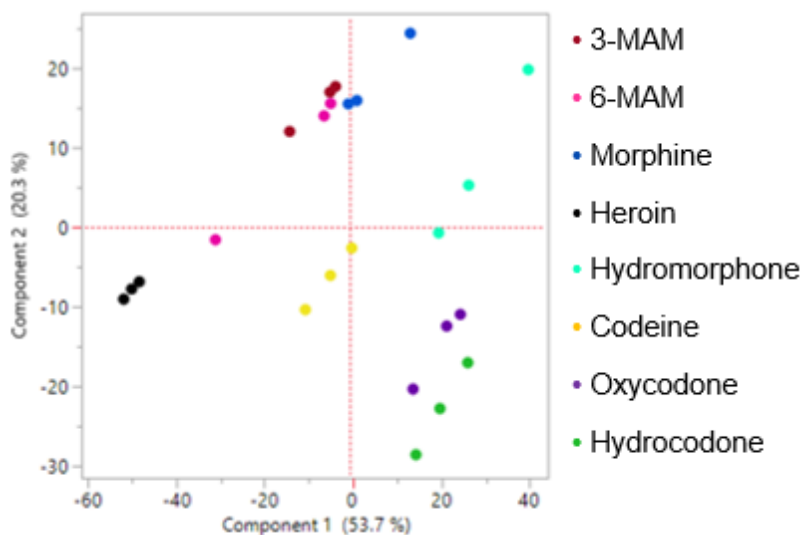
Figure 3.4 2-dimensional PCA scores plot of the first and second principal components (% of variance = 74%) demonstrating the distribution of the opioids based on their corresponding VUV spectra.

Based upon inspection of the Scree plot of the PCs, the first five principal components were selected for inclusion in LDA. These five PCs encompassed 88.5% of the variance. The linear grouping for the VUV spectra from morphine, acetylated morphine and heroin is also evident in DA. The three-dimensional canonical plot is shown in Figure 3.5.
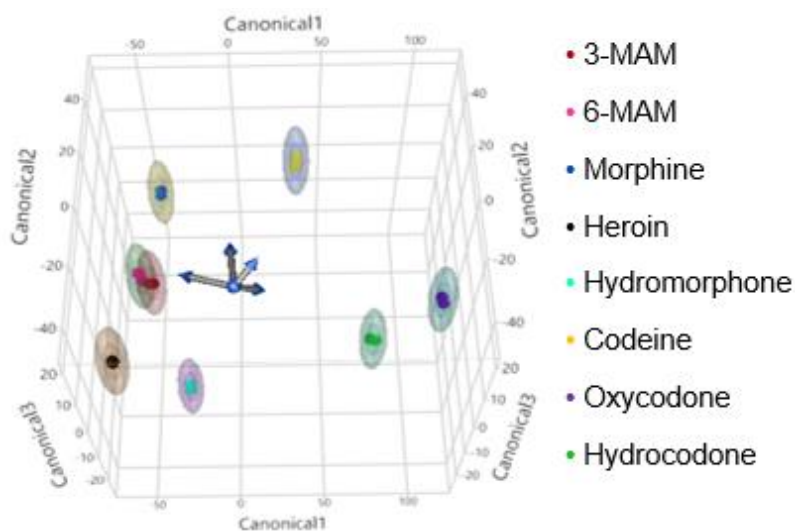
Figure 3.5 3-dimensional DA canonical plot illustrating the linear grouping of the compounds involved with morphine acetylation and differentiation of these compounds from other opioids. Ellipsoids indicate the 95% confidence interval for classification of each compound.

Validation of the classification model resulted in 100% classification accuracy for the test set, which consisted of 33% of the total data set. While the chemometric analysis of the opioid class showed some overlap in the confidence intervals, it was able to resolve 3-MAM and 6-MAM.

3.3.3 Spectra of Adulterants

Standard solutions of eight adulterants (lidocaine, procaine, benzocaine, acetaminophen, caffeine, diphenhydramine, quinine, and guaifenesin) were prepared individually at a concentration of 0.5 mg/mL and analyzed by GC-VUV in triplicate. The spectra obtained were normalized and are shown stacked in Figure 3.6. The spectrum of caffeine has been previously reported [59].
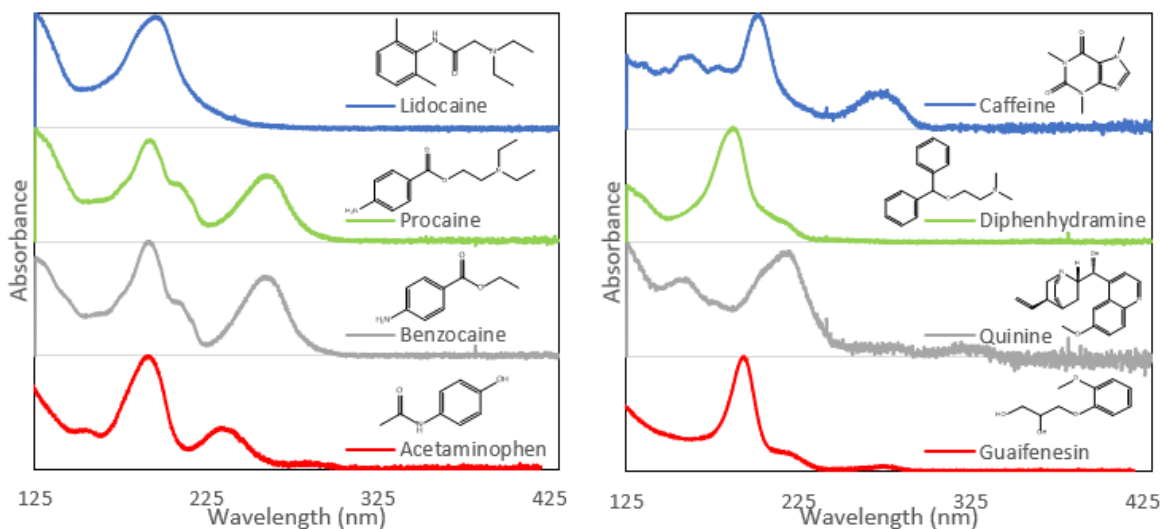
Figure 3.6 Normalized and stacked spectra with structures of A) lidocaine, procaine, benzocaine, acetaminophen. B) caffeine, diphenhydramine, quinine, and guaifenesin.

3.3.4 "Real World" Samples

Three "street" samples of heroin from the Indiana State Police Laboratory, were analyzed by GC-MS and GC-VUV to demonstrate "real world" performance. IR analysis identified caffeine in sample A and lactose in sample B. All analyzed heroin samples included acetylcodeine, 6-MAM, and heroin. The acetylcodeine and 6-MAM are by-products of heroin acetylation. The 6-MAM indicates that the heroin de-acetylated. Chromatograms from the GC-VUV analyses are shown in Figure 3.7.
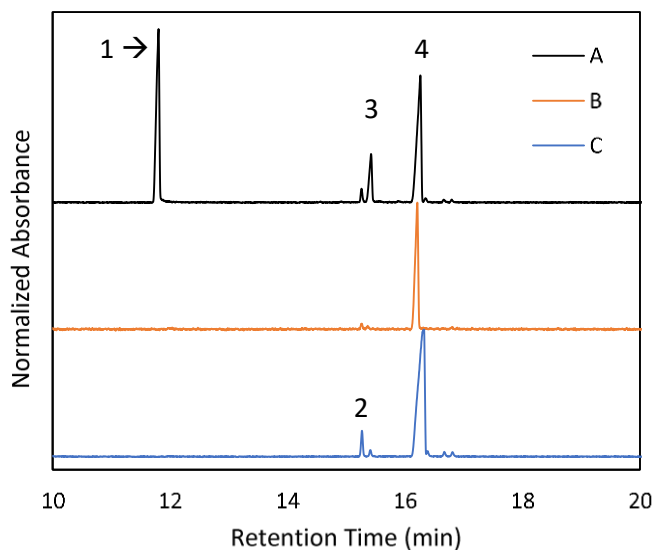
Figure 3.7 Chromatograms obtained of three seized samples of heroin. Peaks: 1) caffeine, 2) acetylcodeine, 3) 6-MAM, 4) heroin.

3.4   Conclusions

The spectra of several forensically important opioids are reported after analysis by GC-VUV. VUV can differentiate all the opioids studied. There are also class similarities between morphine and its various acetylated products, including heroin. Specificity of the spectra was supported by chemometrics, correlation coefficients, and sums of square residuals. VUV spectra of seven adulterants common to heroin were also reported. Finally, three seized samples of heroin were analyzed to demonstrate "real world" performance. Overall, GC-VUV continues to show promise as an analytical instrument providing complimentary data to mass spectrometry.

CHAPTER 4.   OPTIMIZATION OF THE QUALITATIVE AND QUANTITATIVE ANALYSIS OF COCAINE AND OTHER DRUGS OF ABUSE VIA GAS CHROMATOGRAPHY – VACUUM ULTRAVIOLET SPECTROPHOTOMETRY (GC – VUV)

4.1   Introduction

The use of a vacuum ultraviolet (VUV) spectrophotometer as a benchtop detector for gas chromatography (GC) has increased since commercial implementation in 2014 [24, 60]. VUV allows for the detection of virtually any analyte by σ and π bond absorption of UV light in the traditional UV, deep UV, and far UV regions [24, 60, 61]. Applications of GC-VUV include the analysis of petroleum products [24, 39, 62-65], explosives [41, 66, 67], pesticides [35], fatty acid methyl esters (FAMEs) [34, 68-71], controlled substances [33, 36, 42, 44, 49, 50, 72, 73], and more [24, 37, 38, 40, 60, 74]. Differentiation of structural isomers and diastereomers are significant advantages to GC-VUV [42, 44, 49, 50, 75]. Combination of VUV with mass spectrometry has been demonstrated in split and in-line configurations [32, 44].

To date, there has not been a published systematic optimization of method parameters for drug detection by GC-VUV. This study sought to obtain a statistically optimized method through response surface methodology (RSM) for the detection of controlled substances. RSM applications to analytical chemistry are vast and have been touched on in the review by Bezerra et al [76]. RSM is used when a statistical optimum is desired from a process involving multiple variables with dependent response [77]. A face centered central composite design (CCF) was used for RSM optimization of method parameters as limits, both instrumental and practical, were used as high and low values. A three-level design containing high, low, and middle values for three variables using six center points and six replicates was chosen to provide ample coverage and representation of the data set [78].

Of the drugs used in this study, the VUV absorbance spectra for heroin, fentanyl, methcathinone, and methamphetamine have been previously reported [33, 42, 44, 50]. To the authors' knowledge, this is the first report of the VUV absorption spectra of cocaine, lorazepam, PCP, and HU-210 [33, 44]. Cocaine, a natural tropane alkaloid extracted from the coca plant, is a common illicit stimulant [79]. Methamphetamine, another commonly encountered drug of abuse, and other amphetamines were analyzed and reported [50]. GC-VUV analysis of 67 synthetic cathinones and

fentanyl opioids have been reported [33, 42, 44]. Methcathinone is a synthetic cathinone used in "bath salts" [80]. Other drugs of abuse analyzed by GC/VUV include PCP which is a hallucinogen, HU-210 a synthetic cannabinoid, and lorazepam a depressant.

This article aims to demonstrate the optimization of parameters for drug detection by GC-VUV. The VUV parameters of flow-cell temperature, make-up gas pressure, and carrier gas flow rate were optimized through RSM, allowing us to examine cross-variable affects. A CCF experiment was used for the optimization due to working within instrumental and practical limits. Limits of detection for cocaine, heroin, and fentanyl as class representative drugs are given pre- and post-optimization and compared to GC-MS. The VUV spectra of four drugs of abuse are presented herein for reference for future work. Finally, to demonstrate "real world" performance and applicability to seized drug analysis, three seized cocaine samples were analyzed.

4.2   Materials/Methods

4.2.1   Instrumentation

An Agilent 7890A gas chromatograph with 7693 liquid autosampler and 30 m X 0.25 mm X 0.25 μm Agilent HP-5MS UI column was connected to a VUV Analytics VGA-101 Vacuum Ultraviolet spectrophotometer for all VUV data collection unless specified otherwise. An Agilent 5975C mass spectral detector connected to an Agilent 7890A gas chromatograph with 30 m x 0.25 mm x 0.25 μm Agilent DB-5MS column and a 7683B liquid autosampler was used for GC-MS data acquisition.

4.2.2   Materials

All vials, caps, acetonitrile, methanol, and methylene chloride were purchased from Fisher Scientific (Fairlawn, NJ). Heroin (≥98% neat solid), PCP (≥98% neat solid), and HU-210 (1 mg in 100 μL of methanol) were purchased from Cayman Chemical (Ann Arbor, MI). Cocaine base (>98.5% powder) bought from Lipomed Inc. (Cambridge, MA). (+)-Methamphetamine hydrochloride (≥98% powder) and (±)-lorazepam (≥98% powder) were purchased from Sigma-Aldrich (St Louis, MO). All scheduled powders were obtained under a DEA license maintained

by IUPUI. Single component solutions of methcathinone, and fentanyl 1 mg/mL in methanol were purchased from Cerilliant Corporation (Round Rock, TX).

4.2.3 GC-VUV Method

GC inlet temperature 250 ºC, splitless, injection volume 1 µL, flow rate of 4 mL/min of hydrogen carrier gas, oven initial temperature 45 ºC for 1.0 minute ramped at 20 ºC min-1 to 255 ºC with a final temperature hold of 5 minutes. VUV scan rate 6 Hz, flow cell temperature 275 ºC, and makeup gas pressure 0.35 PSI of nitrogen. All analyses performed under these conditions unless specified otherwise. Peak area data were collected for the optimization without the use of spectral filters.

4.2.4 GC-MS Method

GC inlet temperature 250 ºC, splitless, injection volume 1 µL, flow rate of 1.8 mL/min of hydrogen carrier gas, oven initial temperature 50 ºC for 0.5 minutes ramped at 20 ºC min-1 to 250 ºC with a final temperature hold of 2.5 minutes. MS transfer line temperature 255 ºC, mass scan range 35 to 480 Th, solvent delay 0.5 min, tuned using Autotune. Method chosen to be representative of methods used in forensic labs.

4.2.5 Figures of Merit

Accuracy and precision values were determined by analysis of five calibrants in triplicate and challenge samples prepared in identical fashion to but separate stock from the calibrants, also analyzed in triplicate with all vials having a single injection. Accuracy and precision, in the form of percent error and relative standard deviation, were determined by calculating the average concentration of the known challenge samples from the corresponding calibration curves. Calibrants were prepared at 25, 50, 100, 150, and 200 µg/mL, the challenge samples were prepared at 75 µg/mL. This process has been described in prior work [50]. LODs were determined by preparing calibration curves with calibrants ranging from 1 µg/mL to 100 µg/mL in triplicate. For GC-VUV LOD's, spectral filters were applied post-acquisition based on the analyte spectrum. Methamphetamine and fentanyl used a filter that doubled the average absorbance from 184 nm to

185 nm, heroin used the sum of the average from 165 to 170 nm and the average from 126 to 127 nm, cocaine used the sum of the average from 183 to 193 nm and the average from 215 to 230 nm.

4.2.6   Design of Experiments

JMP 13 by SAS Institute was used for design of experiments and optimization by response surface methodology. A face centered central composite design with six center points and six replicates was chosen with three levels (high, middle, and low) and three variables (flow-cell temperature, make-up gas pressure, and carrier gas flow rate). High/middle/low values of 300/275/250 ℃, 0.30/0.20/0.10 psi, and 3.0/2.0/1.0 mL/min were used for flow-cell temperature, make-up gas pressure, and carrier gas flow rate, respectively. Desirability was set to maximize chromatographic peak area for three analytes.

4.3   Results/Discussion

4.3.1   VUV Spectra of Common Drugs of Abuse

Standard samples of cocaine, fentanyl, methcathinone, PCP, lorazepam, and HU-210 were analyzed by GC-VUV as representatives of classes of common controlled substances. Cocaine for tropane alkaloids, fentanyl for synthetic opioids, methcathinone for synthetic cathinones, PCP is a hallucinogen, lorazepam for the barbiturate class, and HU-210 for synthetic cannabinoids. The VUV spectra of these compounds are shown in Figure 4.1. The VUV spectra for all but HU-210 have an aromatic absorption around 180 nm as the maxima. Of these spectra, lorazepam has a complicated absorbance spectrum with many peaks, unlike many VUV spectra of drugs. Possible reasons for the complex spectrum are the high percentage of conjugated bonds and possible vibronic influence of the electronegative chlorine substituents, which yield a characteristic peak at 142 nm.
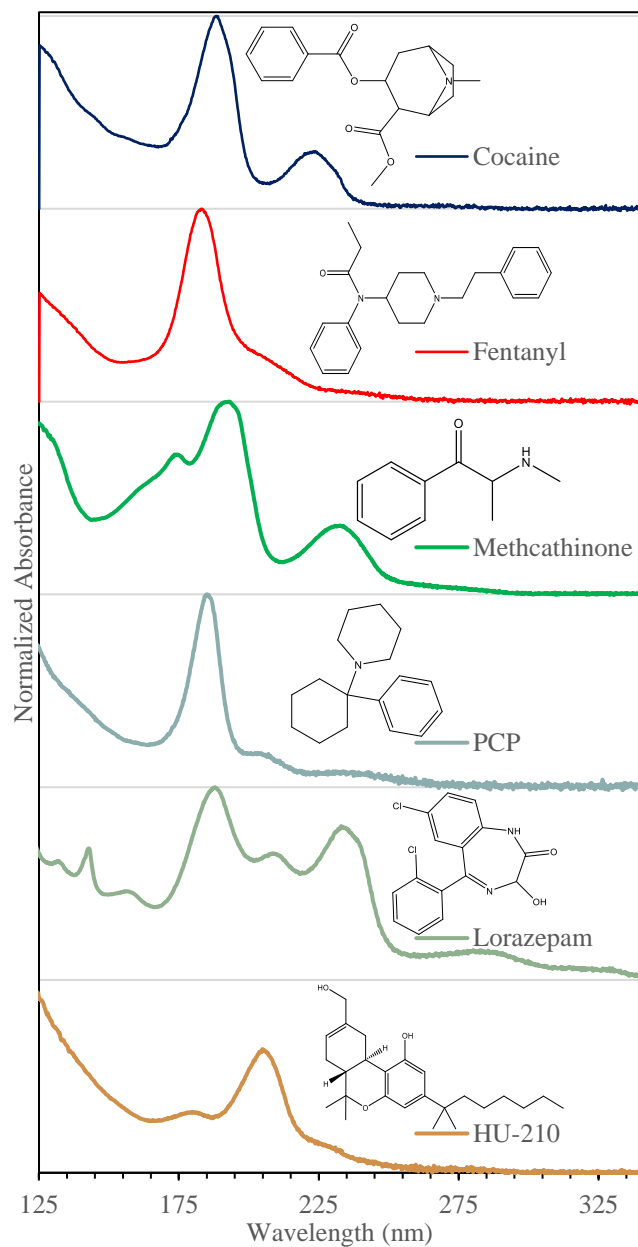
Figure 4.1 VUV absorbance spectra and structures of cocaine, fentanyl, methcathinone, PCP, lorazepam, and HU-210. Spectra were truncated at 340 nm as no sample absorbed at longer wavelengths.

4.3.2 Figures of Merit and Optimization

The accuracy and precision of the GC-VUV for several representative compounds were determined as described in prior work [50]. The samples were single analyte solutions analyzed in triplicate. Since the figures of merit were obtained prior to optimization, it is possible that some values such as the linearity for fentanyl could be improved. The linearity ($R2$) for fentanyl was

0.9752 and is the only analyte of the three less than 0.999. All accuracies, in average percent error, were less than or equal to 1.5%. All values of precision, in percent relative standard deviation, were less than or equal to 1.7%. Error less than 5% and precision less than 2% was considered reasonable. The values obtained for cocaine, heroin, and fentanyl are in Table 4.1. The values for the figures of merit obtained for *N*-amphetamine-TFA in prior work have been included for comparison.

Table 4.1 Accuracy and precision values represented by average error and relative standard deviation (%RSD) for averages of the 75 ng on-column challenge samples and linearity (R2) of the calibration curves of cocaine, heroin, fentanyl, and *N*-amphetamine-TFA from 25 to 200 ng on-column.

Compound	Avg. error	RSD	Linearity (R^2)
Cocaine	1.5%	1.2%	0.9998
Heroin	0.70%	0.94%	0.9998
Fentanyl	1.5%	1.7%	0.9752
N-amphetamine-TFA	-0.26% [50]	0.62% [50]	0.9970

An optimization was performed using face centered central composite design (CCF) to determine optimum VUV flowcell temperature, makeup gas pressure, and GC flow rate. GC oven ramp rate, starting and ending temperatures, hold times, split ratios, injection volumes, and other parameters were not chosen for optimization due to not having a direct effect on conditions inside the VUV flow-cell. Parameters not chosen for optimization have been chosen at common values. The CCF included six replicates of high, low, and center values for each of the variables totaling 120 analyses. The peak area was chosen as the value to maximize for methamphetamine, cocaine, heroin, and fentanyl. Methcathinone was included in the test solution but was found to degrade before the optimization could complete so the data was excluded from consideration. The desirability obtained in the optimization was 0.78, producing values between the limits for all but one value. GC flow rate was found to be optimum at the set lower limit of 1.0 mL/min. Flow cell temperature and make-up gas pressure were optimized at 295 $^\circ$C and 0.13 PSI, respectively. The optimum values were the same for all analytes. The response surfaces for the analytes are given in Figure 4.2. When viewed at full scale, there does not appear to be extensive curvature to the response surfaces. This means that the overall performance of the system is not highly sensitive to

the parameters studied here. However, it is also true that "zoomed in" surfaces such as in Figure 4.2D show a clear maximum curvature.
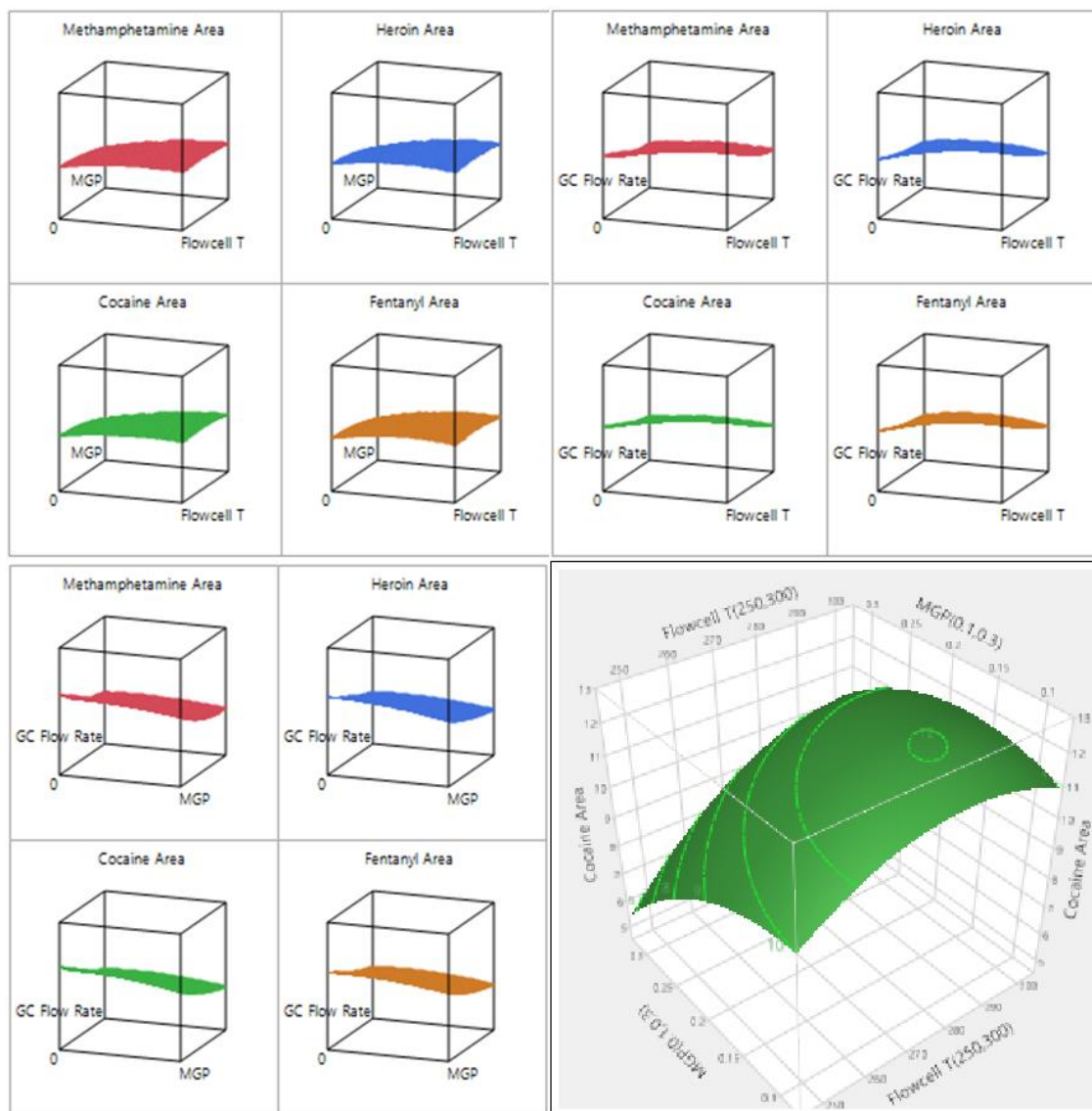
Figure 4.2 Area response surfaces for methamphetamine, heroin, cocaine, and fentanyl varying A) Make-up gas pressure (MGP) and Flowcell Temperature (T), B) GC carrier gas flow rate and Flowcell T, and C) GC carrier gas flow rate and MGP. D) Cocaine response surface with contours area vs MGP vs Flowcell T.

The most influential variable to peak area was found, by response surface analysis, to be GC carrier gas flow rate. Flowcell temperature and make-up gas pressure had the second and third most influential effects, respectively. The cross-variable effects of flowcell temperature x make-

up gas pressure as well as flowcell temperature x GC carrier gas flow rate was found to be significant. Changing flowcell temperature would change the flow rate characteristics in the make-up cell thus affecting mobile phase velocities, which should be taken into consideration in future studies. The overall optima were:

Flowcell temperature: 295 °C

GC column flow rate: 1.0 mL/min

Make-up gas pressure: 0.13 PSI

These optimal values are reasonable for the studied compounds. Thermally unstable or high boiling point compounds would need different flowcell temperatures and thus, based on cross-variable effects being significant, would likely be optimized at different flow rates or make-up gas pressures. A chromatogram of the test solution at the optimized parameters is given in Figure 4.3. Methcathinone degraded throughout testing, which is indicated by the tailing of the peak.
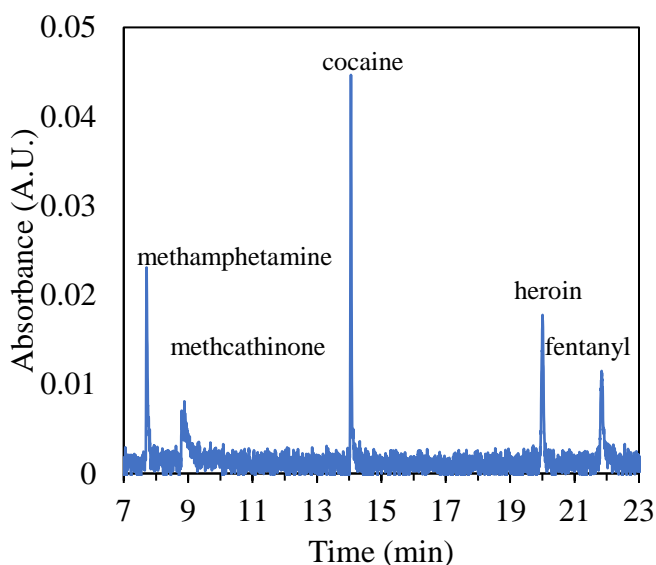
Figure 4.3 Chromatogram of mixture containing 67 ng on-column each of methamphetamine, methcathinone, cocaine, heroin, and fentanyl at the following conditions: GC flow 1 mL/min, oven 30 °C to 250 °C at 20 °C/min, VUV MGP 0.13 PSI of nitrogen, and flow cell temperature 295 °C.

Peak width at half max (PWHM) data was also obtained during the optimization and analyzed separately through RSM. The results of the response surface analysis show that carrier gas flow rate had the most significant impact on peak broadening with make-up gas pressure having minimal impact under these conditions. Flow rates having the most significant effect on

PWHM is reasonable given that chromatographic efficiency is heavily reliant on mobile phase velocities. The optimum values minimizing PWHM for the four analytes were found to be 250 ℃, 2.8 mL/min, and 0.3 PSI, though values mostly did not exceed 0.18 minutes for heroin and fentanyl and 0.05 minutes for methamphetamine and cocaine across the entire tested range.

Calibration curves were obtained pre-optimization for the compounds using the GC-VUV and an equivalent GC-MS method in "scan mode" to obtain limits of detection. As was stated prior, methcathinone degraded between sequential analyses and was thus not able to obtain an accurate LOD and excluded from this data set. Methamphetamine was not reported due to non-gaussian peak characteristics which are required for accurate peak area measurements. A calibration was performed using the optimized parameters to obtain limits of detection for comparison to the pre-optimized conditions. Filters were applied post-acquisition in the GC-VUV that were specific to the type of spectrum of each molecule (see above). The LOD's are given in Table 4.2. The optimization generally produced lower LOD's, particularly with fentanyl where the LOD decreased by more than a factor of 6 to below 10 μg/mL or 10 ng on-column. Heroin increased slightly, but not by a statistically significant margin. The LOD's obtained are acceptable for seized drugs analysis, even within the range of cocaine on common currency [81]. Lower LOD's would be needed for toxicological concentrations of some drugs, e.g. fentanyl can be found in urine at the ng/mL level which is three orders of magnitude lower than the presented LOD's [82]. To further lower LOD's in future research, pre-concentration techniques such as solid phase microextraction (SPME) are recommended.

Table 4.2 LODs in mass-on-column calculated for cocaine, heroin, and fentanyl using GC-MS in scan mode and GC-VUV aided with wavelength filters.

Drug	GC-MS LOD (scan)	GC-VUV LOD (filters)	Optimized GC-VUV LOD (filters)
Cocaine	1.1 ng	2.0 ng	1.5 ng
Heroin	2.8 ng	1.4 ng	2.0 ng
Fentanyl	38 ng	44 ng	9.7 ng
Methamphetamine	31 ng	43.9 ng	6.6 ng

Difference in analyte response between nitrogen and argon make-up gas was tested and no statistical difference was found. It was believed that since nitrogen absorbs faintly in the region of

interest, argon would provide better signal to noise characteristics and improved peak detection. Analysis of the prior five component test mixture using each make-up gas at equal flow resulted in no statistical improvements from one gas to another.

4.3.3 "Real World" Samples

Three "street" samples of cocaine donated by the Indiana State Police were analyzed by GC-VUV and confirmed by GC-MS. The chromatograms of the three samples are given in Figure 4.4. Phenyltetrahydroimidazothiazole (PTHIT), usually in levamisole form, is a common adulterant to cocaine and was found in sample C [83, 84]. Ecgonidine methyl ester and two unidentified compounds were also found in all samples at trace levels around the 6-minute mark in Figure 4.4.
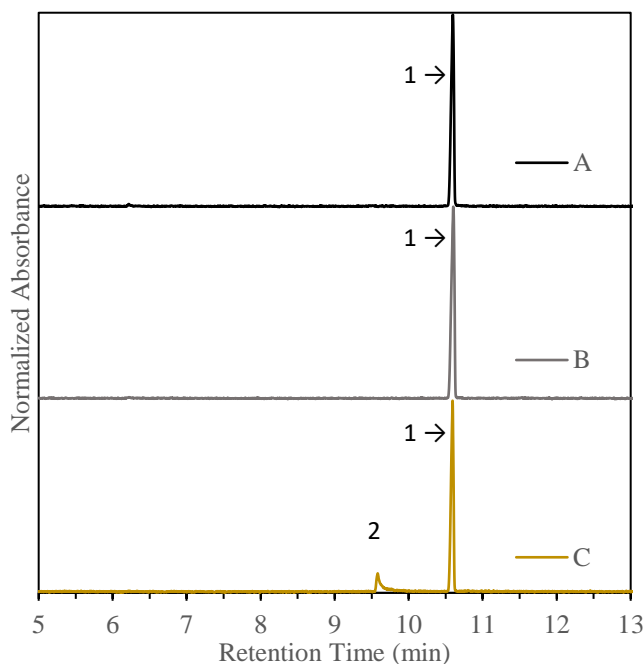
Figure 4.4 Chromatogram obtained of three seized samples of cocaine. Peaks: 1) Cocaine, 2) PTHIT (in sample C). The samples were analyzed at the following conditions: GC flow 1 mL/min, oven 90 $^{\circ}$C held for 1 minute then ramped at 20 $^{\circ}$C/min to 280 $^{\circ}$C held for 10 minutes, VUV MGP 0.13 PSI, and flow cell temperature 295 $^{\circ}$C.

4.4 Conclusions

The VUV absorbance spectra of four compounds were reported for the first time in the literature. Figures of merit were reported for cocaine, heroin, and fentanyl. Parameters influencing conditions in the VUV flow-cell, flow-cell temperature, make-up gas pressure, and carrier gas flow

rate, were optimized for drug detection using RSM on a CCF based experiment. LOD's were reported for cocaine, heroin, and fentanyl from before and after optimization with comparison to a non-optimized GC-MS method. LOD's for the three compounds were determined to be less than 10 ng on-column. Lastly, three seized cocaine exhibits were analyzed by GC-VUV for applicability to "real world" samples. The applicability of GC-VUV to trace level analyses (e.g., drug residue on surfaces/paraphernalia, drugs/metabolites in bodily fluids, determination of volatiles, etc.) remains to be seen.

CHAPTER 5.   DETECTION AND DIFFERENTIATION OF DERIVATIZED DRUGS OF ABUSE BY GAS CHROMATOGRAPHY– VACUUM ULTRAVIOLET (GC–VUV) SPECTROPHOTOMETRY

5.1   Introduction

Analyzing suspected controlled substances comprises much of the casework of many forensic laboratories. GC-MS, considered the "gold standard" instrument [32, 45, 85, 86], is commonly used for drug analysis as it covers the necessary tests recommended by the Scientific Working Group for the Analysis of Seized Drugs (SWGDRUG). Gas chromatography coupled to vacuum ultraviolet spectroscopy (GC-VUV) has been used to analyze controlled substances and, despite producing compound specific data similar in quality to GC-MS, would be considered insufficient for compound identification under SWGDRUG guidelines [24, 31, 36, 64, 65, 87]. Use of the GC in GC-VUV is the same as in GC-MS, such that it provides separation of the components in a mixture of controlled substances.

In GC, using PDMS based columns, active compounds such as amphetamines produce poor chromatographic peaks which leads to poor detector response [60, 72, 85]. A compound that is easily analyzed by GC must be volatile, thermally stable, and have few to no active hydrogens [39, 46, 60, 66, 74, 88]. An active hydrogen refers to a functional group on a controlled substance that will react with the column and cause strong dipole moments and decreased volatility [45, 50, 73, 87]. Such performance can be seen in peak broadening and poor limits of detection [79]. Derivatization removes the active hydrogens and substitutes a protecting group that reduces the dipole moment and increases volatility, resulting in better chromatographic performance and, as shown herein, better detector response with a chosen chromophore [42, 49, 87, 89, 90].

This paper discusses the change in spectra and the improvement of limits of detection for four controlled substances, structures shown in Figure 5.1, using four derivatization agents analyzed by GC-VUV.
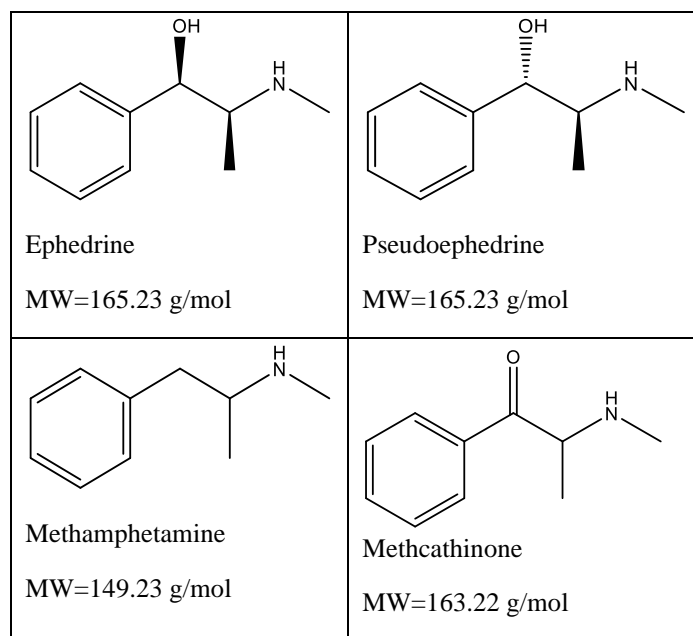
Figure 5.1 Chemical structures and molecular weights of ephedrine, pseudoephedrine, methamphetamine, and methcathinone.

Acylation and silylation were the forms of derivatization in this experiment used to compare the functional groups as chromophores. Common acylation agents, used herein, are carboxylic acid anhydrides such as trifluoroacetic anhydride (TFAA) and 2,3,4,5,6-pentafluorobenzoyl chloride (PFBCl). The most common silylation agent is *N,O*-bis(trimethylsilyl)trifluoroacetamide (BSTFA), which was used herein [87]. The functional groups targeted were hydroxyl, secondary amines, and ketones. The reagents used compared trimethylsilyl groups versus fluorinated groups. The use of fluorinated anhydride groups as a chromophore was used to observe the effect of highly electronegative substituents on detection limits. Then, using pentafluoro benzene groups, the effect of conjugation on detection limits was observed.

Certain reagents had the ability to form multiple reaction products since there are two active hydrogens on ephedrine and pseudoephedrine [33, 90-95]. The preferred reactions for the reagents used are shown in Figure 5.2.
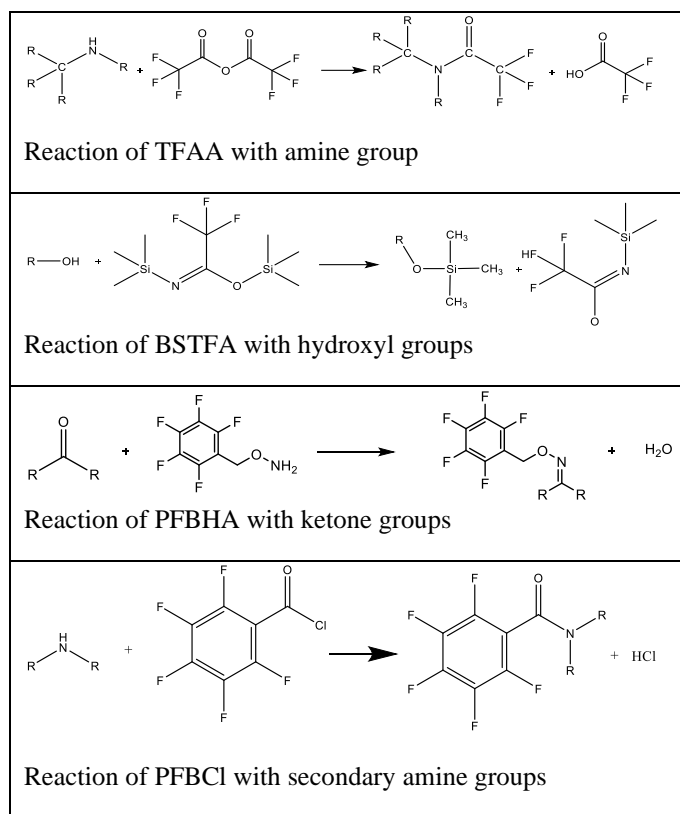
Figure 5.2 Reaction schemes for the preferred reactions of TFAA, BSTFA, PFBHA, and PFBCl.

5.2   Materials/Methods

5.2.1   Instrumentation

An Agilent 7890A gas chromatograph with 7693 liquid autosampler and 30 m x 0.25 mm x 0.25 μm Agilent HP-5MS UI column was connected to a VUV Analytics VGA-101 Vacuum Ultraviolet spectrophotometer for all data collection.

5.2.2   Materials

All vials, caps, and dichloromethane (HPLC grade) were purchased from Fisher Scientific (Fairlawn, NJ) and methanol (ACS reagent grade) was purchased from Sigma-Aldrich (St Louis, MO). Methamphetamine, ephedrine, and pseudoephedrine were purchased from Sigma Aldrich (St Louis, MO) as ≥98% neat solids under a DEA license maintained by IUPUI. Methcathinone solution (1 mg/mL in methanol) from Cerilliant Corporation (Round Rock, TX). Derivatization

agents TFAA and BSTFA (BSTFA + 1% TMS) were purchased from Regis Tech (Morton Grove, IL), and pentafluorobenzyl hydroxylamine (PFBHA) was purchased from Sigma-Aldrich (St Louis, MO).

5.2.3   Sample Preparation

A 100 ppm w/v stock of each sample was prepared and reacted with 5% v/v of derivatization agent. Ephedrine, pseudoephedrine, and methamphetamine were dissolved in DCM and reacted with TFAA, BSTFA, and PFBCl. Methcathinone was diluted with methanol and reacted with PFBHA. Reaction time was 20 minutes to ensure full reaction. Samples were then diluted to make calibration standards of 1mL sample volume and analyzed in triplicate.

5.2.4   GC Methods

The inlet temperature was 250 ^{o}C, splitless, 1μL injection volume, 1 mL/min flow rate of hydrogen carrier gas (85 cm/sec linear velocity), initial oven temperature of 30 ^{o}C held for 1 minute, ramped at 20 ^{o}C/min to 250 ^{o}C final temperature held 13 minutes and total run time of 25 minutes. The VUV scan rate was 6 Hz with a flow cell temperature of 295 ^{o}C, and nitrogen makeup gas pressure of 0.13 psi.

5.2.5   Chemometrics

Spectra were baseline subtracted and the absorbance normalized to the square root of sum of squares of all wavelengths prior to multivariate analyses. JMP 13 by SAS Institute was used for all multivariate analyses.

5.3   Results/Discussion

5.3.1   Illicit Drugs Spectra, Derivatized and "as-is"

The spectra of ephedrine, pseudoephedrine, methamphetamine, and methcathinone "as-is", pre-derivatization, were obtained as a reference point to compare the influence of four substituents on the absorbance spectra. The analytes were then derivatized using TFAA, BSTFA, PFBCl, and

PFBHA where appropriate. The spectra of the compounds "as-is" and derivatized are given in Figure 5.3.
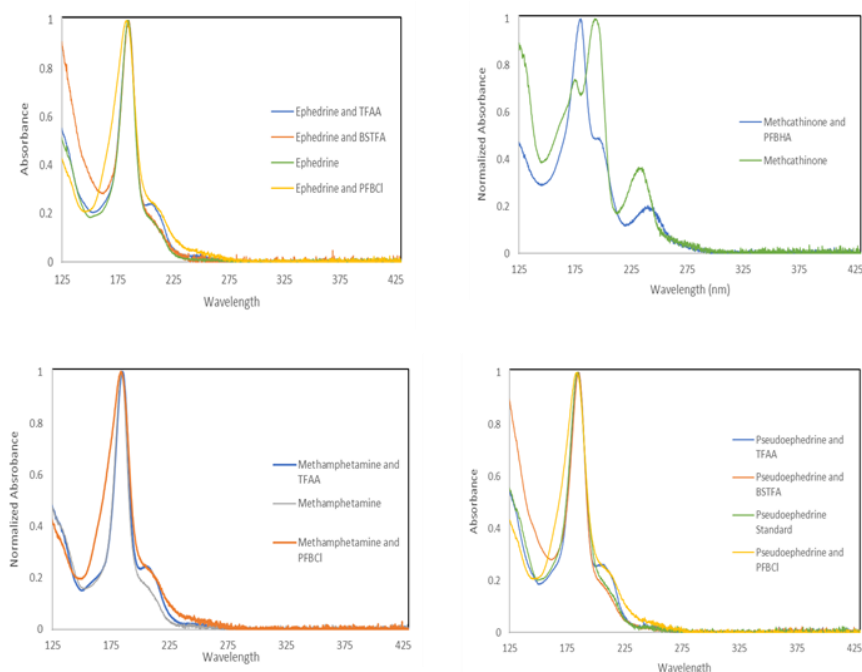
Figure 5.3 Spectra of the "as-is" and derivatized forms of ephedrine, methcathinone, methamphetamine, pseudoephedrine, and the respective derivatized forms with TFAA, BSTFA, PFBCl, and PFBHA.

Addition of trimethylsilyl (TMS) groups increased absorbance in the sigma bonding region from 125 to 175 nm relative to the peak at 185 nm. Addition of trifluoroacetyl (TFA) groups increased absorbance at 208 nm. Addition of pentafluorobenzoyl (PFBO) group increased absorbance from 150 to 250 nm. The oxime formed from methcathinone and PFBHA showed an increase in absorbance at 180 nm that became the maximum in the spectrum.

5.3.2 Limits of Detection

The methamphetamine, ephedrine, and pseudoephedrine "as-is" and derivatized were analyzed at various concentration to determine the Limits of Detection (LOD's). The LOD results for the derivatized and as-is compounds are given in Table 5.1. The LOD's in Table 5.1 indicate that fluorinated groups tend to increase absorptivity more than TMS groups. PFBO addition in

65

ephedrine and pseudoephedrine resulted in two derivatized peaks and thus decreased detectability as the calculated mass on column was split between two peaks. The lowest LOD obtained for methamphetamine was through PFBO addition, this may indicate that the highly conjugated fluorinated substituent is more absorptive than TFA groups.

Table 5.1 Limits of Detection in mass on-column for ephedrine, pseudoephedrine, and methamphetamine "as-is" and derivatized with TFAA, BSTFA, and PFBCl.

	Ephedrine	Pseudoephedrine	Methamphetamine
"as-is"	10.62 ng	13.79 ng	13.54 ng
TFAA	6.11 ng	2.06 ng	13.96 ng
BSTFA	4.81 ng	3.70 ng	N/A
PFBCl	26.437 ng	10.261 ng	4.51 ng

The sensitivities and linearities obtained from the limit of detection determination are given in Table 5.2. The larger sensitivities indicate that adding a fluorinating group increases distinction between similar chemical structures. Ephedrine and pseudoephedrine are diastereomers and their increased sensitivity after derivatization supports the use of these derivatization agents. Future work should look at other fluorinated reagents such as heptafluorobutyric anhydride.

Table 5.2 Sensitivities in mAU/ng and linearity (R^2) for the "as-is" and derivatized methamphetamine, ephedrine, and pseudoephedrine.

Drug Name	Sensitivity (mAU/ng)	R^2
Methamphetamine	14.5	0.9807
Methamphetamine-PFBO	23.1	0.9975
Methamphetamine-TFA	7.5	0.9872
Ephedrine	2.9	0.9822
Ephedrine-TFA	19.4	0.9927
Ephedrine-TMS	8.4	0.9750
Pseudoephedrine	0.5	0.8871
Pseudoephedrine-TFA	25.7	0.9882
Pseudoephedrine-TMS	27.4	0.9962

5.3.3 Chemometric Analyses

The diastereomers, theoretically the most difficult to distinguish, were chosen to model the differentiability of the VUV spectra. The principal component plot in Figure 5.4 shows differentiability of the "as-is" and derivatized forms of ephedrine and pseudoephedrine. The plot indicates that the spectra are distinguishable, something that is difficult to achieve with GC-MS. The trifluoroacetyl (TFA) substituted compounds show greater separation than the trimethylsilyl (TMS) substituted compounds.
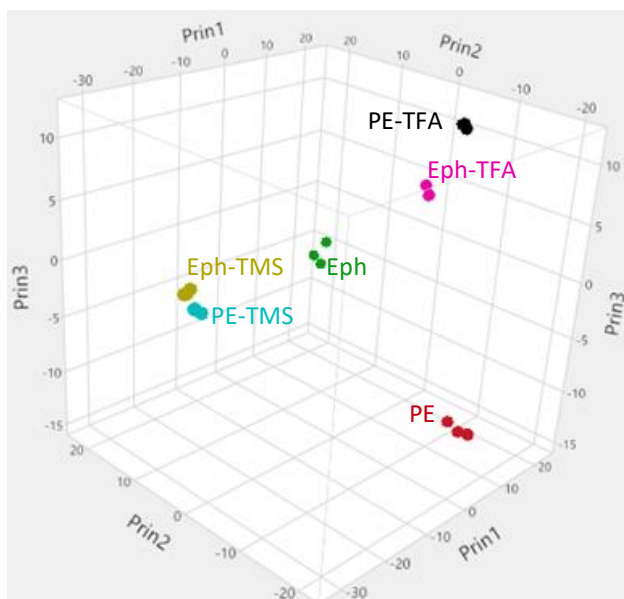
Figure 5.4 3-dimensional principal component plot of the VUV spectra of ephedrine, pseudoephedrine, and the respective TFA and TMS derivatives.

The discriminant analysis plot, shown in Figure 5.5, confirms the ability to distinguish the diastereomers and their derivatives. Each grouping is separated such that no overlap exists in the 95% confidence intervals, leading to 100% classification accuracy. The BSTFA derivatives have no overlap in confidence intervals and are distinguishable by the VUV software. As the TFA substituted points show the best separation, other fluorinated groups may show similar results.
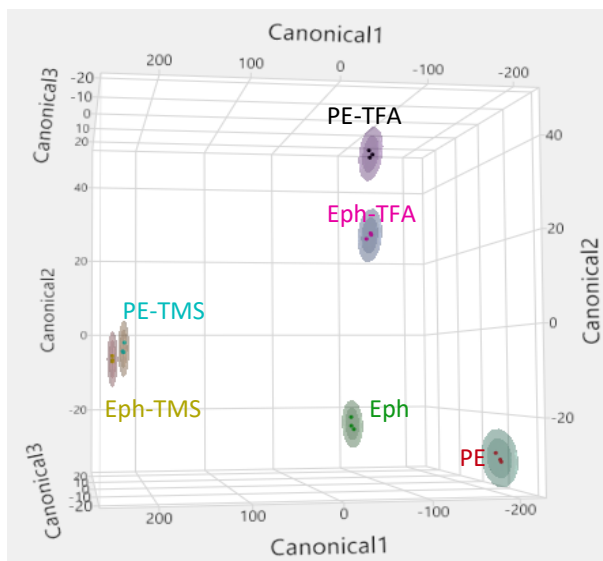
Figure 5.5 3-dimensional canonical plot of ephedrine, pseudoephedrine, and the respective TFA and TMS derivatives with 95% confidence intervals shown by rings.

5.4 Conclusions

The use of derivatization agents has lowered the limits of detection by as much as a factor of six for the compounds analyzed. Fluorinated substituents tend to increase absorptivity and should be further explored by experimentation with other reagents such as heptafluorobutyric anhydride. Future work should include different derivatization agents as well as other compounds outside the phenethylamines to investigate whether fluorinated substituents provide the greatest increase in absorptivity.

CHAPTER 6.   ANALYSIS OF FENTANYL ANALOGUES BY GAS CHROMATOGRAPHY – VACUUM UV SPECTROPHOTOMETRY AND CHEMOMETRICS

6.1   Introduction

Fentanyl and associated analogues, the main culprits in the opioid epidemic, [96] are a synthetic class of opioids first derived in 1960 [44, 97]. Post-mortem serum levels for fentanyl as low as 3 ng/mL have been seen [98]. Fentanyl analogues, remifentanil and carfentanil, were used as chemical warfare agents [99]. These factors indicate the need for a sensitive and specific method of detection. The typical method of detection in forensic chemistry, GC-MS, is known to have difficulties with some fentanyl analogues [44].

Vacuum UV (VUV) detection has shown the capability to distinguish structural isomers, cis/trans isomers, diastereomers, and isotopomers [35, 44, 47, 50, 71]. One interesting capability of VUV is the ability to deconvolute coeluting peaks, this has been shown by Reiss et al. [66] and could be used to decrease analysis times. While deconvolution is interesting, forensic analyses rely on good resolution of analyte peaks to prevent false identifications. Whether or not one chooses to use deconvolution, a reference spectrum is needed. Reference spectra of phenethylamines [49, 50, 100], synthetic cathinones [33, 49], opiates [73], synthetic cannabinoids [72], cocaine and others [101] have been reported. Buchalter et al. reported 24 fentanyl analogues analyzed by VUV and cold EI MS [44]. This work reports additional spectra of fentanyl analogues and three spectra of derivatized fentanyl analogues.

This study sought to analyze and report 17 previously unpublished spectra of fentanyl analogues by GC-VUV. Ten para-substituted chlorinated fentanyl analogues were analyzed by GC-VUV with the resultant spectra analyzed by PCA and DA. And two pairs of cis/trans isomers were analyzed to test and reinforce the capability of VUV to distinguish cis/trans-isomers as reported by Fan et al [71]. Upon chemometric analysis, GC-MS differentiated the cis/trans isomers. Two analogues and the precursor 4-ANPP were analyzed before and after derivatization with pentafluorobenzoyl chloride to study the effect of the derivatization agent on the spectra and detectability of these substances.

6.2 Materials/Methods

6.2.1 Instrumentation

An Agilent 7890A gas chromatograph with 7693 liquid autosampler and 30 m X 0.25 mm X 0.25 μm Agilent HP-5MS UI column was connected to a VUV Analytics VGA-101 Vacuum Ultraviolet spectrophotometer for VUV data collection. An Agilent 5977B mass spectral detector connected to an Agilent 7890B gas chromatograph with 30 m x 0.25 mm x 0.25 μm Agilent HP-5MS UI column and a PAL RTC 120 autosampler with liquid syringe was used for GC-MS data acquisition.

6.2.2 Materials

All vials, caps, methanol, and methylene chloride were purchased from Fisher Scientific (Fairlawn, NJ). Pentafluorobenzoyl chloride (PFBCl) was obtained from Acros Organics (China). Fentanyl analogues were obtained as part of the FAS kit from Cayman Chemical (Ann Arbor, MI) and CRM kit from Cerilliant Corporation (Round Rock, TX) made possible, in part, by the Centers for Disease Control and Prevention's design and support of Traceable Opioid Material Kits. 4-ANPP, norfentanyl, and norcarfentanil were provided in the CRM kit at 1 mg/mL in methanol. All other fentanyls were provided in the FAS kit and reconstituted per instructions in methanol. All scheduled substances were obtained under a DEA license maintained by IUPUI.

6.2.3 GC-VUV Method

GC inlet temperature 265 °C, splitless, injection volume 1 μL, flow rate of 1 mL/min of hydrogen carrier gas, oven initial temperature 150 °C for 1.0 minute ramped at 20 °C/min to 300 °C with a final temperature hold of 13.5 minutes. VUV scan rate 6 Hz, flow cell temperature 295 °C, and 0.13 PSI of nitrogen makeup gas. All analyses performed under these conditions unless specified otherwise. Carfentanil samples were analyzed using an inlet temperature of 280 °C and an initial oven temperature of 200 °C. Peak height data were collected for the limit of detection determinations with the use of a spectral filter that summed the averages of the ranges 183-193 nm and 215-230 nm.

6.2.4   GC-MS Method

GC inlet temperature 280 ^{o}C, splitless, injection volume 1 μL, flow rate of 1.5 mL/min of helium carrier gas, oven initial temperature 150 ^{o}C for 1 minute ramped at 20 ^{o}C/min to 290 ^{o}C with a final temperature hold of 10 minutes. MS transfer line temperature 300 ^{o}C, mass scan range 40 to 500 Th, solvent delay 1.5 min, tuned using Etune.

6.2.5   Chemometrics

All multivariate analyses were completed using JMP 13 by SAS Institute. All spectra were baseline subtracted and normalized to the square root of sum of squares of all wavelengths prior to analysis. All spectra were truncated at 330 nm for PCA since no sample absorbed at longer wavelengths. The linear discriminant analyses were performed using several principal components chosen from the PCA based on the generated Scree plots. All DA were performed with a one-third test set.

6.3   Results/Discussion

6.3.1   Spectra and Chemometric Analysis of Cis/Trans Fentanyl Analogues

A pair of methyl fentanyl standard solutions and methyl thiofentanyl standard solutions were analyzed in triplicate. The spectra obtained are given in Figure 6.1. The methyl fentanyl cis/trans pair differ the most for wavelengths shorter than 175 nm and the methyl thiofentanyl pair differ the most from 180 to 185 nm and the region from 130 to 145 nm. The subtle differences are enough to differentiate the pairs as in previous work[50] this is highlighted by the statistical analyses that follow in Table 6.1 and Figure 6.2.
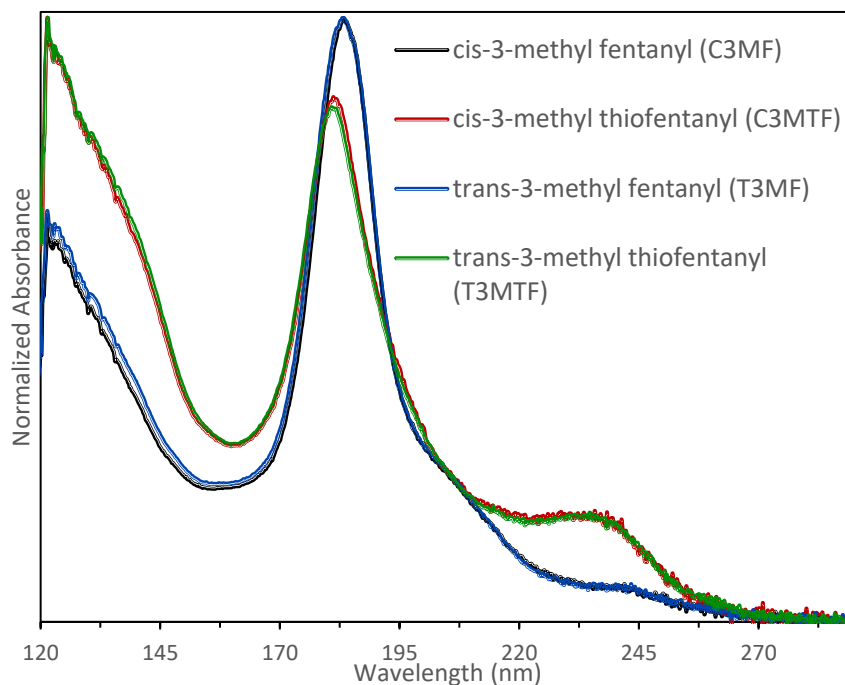
Figure 6.1 Overlaid spectra of the cis/trans pairs of 3-methyl fentanyl and 3-methyl thiofentanyl.

The spectra from Figure 6.1 were analyzed by principal component analysis (PCA) and discriminant analysis (DA). The first three principal components, encompassing 80.1% of the variability, were chosen for DA based on the obtained Scree plot. The ability of the PCA to group the analytes properly and subsequent DA to correctly classify the data with 100% accuracy including a one-third test set indicates the ability to distinguish between the spectra. The results of the analyses are given in plots in Figure 6.2. The methyl fentanyl pair was separated from the methyl thiofentanyl pair by Component 1 and Canonical 1, the cis and trans pairs were separated by Component 2 and Canonical 2 in the PCA and DA, respectively. There was one data point of cis-3-methyl thiofentanyl along Component 2 that indicates an outlier, this did not significantly affect the DA results.

Figure 6.2 A) 2-dimensional PCA scores plot of the first and second principal components (% of variance = 74%) demonstrating the distribution of the compounds based on their corresponding VUV spectra, and B) 2-dimensional canonical plot demonstrating separation of the four classes.

Sums of squares residuals (SSR) and correlation coefficient (COR) analyses of the spectra in Figure 6.1 was conducted as in prior work[73] to give a measure of the similarity or dissimilarity of the spectra. The data obtained is given in Table 6.1. The *cis*-3-methyl thiofentanyl SSR and Cor were lower and higher, respectively, for the *trans*-3-methyl thiofentanyl which would normally indicate a high degree of similarity, though the *trans*-3-methyl thiofentanyl does not show this same pattern. When taken into consideration with the principle component analysis, an outlier in the *cis*-3-methyl thiofentanyl data likely caused the values for COR and SSR against itself to be respectively lower and higher than expected.

Table 6.1 Matrix of average correlation coefficients (COR) and sums of square residuals (SSR) for *cis*-3-methyl fentanyl (C3MF), *cis*-3-methyl thiofentanyl (C3MTF), *trans*-3-methyl fentanyl (T3MF), and *trans*-3-methyl thiofentanyl (T3MTF). Averages taken from three by three matrices of triplicates. COR are shown in blue on the left of each cell whereas SSR are shown in red on the right of each cell.

COR \ SSR	C3MF	C3MTF	T3MF	T3MTF
C3MF	0.0006171 / 0.9996	0.08005	0.001672	0.08725
C3MTF	0.9438	0.002650 / 0.9981	0.071034	0.002014
T3MF	0.9989	0.9510	0.0008921 / 0.9994	0.076110
T3MTF	0.9395	0.9985	0.9466	0.0009486 / 0.9993

6.3.2 Spectra and Chemometric Analysis of Chlorinated Fentanyls

Lagesson et al. reported the effect of halogens on straight chain compounds in the region from 168-330 nm [91]. The peaks common to chlorinated compounds below 168 nm can be seen in the spectra of 4-chloroaniline, [47] chlorobenzene and trichlorobenzene, [74] chloroform, [102] and dichlorobenzenes [32]. Ten standard solutions of chlorinated fentanyl analogues were analyzed in triplicate to further explore this absorbance trend. All spectra showed a maximum absorbance around 185 nm. The spectra in Figure 6.3 show peaks common to chlorinated compounds at 136 nm and 145 nm.
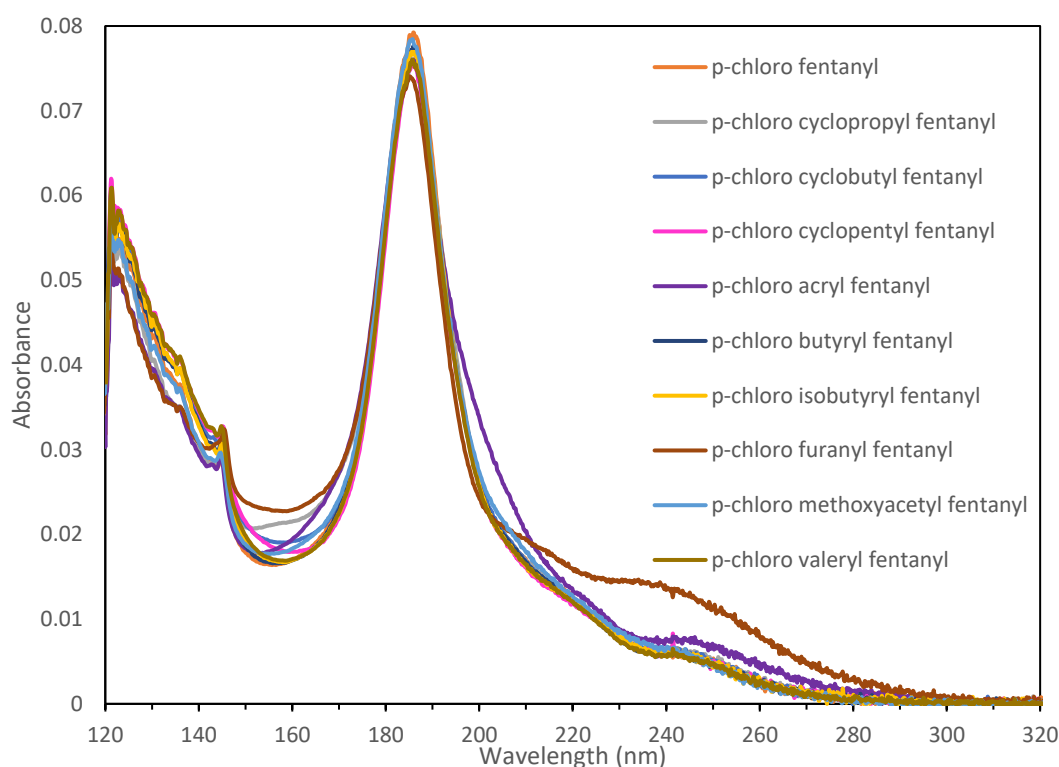
Figure 6.3 Overlaid VUV spectra of the ten chlorinated fentanyl analogues.

The spectra in Figure 6.3 were analyzed by PCA then by DA. Based on the obtained Scree plot the first five principal components, covering 91.5% of the variance, were input into DA and achieved 100% classification accuracy including a one-third test set. The plots produced by the chemometric analyses are given in Figure 6.4 A and B. The perfect classification accuracy and separated groupings in the PCA indicate that the spectra, while similar, are differentiable.

Figure 6.4 A) 2-dimensional PCA scores plot of the first and second principal components (% of variance = 78%) demonstrating the distribution of the compounds based on their corresponding VUV spectra, and B) 2-dimensional canonical plot showing the separation of the ten classes.

6.3.3 GC-MS Analysis of Fentanyl Analogues

The fentanyl analogues analyzed in section 6.3.1 were analyzed by GC-MS in triplicate. The molecular ions of *cis*-3-methyl fentanyl and *cis*-3-methyl thiofentanyl were observed in low abundance. The mass spectra of the *cis*/*trans* fentanyls are given in Figures 6.5-6.8.
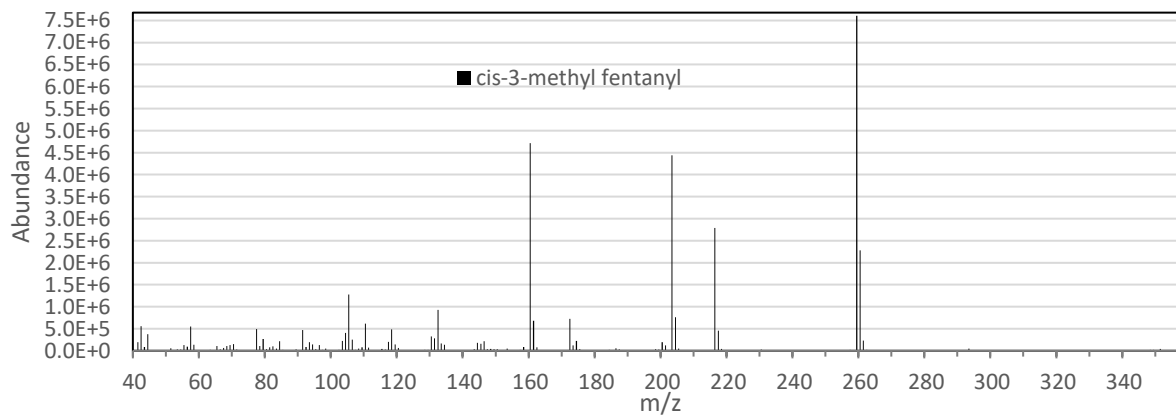
Figure 6.5 Mass spectrum of *cis*-3-methyl fentanyl.
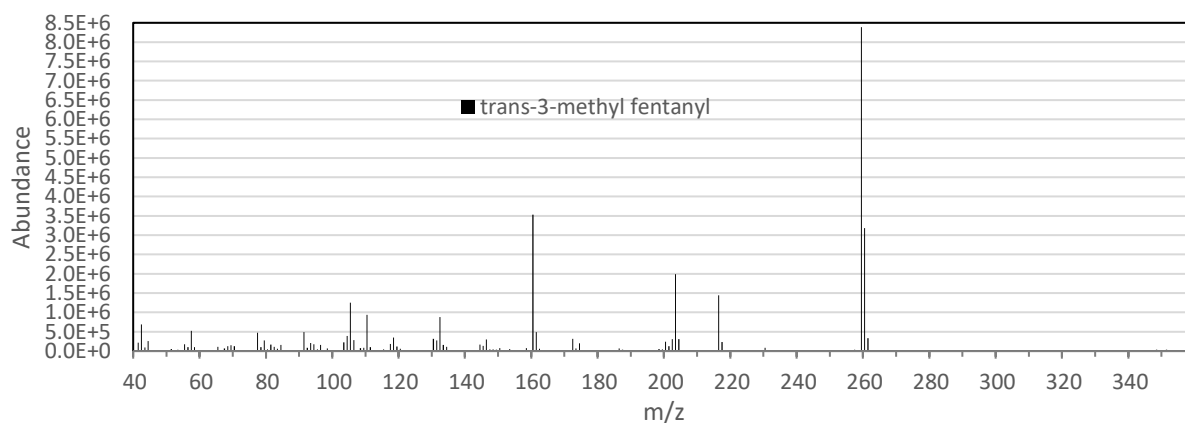
Figure 6.6 Mass spectrum of *trans*-3-methyl fentanyl.
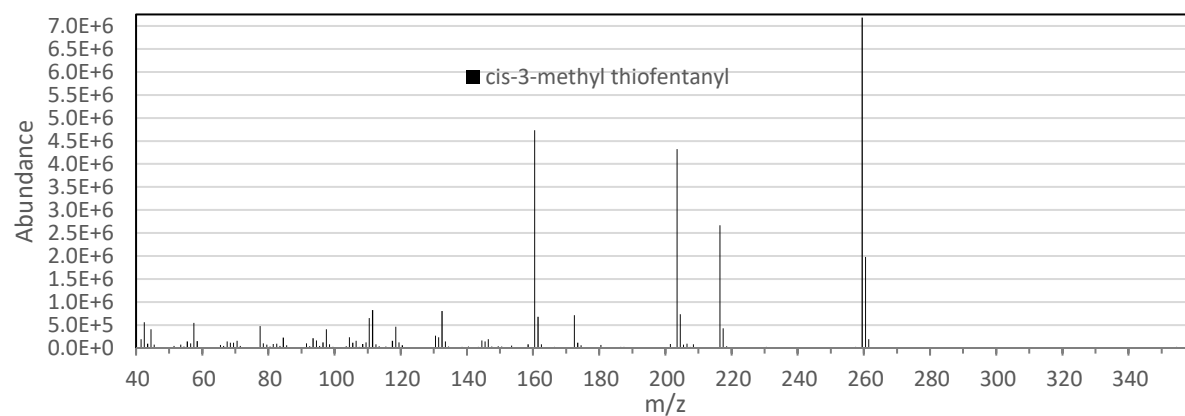
Figure 6.7 Mass spectrum of *cis*-3-methyl thiofentanyl.
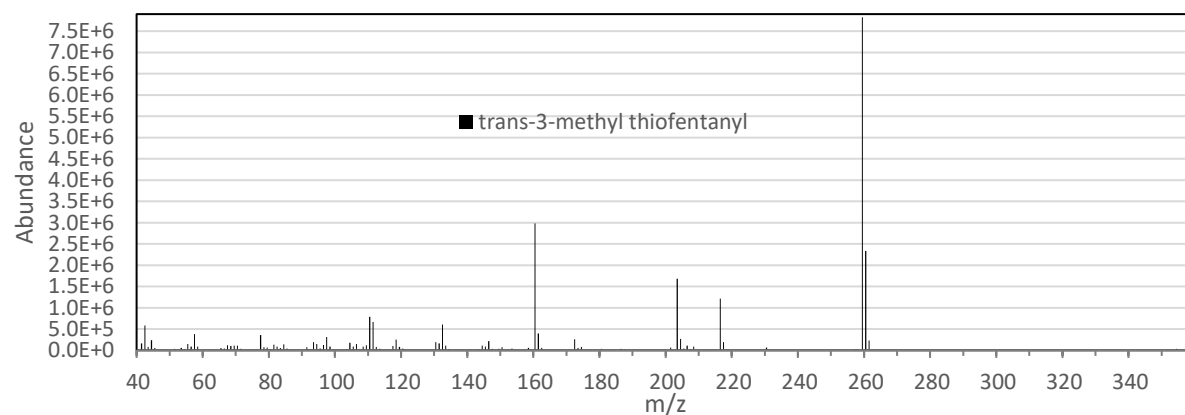
Figure 6.8 Mass spectrum of *trans*-3-methyl thiofentanyl.

The fentanyl analogues analyzed in section 6.3.2 were analyzed by GC-MS in triplicate. The molecular ions of *p*-chloro fentanyl, *p*-chloro cyclopropyl fentanyl, *p*-chloro cyclobutyl fentanyl, *p*-chloro butyryl fentanyl, *p*-chloro isobutyryl fentanyl, and *p*-chloro acrylfentanyl were observed in low abundance. The mass spectra of the chlorinated fentanyls are given in Figures 6.9-6.18.
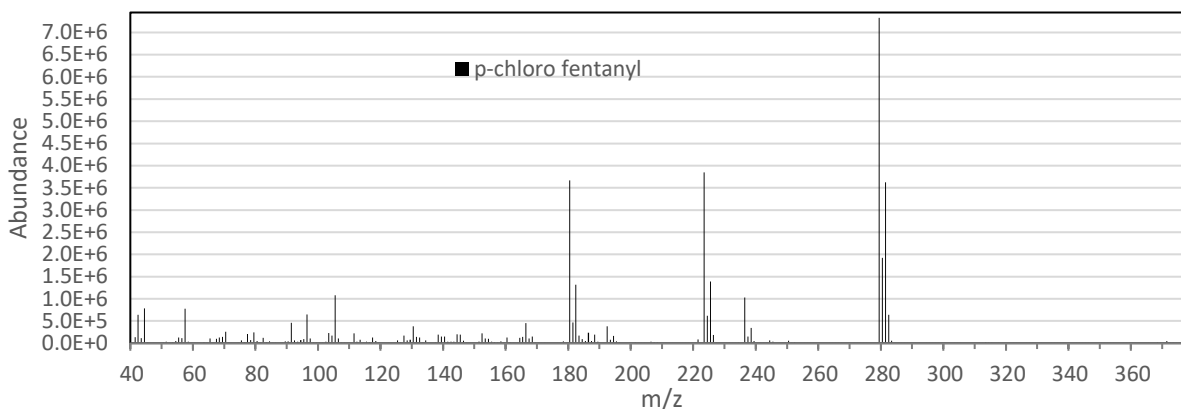
Figure 6.9 Mass spectrum of *p*-chloro fentanyl.
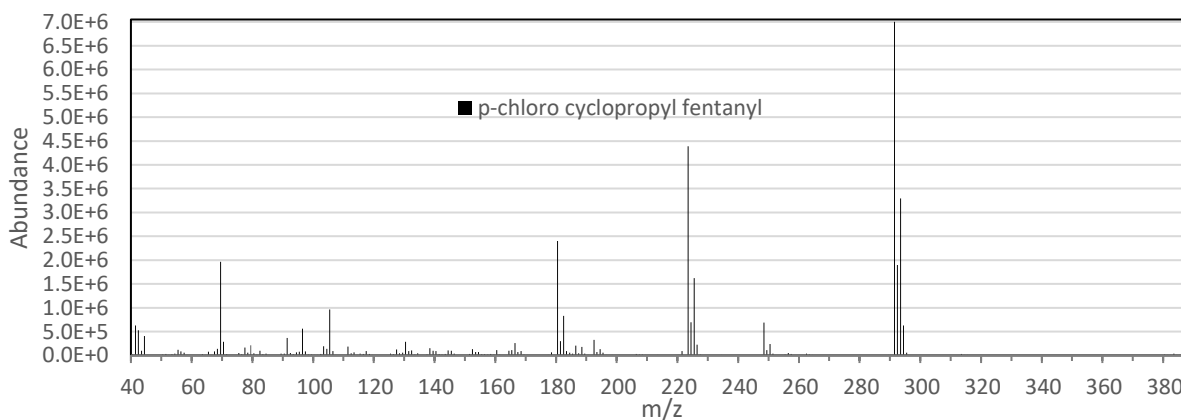
Figure 6.10 Mass spectrum of *p*-chloro cyclopropyl fentanyl.
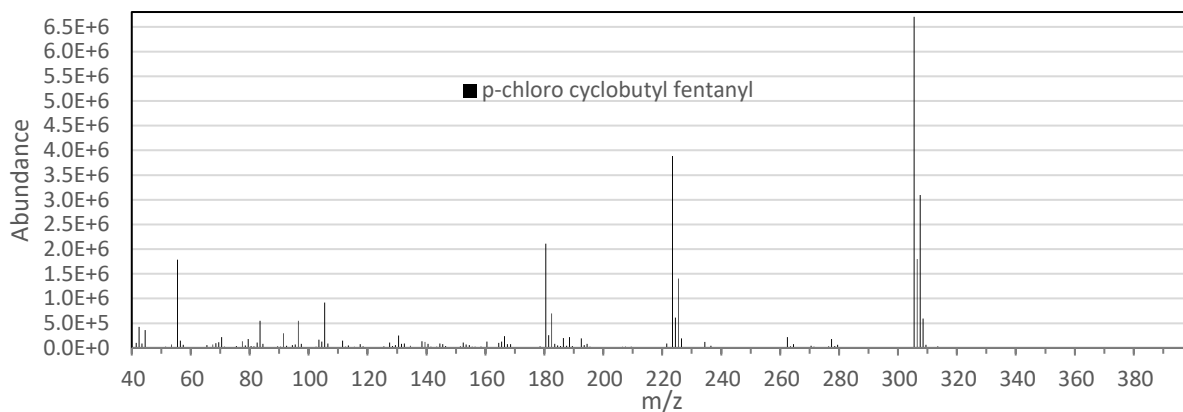
Figure 6.11 Mass spectrum of *p*-chloro cyclobutyl fentanyl.
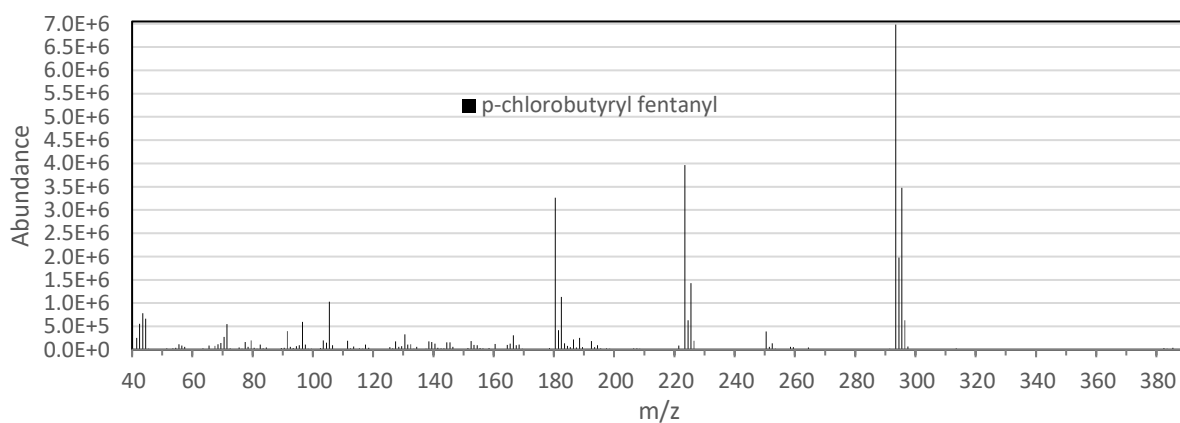
Figure 6.12 Mass spectrum of *p*-chlorobutyryl fentanyl.
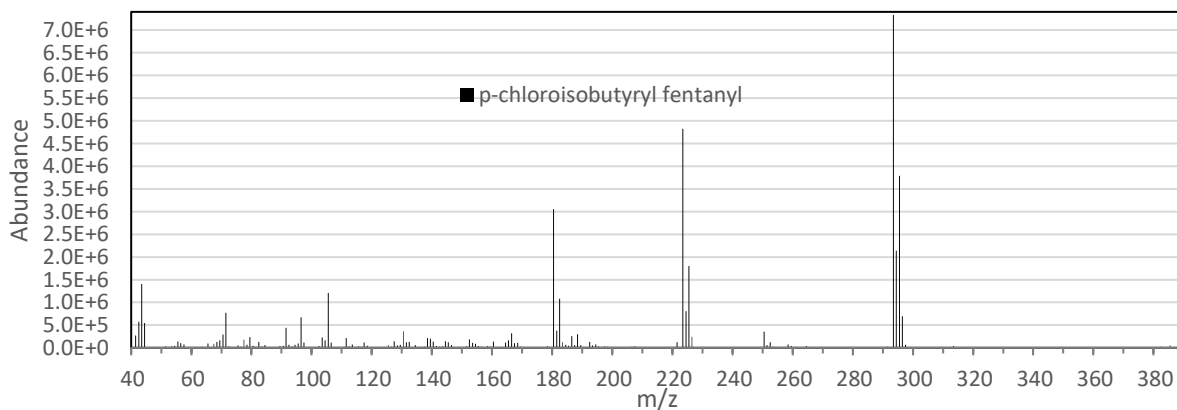
Figure 6.13 Mass spectrum of *p*-chloroisobutyryl fentanyl.
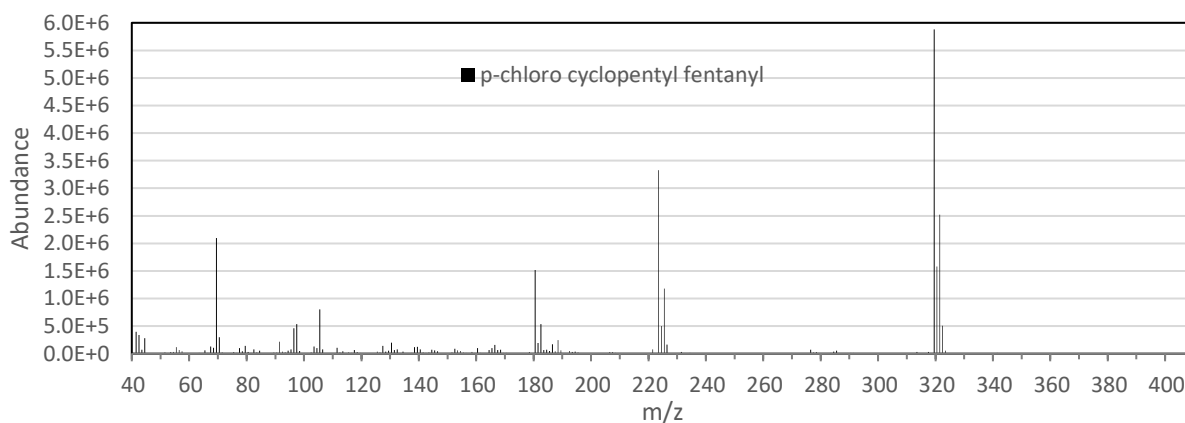
Figure 6.14 Mass spectrum of *p*-chloro cyclopentyl fentanyl.
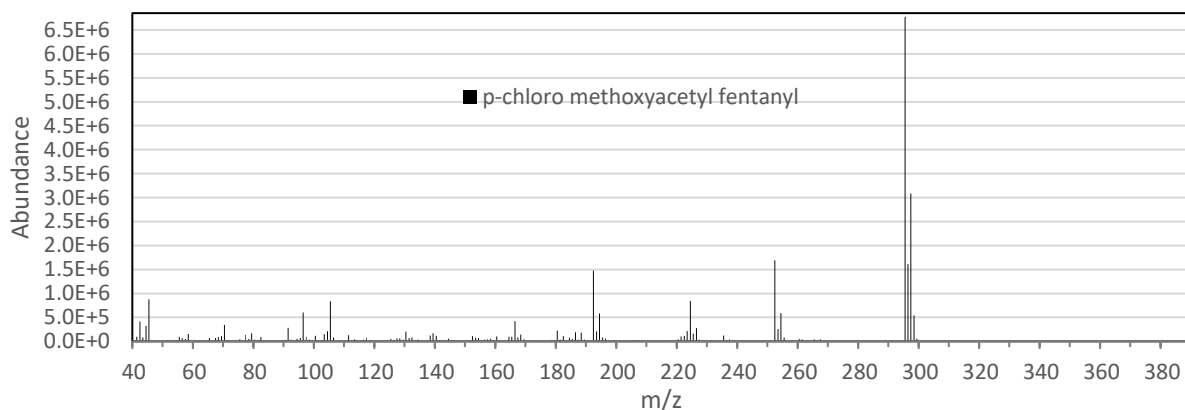
Figure 6.15 Mass spectrum of *p*-chloro methoxyacetyl fentanyl.
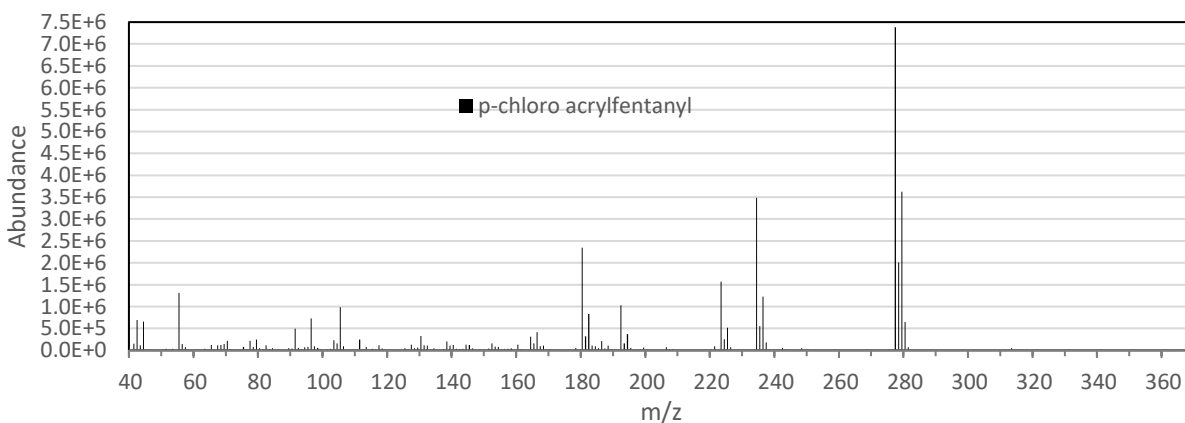
Figure 6.16 Mass spectrum of *p*-chloro acrylfentanyl.
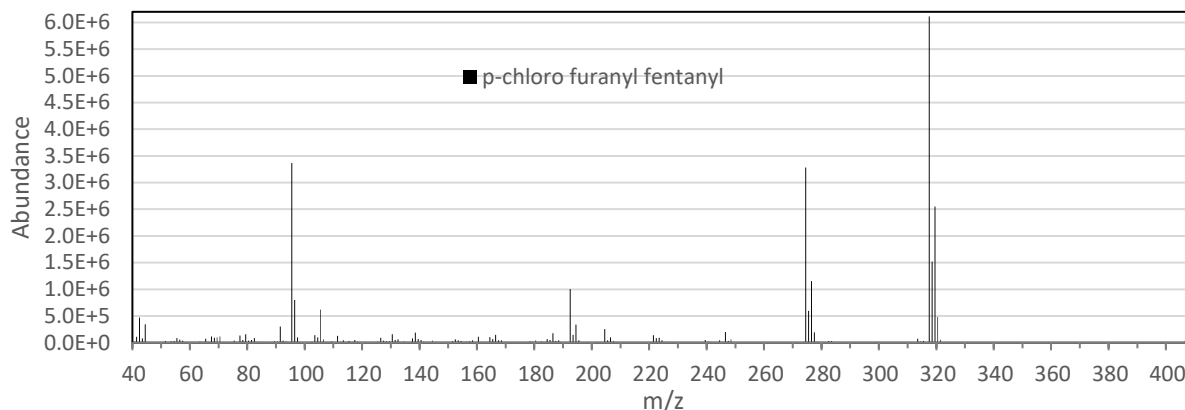
Figure 6.17 Mass spectrum of *p*-chloro furanyl fentanyl.
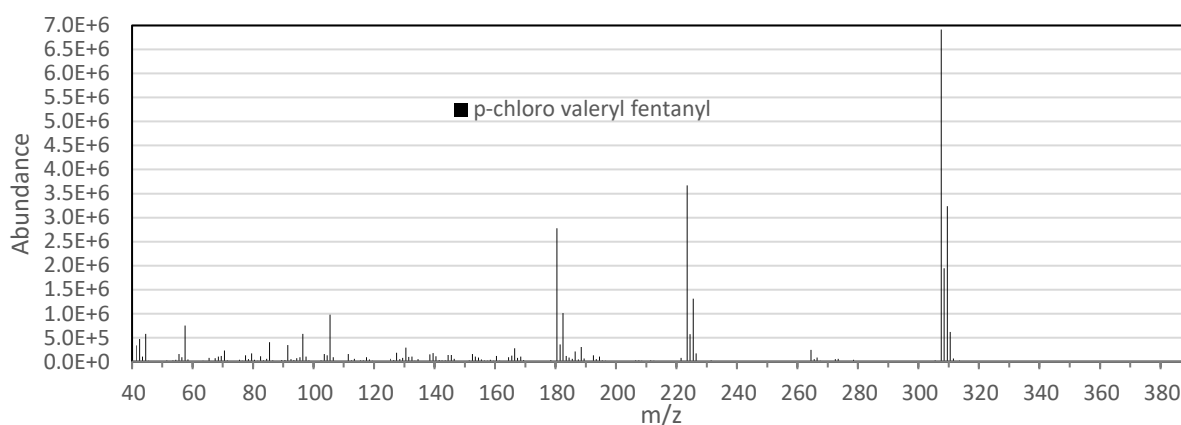
Figure 6.18 Mass spectrum of *p*-chloro valeryl fentanyl.

The mass spectra for the chlorinated fentanyls were analyzed by principle component analysis. The first 8 principal components, covering 84.7% of the variance, were analyzed by DA resulting in a classification accuracy of 96.7% using a one-third test set. The misclassified sample of *p*-chloro isobutyryl fentanyl was said to be *p*-chloro butyryl fentanyl. The results from the PCA and DA are shown in Figure 6.19.
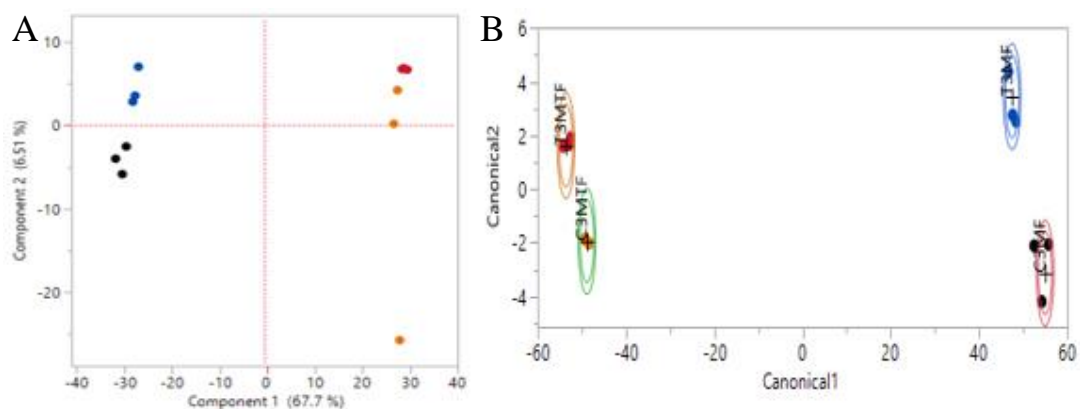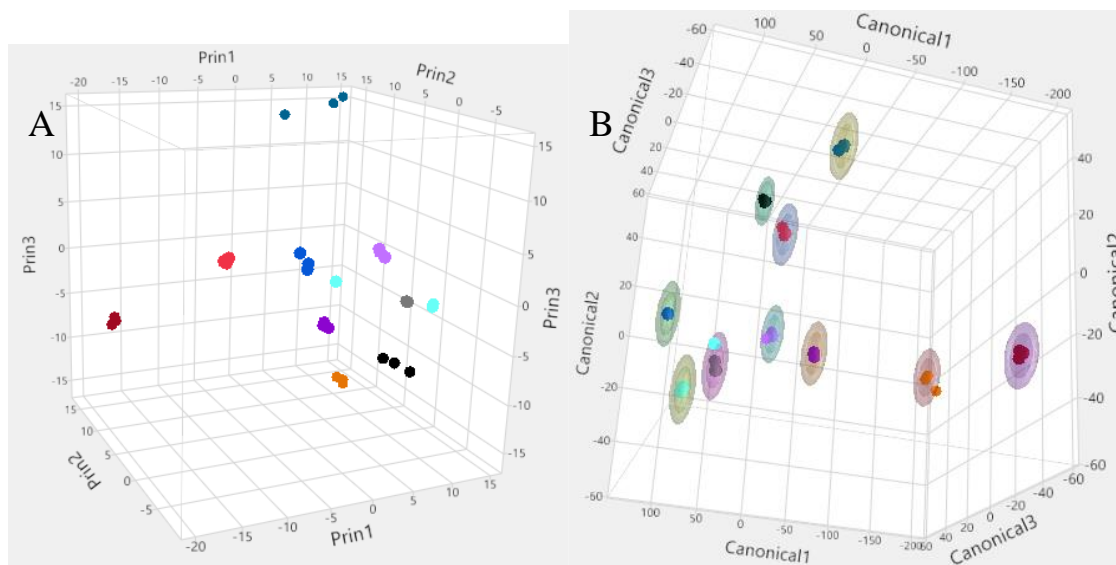
Figure 6.19 A) 3-dimensional PCA scores plot of the first three principal components (% of variance = 72%) demonstrating the distribution of the chlorinated fentanyls based on their corresponding mass spectra, and B) 3-dimensional canonical plot showing the ten classes in canonical space with rings indicating 95% confidence intervals.

The mass spectra of the cis/trans methyl fentanyl pairs were analyzed by PCA. Four principal components, covering 72.3% of the variance, resulted in a DA classification accuracy of 100% using a one-third test set. The results are shown in Figure 6.20.
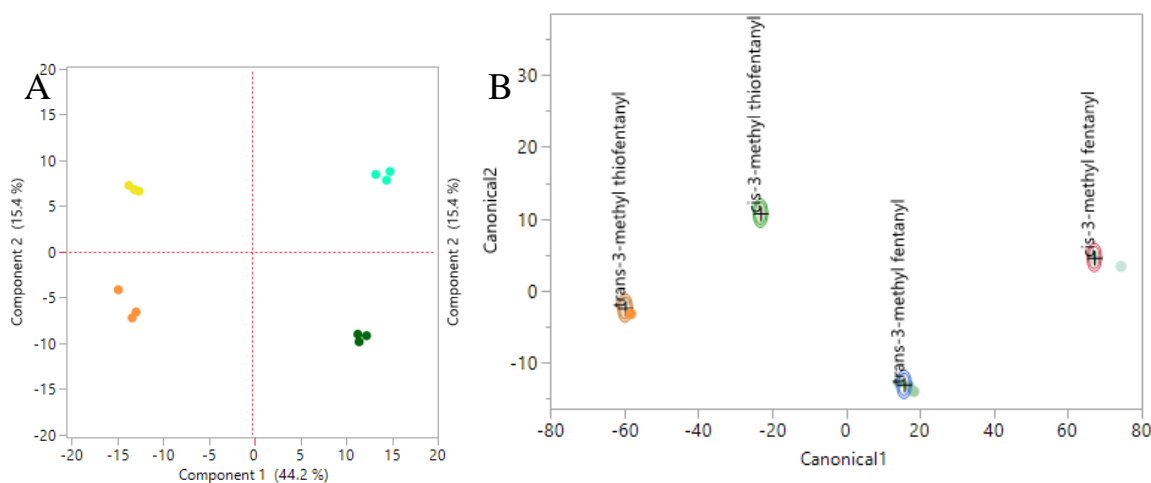
Figure 6.20 A) 2-dimensional PCA scores plot of the first and second principal components (% of variance = 59.6%) demonstrating the distribution of the cis/trans methyl fentanyls based on their corresponding mass spectra, and B) 2-dimensional canonical plot showing the four classes with rings indicating 95% confidence intervals.

6.3.4 Derivatization of norfentanyls, spectra, chemometrics, and changes in LOD

Norfentanyl, 4-ANPP, and norcarfentanil were analyzed as standard solutions in triplicate "as-is" and derivatized by pentafluorobenzoyl chloride in a dilution series to obtain spectra, LODs and sensitivities which are given in Figure 6.21. The pre-derivatization main absorbance peak was from 160-230 nm for norfentanyl and 4-ANPP, and 120-160 nm for norcarfentanil. Upon derivatization the main absorbance peak was 150-250 nm for all three analytes. The limits of detection for each analyte improved upon addition of the pentafluorobenzoyl group at the secondary amine. The least improvement was seen for 4-ANPP which went from 27 ng on-column to 11 ng on-column. The greatest improvement was seen for norcarfentanil which went from 28 ng on-column to 0.67 ng on-column. These numbers approach the amount of fentanyl in a milliliter of urine [82]. Pre-concentration techniques, such as solid phase microextraction (SPME), would be recommended to further decrease LODs and for non-derivatizable fentanyls.
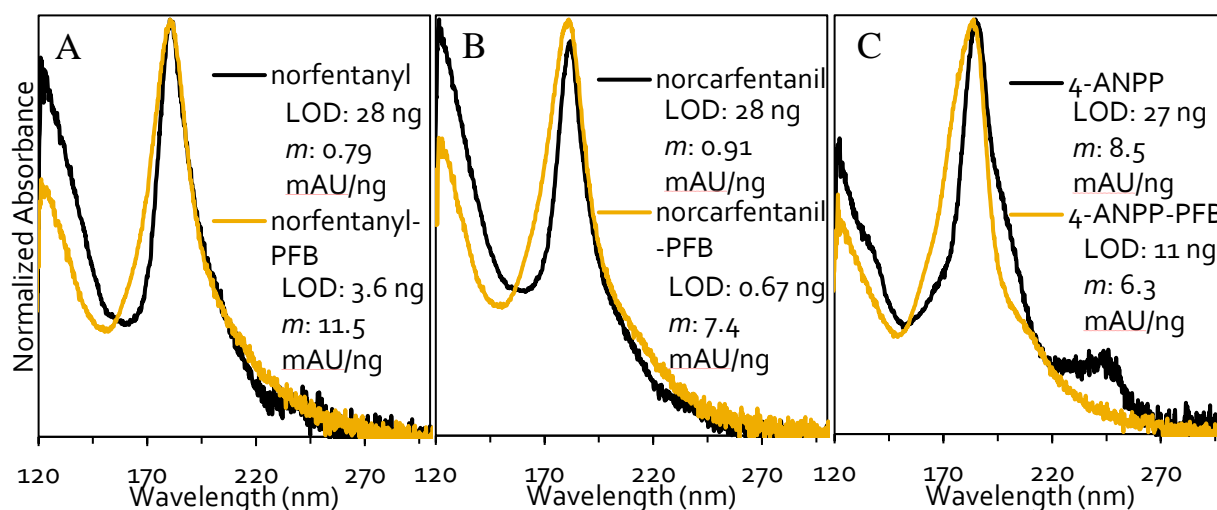
Figure 6.21 Overlaid spectra, limits of detection (LODs) in mass on-column, and sensitivities (*m*) of A) norfentanyl and the pentafluorobenzoyl (PFB) derivative, B) norcarfentanil and the PFB derivative, and C) 4-ANPP and the PFB derivative.

The similarities in the derivatized spectra prompted further analysis by chemometrics, the results of which are given in Figure 6.22. PCA grouped the data mostly by analyte. The DA achieved 100% classification accuracy using the first five principal components as determined through Scree plot analysis. Despite appearing similar, the spectra are differentiable.
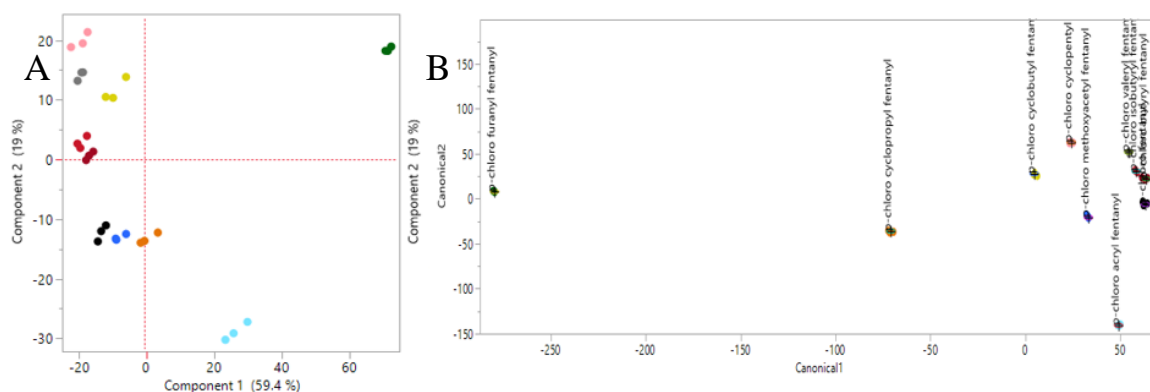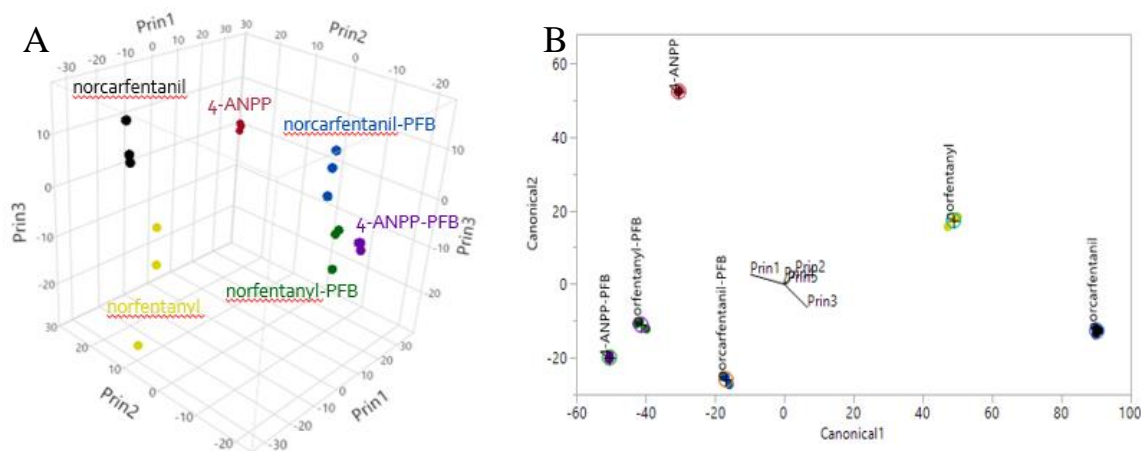
Figure 6.22 A) 3-dimensional PCA scores plot of the first three principal components (% of variance = 83%) demonstrating the distribution of the chlorinated fentanyls based on their corresponding mass spectra, and B) 2-dimensional canonical plot showing the six classes with rings indicating 95% confidence intervals.

Each of the six compounds, 4-ANPP, norfentanyl, norcarfentanil, and the PFB derivatives were analyzed by GC-MS. The obtained mass spectra are given in Figures 6.23-6.28.
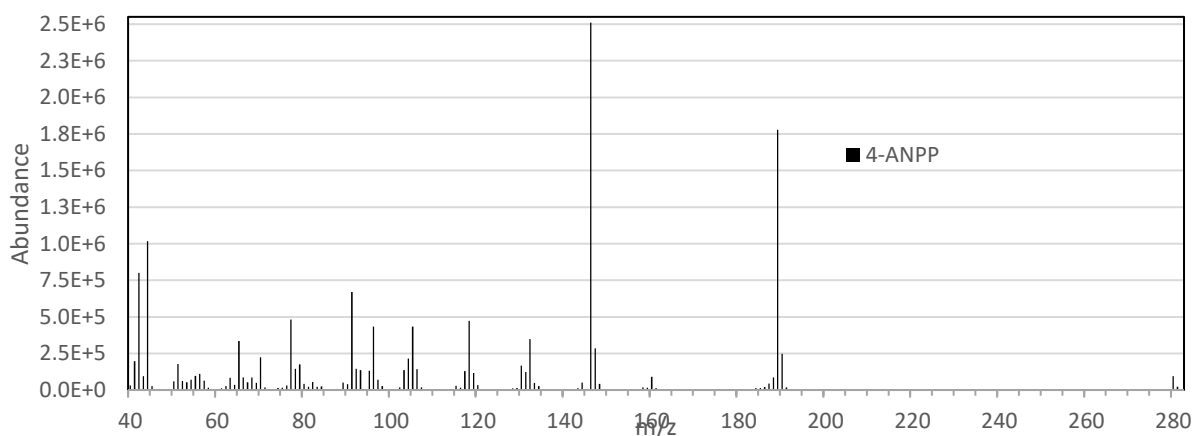
Figure 6.23 Mass spectrum of 4-ANPP.
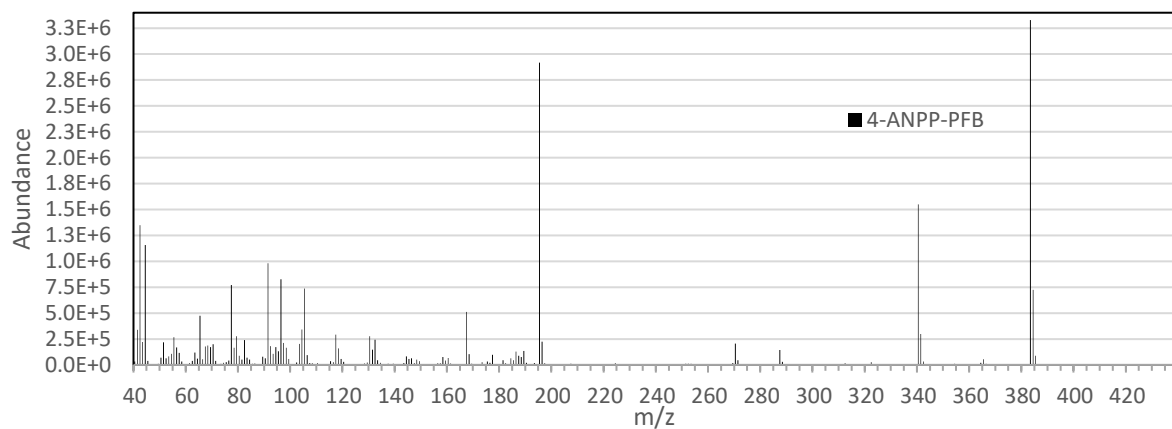
Figure 6.24 Mass spectrum of 4-ANPP-PFB.
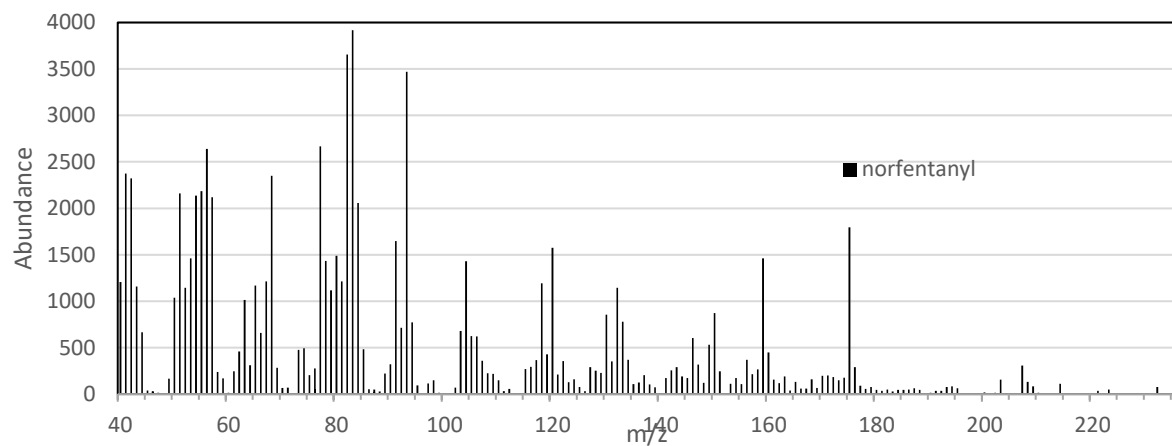
Figure 6.25 Mass spectrum of norfentanyl.
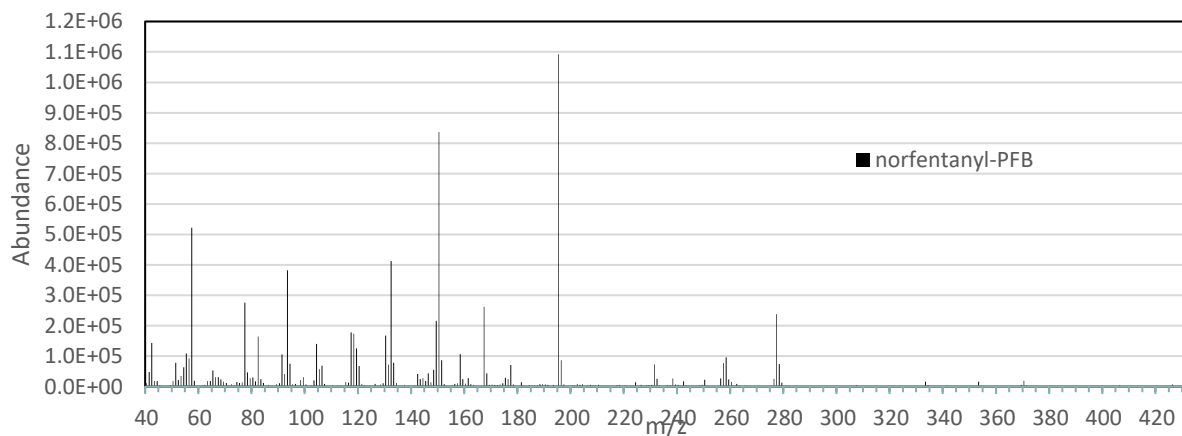
Figure 6.26 Mass spectrum of norfentanyl-PFB.
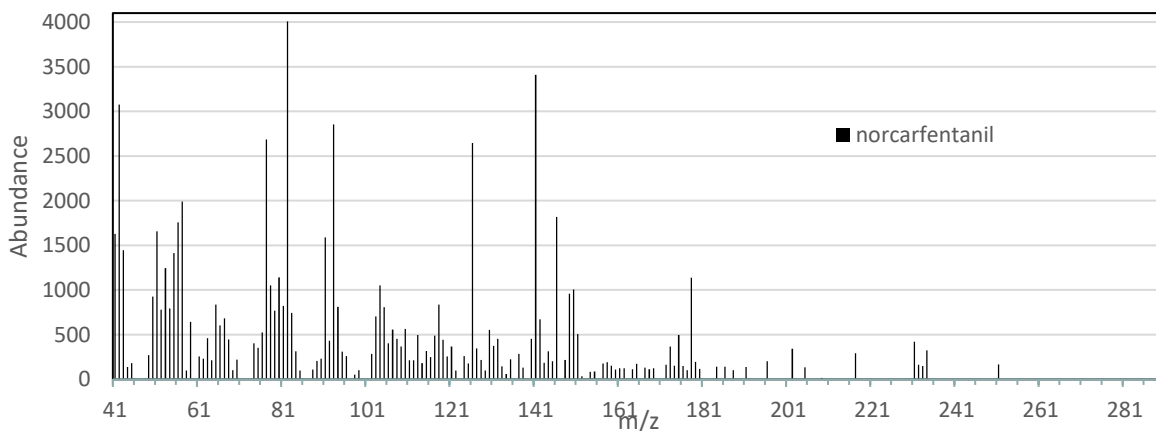
Figure 6.27 Mass spectrum of norcarfentanil.
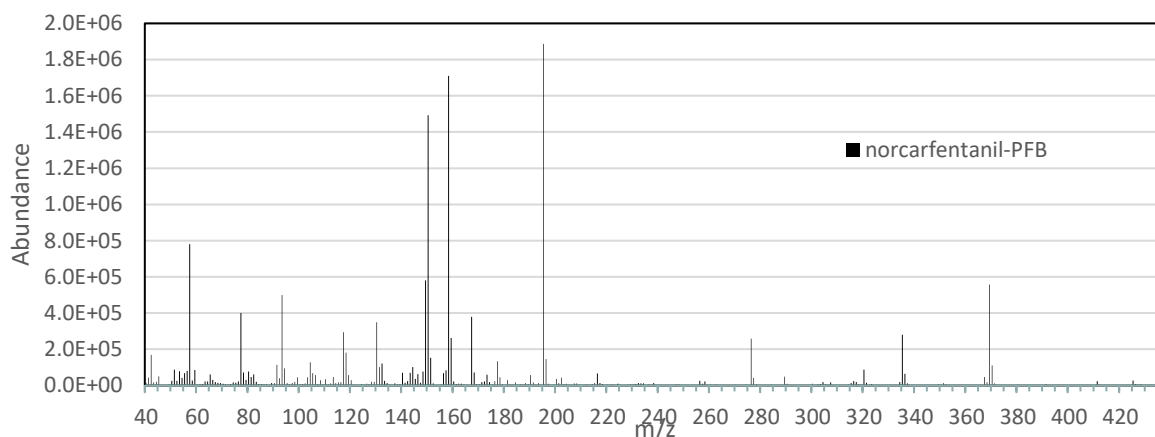
Figure 6.28 Mass spectrum of norcarfentanil-PFB.

6.4 Conclusions

Several spectra of fentanyl analogues have been reported and analyzed by chemometric methods. While this work brings the total fentanyl analogues to over 40, there are at least 70 other known fentanyl analogues that should be reported in future work. Three fentanyl analogues that contained active hydrogens were derivatized and showed lower LODs upon derivatization. Future work should strive to find an optimum derivatization agent or one that can derivatize amides to push the LODs of more fentanyls to the trace levels needed for fentanyl analogues in toxicological samples.

6.5 Acknowledgements

CHAPTER 7. FUTURE WORK

7.1 GC-VUV Analysis of Benzodiazepines:

Benzodiazepines, a somewhat less common class of drugs of abuse seen more in certain jurisdictions than others, are muscle relaxants and anti-convulsants with amnesic properties that are sometimes used in drug facilitated sexual assaults (DFSA). Detecting the compounds used in DFSA requires the ability to detect trace amounts of the substance(s) in either toxicological samples or residues on drinkware. The reason that analysis of benzodiazepines would be interesting for VUV purposes is that they largely contain the halogens chlorine and fluorine. Halogens can cause distinct absorbance bands in the far-UV (FUV), such as the 144 nm peak common to chlorinated compounds shown in the spectra of fentanyls in Figure 7.1 below. This highlights the region of interest from Figure 6.3 and in the spectra of lorazepam in Figure 4.1.
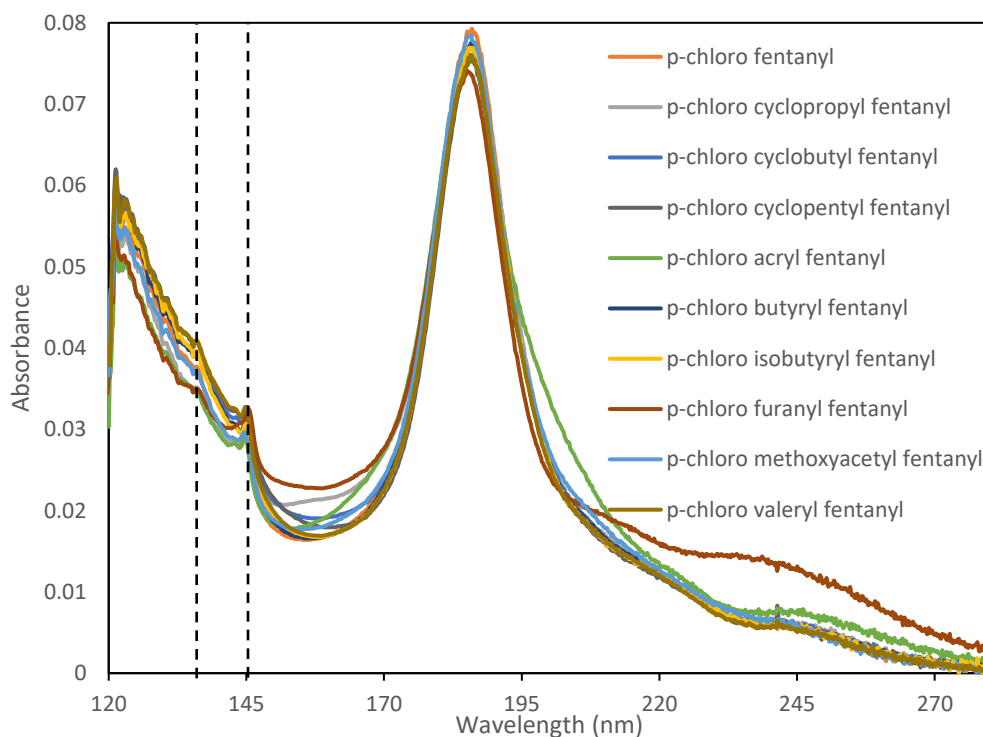
Figure 7.1 Spectra of ten chlorinated fentanyl analogues with peaks most likely caused by the chlorinated group indicated by dashed lines.

7.2 Determination of Optimum VUV Derivatization Agent

Expanding on Chapter 5, where it was shown that derivatization can lower limits of detection, various derivatization agents and host compounds should be analyzed towards finding an "ideal" derivatization agent for VUV detection. The highly electronegative and conjugated substituents used in Chapter 5 provide a starting point for this investigation since it was seen that these groups provided greater detectability than addition of trimethylsilyl groups and addition of alkyl chains would not provide any additional benefit. The effect of derivatization is further seen in the improved limits of detection found in Chapter 6 section 6.3.4 on derivatization of norfentanyls and 4-ANPP with pentafluorobenzoyl chloride. Reagents previously used for electron capture detection (ECD), such as heptafluorobutyric anhydride, may be of interest. Another important direction is to see if ionization efficiency is related to absorptivity since fluorinated compounds tend to ionize well and absorb well in the FUV.

7.3 Coupling GC-VUV with MS

Combining VUV in-line with MS has many benefits which have been well presented by Anthony et al. [32] and Buchalter et al. [44]. Since VUV is non-destructive and orthogonal to MS, combining the two could create a new "gold standard" for forensic chemistry that provides structural information from the MS with spectral information from the VUV while also obtaining relative retention times. The largest critique against VUV has been the relatively high detection limits compared to mass spectrometry. By adding an MS after the VUV without any splitting or dilution, it would allow for the lower detection limits provided by MS without having to analyze a sample multiple times.

Connecting the VGA-101 to an MSD could be performed with little difficulty by orienting the MS transfer line to be in close proximity to the outlet of the VUV flow-cell, not the exhaust outlet, and using a deactivated metal capillary from the flow-cell into the MSD source. Using a metal capillary and placing the heated transfer line in close proximity to the flow cell should minimize cold spots and allow for little to no condensation in the transfer line especially since the molecules would be approaching supersonic velocities going into the MS. Controlling the systems would require the use of an appropriate GC-MSD control software and the VUV software, both detectors can be configured to begin acquisition upon signal from the GC via a split rs-232 cable.

The vacuum used for the MSD would eliminate the need for a make-up gas in the flow-cell and the valves on the VUV can be set to remain closed, if the valves do not seal appropriately a plug can be screwed into the make-up gas inlets for the cell. Work by Anthony et al. has been done in attempting to combine GC-VUV and MS in-line, though the connection was sub-optimal and involved a rather long transfer line of 76 cm and a lower than recommended 210 °C transfer line temperature [32]. The proposed setup would allow for a transfer line of less than half that length which would limit any peak broadening and would allow for transfer line temperatures more in line with column limits, i.e. 300 °C. Further reduction of peak broadening in the transfer line may be achieved by using a steel capillary column. An in-line configuration eliminates the complexity of the currently recommended split configuration such as that used by the Lurie group [44].

7.4   Diode Array VUV for Alcohols

As has been mentioned, currently VUV has higher than desired detection limits. One possible method for improving detection limits would be to use a different detection method. The back-illuminated thin-film CCD currently used for VUV is not as sensitive as a photodiode array detector, but it does capture data for more wavelengths at once as the trade-off. In speaking with an instrument manufacturer, a new PDA-VUV using two or three wavelength ranges in a more sensitive detector for targeted compound detection is in development. Using the ratio of the absorbance at two/three windows should be specific within a particular class of compounds such as alcohols and very small polar molecules.

An example of a viable application would be to blood alcohol concentration (BAC) determination. The GC-PDA-VUV would be more specific than the currently common GC-FID and would allow for a one column system which is simpler than the current two-column method. Quantitation using the PDA-VUV would be facile since the Beer-Lambert Law is the basis for quantitative analysis using any UV absorption technique. For BAC analyses it would be crucial to differentiate water, acetone, methanol, and ethanol, all of which exhibit distinct absorption spectra in the VUV as seen in Figure 7.2.
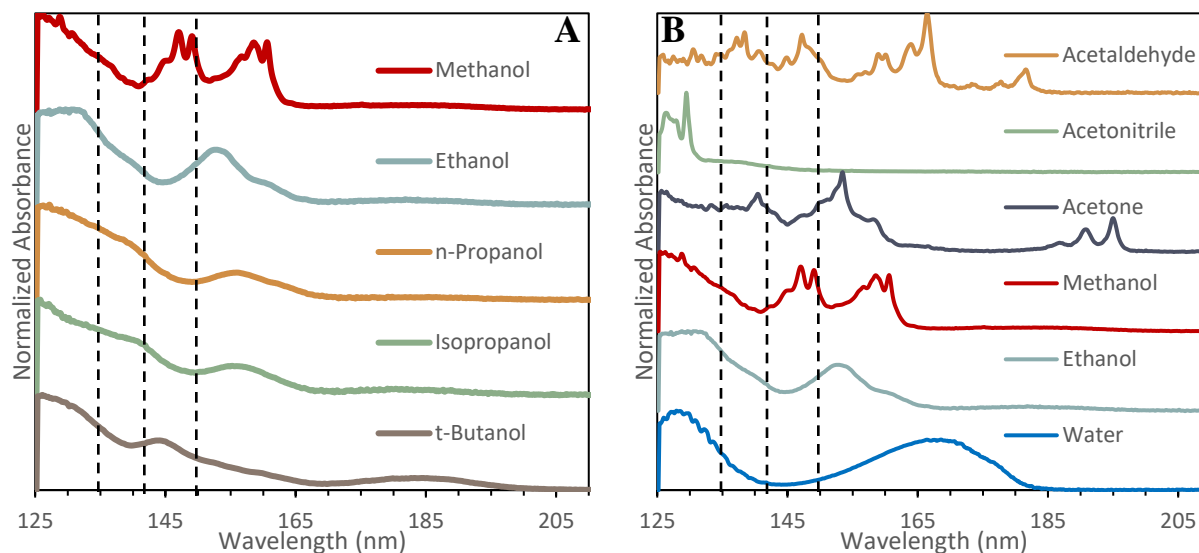
Figure 7.2 Spectra with regions at 135, 142, and 150 nm indicated with dashed lines of A) methanol, ethanol, *n*-propanol, isopropanol, and *t*-butanol and B) acetaldehyde, acetonitrile, acetone, methanol, ethanol, and water.

While the full spectra would not be obtained, regions such as those at 135, 142, and 150 nm would result in a response peak ratio with which each could be distinguished. These wavelengths are indicated by the dashed lines in Figure 7.2. For an example, the average response was taken from the data in Figure 7.2 at these wavelengths with a window of ± 1 nm and the absorbance ratios determined. The ratios of the three values with the lower wavelength as the numerator are shown in Table 7.1.

Table 7.1 Ratios of the absorbance of acetonitrile, *t*-butanol, isopropanol, *n*-propanol, ethanol, methanol, acetone, acetaldehyde, and water at 135, 142, and 150 nm ± 1 nm.

Compound	Acetonitrile	*t*-Butanol	Isopropanol	*n*-Propanol	Ethanol	Methanol	Acetone	Acetaldehyde	Water
135/150 nm	6.141	1.966	2.833	3.824	1.642	1.057	0.915	1.178	3.327
135/142 nm	1.830	1.314	1.352	1.680	2.318	1.846	1.016	1.216	5.299
142/150 nm	3.356	1.495	2.096	2.276	0.708	0.573	0.901	0.969	0.628

7.5   Deposition/Solid Phase VUV Detector

Perhaps the most ambitious proposition is the development of a deposition solid phase VUV using a sapphire disc in like manner to the DiscovIR deposition IRD [103]. The proposed instrument

would include a liquid N2 cooled aluminum platform supporting a spinning disc of sapphire (or MgF) programmed to spin at a variable rate based on the sampling rate and flow rate from the instrument, a motorized wheel and two concave bumpers that allow the disc to turn while held in place, and heating coils that would be used to quickly heat the disc above the boiling point of the analytes which could be removed via vacuum or purged with inert gas. A possible pitfall in quick heat/cool cycles is that it could cause cracking and possible destruction of the sapphire or MgF disc. MgF is slightly more transparent than sapphire but is less robust. The aluminum base would have a light path cut out in the path after the column outlet allowing transmission measurements to be taken. A simplified diagram of such an instrument is given in Figure 7.3.
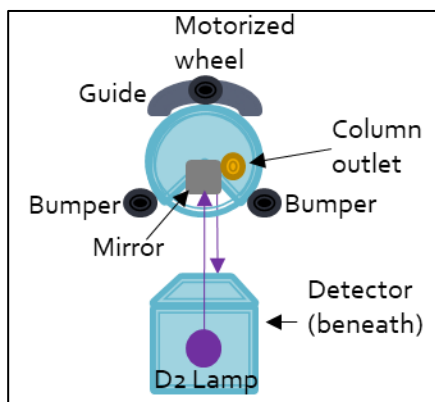
Figure 7.3 Simplified diagram of proposed deposition VUV instrument.

The advantages of such an instrument include spectra that are more similar to computationally predicted spectra due to the lower thermal energy, more specific spectra due to the narrower absorption bands and potential to resolve close absorption bands, possible lower noise levels due to lower thermal noise, and the option to increase dwell time and re-analyze each sample after the initial run. Lower temperatures should result in sharper peaks since energy gaps in rotational and vibrational energy levels are temperature dependent. This may lead to less ambiguous absorption spectra with narrower absorption peaks and potentially teasing out overlapping absorption bands, thus allowing better assignment of absorption bands to the corresponding electronic transition. The ability to increase dwell time, even if after the "first pass", would allow for a greater number of scans averaged thus providing better signal-to-noise and potentially lower detection limits than in the gas phase.

Possible pitfalls include the challenges in designing the instrument so that it does not infringe on any patents held by the current deposition IR instrument makers, the mentioned thermal stressing of materials, and the decreased pathlength. Not infringing on patents would require creative engineering but is a solvable problem. Thermal stresses on the materials could cause short periods between maintenance, need for more expensive materials, or even the breakage of parts in the middle of an analysis. With carefully chosen materials and limitations imposed on the heating and cooling cycles, thermal stress can be accounted for. The decrease in pathlength could still result in the same or even worse detectability than the gas phase, though it is offset by the increase in dwell time and the lower thermal noise.

REFERENCES

1. Korytar, P.; Janssen, H. G.; Matisova, E.; Brinkman, U. A. T., Practical fast gas chromatography: methods, instrumentation and applications. *Trac-Trend Anal Chem* **2002,** *21* (9-10), 558-572.

2. Cramers, C. A.; Janssen, H. G.; van Deursen, M. M.; Leclercq, P. A., High-speed gas chromatography: an overview of various concepts. *Journal of Chromatography A* **1999,** *856* (1-2), 315-329.

3. van Deursen, M. M.; Beens, J.; Janssen, H. G.; Leclercq, P. A.; Cramers, C. A., Evaluation of time-of-flight mass spectrometric detection for fast gas chromatography. *Journal of Chromatography A* **2000,** *878* (2), 205-213.

4. Matisová, E.; Dömötörová, M., Fast gas chromatography and its use in trace analysis. *Journal of Chromatography A* **2003,** *1000* (1-2), 199-221.

5. Van Es, A.; Janssen, J.; Bally, R.; Cramers, C.; Rijks, J., Sample introduction in high speed capillary gas chromatography; input band width and detection limits. *HRC CC, J. High Resolut. Chromatogr. Chromatogr. Commun.* **1987,** *10* (5), 273-9.

6. Tranchida, P. Q.; Mondello, L., Current-day employment of the micro-bore open-tubular capillary column in the gas chromatography field. *Journal of Chromatography A* **2012,** *1261*, 23-36.

7. Leclercq, P. A.; Schutjes, C. P. M.; Cramers, C. A., Roads to Faster and More Sensitive Capilary GC/MS. Application of 50mum Columns. *Journal of Chromatography library* **1985**, 55-65.

8. Sapozhnikova, Y.; Lehotay, S. J., Review of recent developments and applications in low-pressure (vacuum outlet) gas chromatography. *Anal Chim Acta* **2015,** *899*, 13-22.

9. Mondello, L.; Tranchida, P. Q.; Casilli, A.; Favoino, O.; Dugo, P.; Dugo, G., Fast GC analysis with a 50 microm ID column: theory, practical aspects, and application to a highly complex sample. *J Sep Sci* **2004,** *27* (14), 1149-56.

10. Ghijsen, R. T.; Poppe, H.; Kraak, J. C.; Duysters, P. P. E., The Mass Loadability of Various Stationary Phases in Gas-Chromatography. *Chromatographia* **1989,** *27* (1-2), 60-66.

11. Snow, N. H., Fast Gas Chromatoography with Short Columns: Are Speed and Resolution Mutually Exclusive? *Journal of Liquid Chromatography and Related Technologies* **2004,** *27* (7-9), 1317-1330.

12. Schutjes, C. P. M.; Leclercq, P. A.; Rijks, J. A.; Cramers, C. A., Model Describing The Role of the Pressure Gradient on Efficiency and Speed of Analysis in Capillary Gas Chromatography. *Journal of Chromatography* **1984,** *289*, 163-170.

13. Grob, K.; Grob, G., Capillary columns with very thick coatings. *HRC CC, J. High Resolut. Chromatogr. Chromatogr. Commun.* **1983,** *6* (3), 133-9.

14. Steenackers, D.; Sandra, P., Capillary GC on 50 micrometer I.D. Columns coated with thick films. Theory and selected practical results. *Journal of High Resolution Chromatography* **1995,** *18* (2), 77-82.

15. Pert, A. D.; Baron, M. G.; Birkett, J. W., Review of analytical techniques for arson residues. *J Forensic Sci* **2006,** *51* (5), 1033-49.

16. International, A., Standard Test Method for Ignitable Liquid Residues in Extracts from Fire Debris Samples by Gas Chromatography-Mass Spectrometry. 2006; Vol. E1618.

17. Giddings, J. C.; Seager, S. L.; Stucki, L. R.; Stewart, G. H., Plate Height in Gas Chromatography. *Analytical Chemistry* **1960,** *32* (7), 867-870.

18. McNair, H. M.; Miller, J. M., *Basic Gas Chromatography*. Second Edition ed.; John Wiley & Sons, In: 2009.

19. Goodpaster, J. V.; Bishop, J. J.; Benner, B. A., Jr., Forensic analysis of hair surface components using off-line supercritical fluid extraction and large volume injection. *J. Sep. Sci.* **2003,** *26* (1/2), 137-141.

20. Onuska, F. I.; Karasek, F. W., *Open Tubular Column Gas Chromatography in Environmental Sciences*. Plenum Press: 1984.

21. Ignatiadis, I.; Gonnord, M. F.; Vidalmadjar, C., Measurement of Thermodynamic Equilibria by Chromatography. *Chromatographia* **1987,** *23* (3), 215-219.

22. Heberger, K.; Kowalska, T., Determination of heats of vaporization and Gibbs free energies of alkylbenzenes on GC stationary phases of different polarity. *Chromatographia* **1998,** *48* (1-2), 89-94.

23. James, M. R.; Giddings, J. C.; Keller, R. A., Thermodynamic Pitfalls in Gas Chromatography. *Journal of Chromatographic Science* **1965,** *3* (2), 57-60.

24. Schug, K. A.; Sawicki, I.; Carlton, D. D., Jr.; Fan, H.; McNair, H. M.; Nimmo, J. P.; Kroll, P.; Smuts, J.; Walsh, P.; Harrison, D., Vacuum ultraviolet detector for gas chromatography. *Anal Chem* **2014,** *86* (16), 8329-35.

25. Kumar, R.; Sharma, V., Chemometrics in forensic science. *TrAC Trends in Analytical Chemistry* **2018,** *105*, 191-201.

26. Liszewski, E. A.; Lewis, S. W.; Siegel, J. A.; Goodpaster, J. V., Characterization of Automotive Paint Clear Coats by Ultraviolet Absorption Microspectrophotometry with Subsequent Chemometric Analysis. *Applied Spectroscopy* **2010,** *64* (10), 1122-1125.

27. Turner, D. A.; Goodpaster, J. V., Comparing the effects of weathering and microbial degradation on gasoline using principal components analysis. *J Forensic Sci* **2012,** *57* (1), 64-9.

28. Barrett, J. A.; Siegel, J. A.; Goodpaster, J. V., Forensic discrimination of dyed hair color: II. Multivariate statistical analysis. *J Forensic Sci* **2011,** *56* (1), 95-101.

29. Sachs, S. B.; Woo, F., A detailed mechanistic fragmentation analysis of methamphetamine and select regioisomers by GC/MS. *J Forensic Sci* **2007,** *52* (2), 308-19.

30. Awad, T.; Belal, T.; DeRuiter, J.; Kramer, K.; Clark, C. R., Comparison of GC-MS and GC-IRD methods for the differentiation of methamphetamine and regioisomeric substances. *Forensic Sci Int* **2009,** *185* (1-3), 67-77.

31. Santos, I. C.; Schug, K. A., Recent advances and applications of gas chromatography vacuum ultraviolet spectroscopy. *J Sep Sci* **2017,** *40* (1), 138-151.

32. Anthony, I. G. M.; Brantley, M. R.; Gaw, C. A.; Floyd, A. R.; Solouki, T., Vacuum Ultraviolet Spectroscopy and Mass Spectrometry: A Tandem Detection Approach for Improved Identification of Gas Chromatography-Eluting Compounds. *Anal Chem* **2018,** *90* (7), 4878-4885.

33. Skultety, L.; Frycak, P.; Qiu, C.; Smuts, J.; Shear-Laude, L.; Lemr, K.; Mao, J. X.; Kroll, P.; Schug, K. A.; Szewczak, A.; Vaught, C.; Lurie, I.; Havlicek, V., Resolution of isomeric new designer stimulants using gas chromatography - Vacuum ultraviolet spectroscopy and theoretical computations. *Anal Chim Acta* **2017,** *971*, 55-67.

34. Santos, I. C.; Smuts, J.; Choi, W. S.; Kim, Y.; Kim, S. B.; Schug, K. A., Analysis of bacterial FAMEs using gas chromatography - vacuum ultraviolet spectroscopy for the identification and discrimination of bacteria. *Talanta* **2018,** *182*, 536-543.

35. Fan, H.; Smuts, J.; Walsh, P.; Harrison, D.; Schug, K. A., Gas chromatography-vacuum ultraviolet spectroscopy for multiclass pesticide identification. *J Chromatogr A* **2015,** *1389*, 120-7.

36. Leghissa, A.; Hildenbrand, Z. L.; Schug, K. A., A review of methods for the chemical characterization of cannabis natural products. *J Sep Sci* **2018,** *41* (1), 398-415.

37. Weston, C.; Smuts, J.; Mao, J. X.; Schug, K. A., Investigation of gas phase absorption spectral similarity for stable isotopically labeled compounds in the 125-240 nm wavelength range. *Talanta* **2018,** *177*, 41-46.

38. Zheng, J. J.; Huang, C. L.; Wang, S., Challenging pharmaceutical analyses by gas chromatography with vacuum ultraviolet detection. *Journal of Chromatography A* **2018,** *1567*, 185-190.

39. Schenk, J.; Mao, J. X.; Smuts, J.; Walsh, P.; Kroll, P.; Schug, K. A., Analysis and deconvolution of dimethylnaphthalene isomers using gas chromatography vacuum ultraviolet spectroscopy and theoretical computations. *Anal. Chim. Acta* **2016,** *945*, 1-8.

40. Garcia-Cicourel, A. R.; Janssen, H. G., Direct analysis of aromatic hydrocarbons in purified mineral oils for foods and cosmetics applications using gas chromatography with vacuum ultraviolet detection. *J Chromatogr A* **2019,** *1590*, 113-120.

41. Cruse, C. A.; Goodpaster, J. V., Generating highly specific spectra and identifying thermal decomposition products via Gas Chromatography / Vacuum Ultraviolet Spectroscopy (GC/VUV): Application to nitrate ester explosives. *Talanta* **2019,** *195*, 580-586.

42. Lurie, I. S.; Tremeau-Cayel, L.; Rowe, W. F., Recent Advances in Comprehensive Chromatographic Analysis of Emerging Drugs. *Lc Gc N. Am.* **2017,** *35* (12), 878-883.

43. Lurie, I.; Szewczak, A.; Vaught, C.; Smuts, J., The Ultitlity of Gc Coupled to Vacuum Uv Spectroscopy for the Analysis of Emerging Drugs. *Forensic Sci.Int.* **2017,** *277*, 129-130.

44.   Buchalter, S.; Marginean, I.; Yohannan, J.; Lurie, I. S., Gas chromatography with tandem cold electron ionization mass spectrometric detection and vacuum ultraviolet detection for the comprehensive analysis of fentanyl analogues. *J Chromatogr A* **2019,** *1596*, 183-193.

45.   Bai, L.; Smuts, J.; Walsh, P.; Qiu, C.; McNair, H. M.; Schug, K. A., Pseudo-absolute quantitative analysis using gas chromatography - Vacuum ultraviolet spectroscopy - A tutorial. *Anal Chim Acta* **2017,** *953*, 10-22.

46.   Liu, H. A.; Raffin, G.; Trutt, G.; Randon, J., Is vacuum ultraviolet detector a concentration or a mass dependent detector? *Journal of Chromatography A* **2017,** *1530*, 171-175.

47.   Weston, C.; Smuts, J.; Mao, J. X.; Schug, K. A., Investigation of gas phase absorption spectral similarity for stable-isotopically labeled compounds in the 125-240nm wavelength range. *Talanta* **2018,** *177*, 41-46.

48.   Kelly, K.; Bell, S., Evaluation of the reproducibility and repeatability of GCMS retention indices and mass spectra of novel psychoactive substances. *Forensic Chemistry* **2018,** *7*, 10-18.

49.   Kranenburg, R. F.; García-Cicourel, A. R.; Kukurin, C.; Janssen, H.-G.; Schoenmakers, P. J.; van Asten, A. C., Distinguishing drug isomers in the forensic laboratory: GC-VUV in addition to GC-MS for orthogonal selectivity and the use of library match scores as a new source of information. *Forensic Sci.Int.* **2019**.

50.   Roberson, Z. R.; Goodpaster, J. V., Differentiation of structurally similar phenethylamines via gas chromatography–vacuum ultraviolet spectroscopy (GC–VUV). *Forensic Chemistry* **2019,** *15*, 100172.

51.   Prebihalo, S. E.; Berrier, K. L.; Freye, C. E.; Bahaghighat, H. D.; Moore, N. R.; Pinkerton, D. K.; Synovec, R. E., Multidimensional Gas Chromatography: Advances in Instrumentation, Chemometrics, and Applications. *Anal Chem* **2018,** *90* (1), 505-532.

52.   Barroso, M.; Gallardo, E.; Vieira, D. N.; Queiroz, J. A.; Lopez-Rivadulla, M., Bioanalytical procedures and recent developments in the determination of opiates/opioids in human biological samples. *Anal Bioanal Chem* **2011,** *400* (6), 1665-90.

53.   Maas, A.; Madea, B.; Hess, C., Confirmation of recent heroin abuse: Accepting the challenge. *Drug Test Anal* **2018,** *10* (1), 54-71.

54.   Dinis-Oliveira, R. J., Metabolism and metabolomics of opiates: A long way of forensic implications to unravel. *J Forensic Leg Med* **2019,** *61*, 128-140.

55.   Burns, S. M.; Cunningham, C. W.; Mercer, S. L., DARK Classics in Chemical Neuroscience: Fentanyl. *ACS Chem Neurosci* **2018,** *9* (10), 2428-2437.

56.   Kaa, E.; Bent, K., Impurities, adulterants and diluents of illicit heroin in Denmark (Jutland and Funen). *Forensic Sci Int* **1986,** *31* (3), 195-210.

57.   Kaa, E., Impurities, adulterants and diluents of illicit heroin. Changes during a 12-year period. *Forensic Sci Int* **1994,** *64* (2-3), 171-9.

58.   Stromberg, L.; Lundberg, L.; Neumann, H.; Bobon, B.; Huizer, H.; van der Stelt, N. W., Heroin impurity profiling. A harmonization study for retrospective comparisons. *Forensic Sci Int* **2000,** *114* (2), 67-88.

59. Santos, I. C.; Smuts, J.; Schug, K. A., Rapid Profiling and Authentication of Vanilla Extracts Using Gas Chromatography-Vacuum Ultraviolet Spectroscopy. *Food Analytical Methods* **2017,** *10* (12), 4068-4078.

60. Lelevic, A.; Souchon, V.; Moreaud, M.; Lorentz, C.; Geantet, C., Gas chromatography vacuum ultraviolet spectroscopy: A review. *J Sep Sci* **2020,** *43* (1), 150-173.

61. Ozaki, Y., Frontiers of Far-Ultraviolet Spectroscopy in the Solid and Liquid States. *Spectroscopy* **2017,** *32* (2), 40-51.

62. Walsh, P.; Garbalena, M.; Schug, K. A., Rapid Analysis and Time Interval Deconvolution for Comprehensive Fuel Compound Group Classification and Speciation Using Gas Chromatography-Vacuum Ultraviolet Spectroscopy. *Anal Chem* **2016,** *88* (22), 11130-11138.

63. Bai, L.; Smuts, J.; Schenk, J.; Cochran, J.; Schug, K. A., Comparison of GC-VUV, GC-FID, and comprehensive two-dimensional GC–MS for the characterization of weathered and unweathered diesel fuels. *Fuel* **2018,** *214*, 521-527.

64. Groger, T.; Gruber, B.; Harrison, D.; Saraji-Bozorgzad, M.; Mthembu, M.; Sutherland, A.; Zimmermann, R., A Vacuum Ultraviolet Absorption Array Spectrometer as a Selective Detector for Comprehensive Two-Dimensional Gas Chromatography: Concept and First Results. *Anal Chem* **2016,** *88* (6), 3031-9.

65. Dunkle, M. N.; Pijcke, P.; Winniford, B.; Bellos, G., Quantification of the composition of liquid hydrocarbon streams: Comparing the GC-VUV to DHA and GCxGC. *J Chromatogr A* **2019,** *1587*, 239-246.

66. Reiss, R.; Gruber, B.; Klingbeil, S.; Groger, T.; Ehlert, S.; Zimmermann, R., Evaluation and application of gas chromatography - vacuum ultraviolet spectroscopy for drug- and explosive precursors and examination of non-negative matrix factorization for deconvolution. *Spectrochim Acta A Mol Biomol Spectrosc* **2019,** *219*, 129-134.

67. Cruse, C.; Pu, J.; Goodpaster, J. V., EXPRESS: Identifying Thermal Decomposition Products of Nitrate Ester Explosives Using Gas Chromatography-Vacuum Ultraviolet Spectroscopy: An Experimental and Computational Study. *Appl Spectrosc* **2020**, 3702820915506.

68. Weatherly, C. A.; Zhang, Y.; Smuts, J. P.; Fan, H.; Xu, C.; Schug, K. A.; Lang, J. C.; Armstrong, D. W., Analysis of Long-Chain Unsaturated Fatty Acids by Ionic Liquid Gas Chromatography. *J Agric Food Chem* **2016,** *64* (6), 1422-32.

69. Santos, I. C.; Smuts, J.; Crawford, M. L.; Grant, R. P.; Schug, K. A., Large-volume injection gas chromatography-vacuum ultraviolet spectroscopy for the qualitative and quantitative analysis of fatty acids in blood plasma. *Anal Chim Acta* **2019,** *1053*, 169-177.

70. Zoccali, M.; Schug, K. A.; Walsh, P.; Smuts, J.; Mondello, L., Flow-modulated comprehensive two-dimensional gas chromatography combined with a vacuum ultraviolet detector for the analysis of complex mixtures. *J Chromatogr A* **2017,** *1497*, 135-143.

71. Fan, H.; Smuts, J.; Bai, L.; Walsh, P.; Armstrong, D. W.; Schug, K. A., Gas chromatography-vacuum ultraviolet spectroscopy for analysis of fatty acid methyl esters. *Food Chem* **2016,** *194*, 265-71.

72. Leghissa, A.; Smuts, J.; Qiu, C.; Hildenbrand, Z. L.; Schug, K. A., Detection of cannabinoids and cannabinoid metabolites using gas chromatography with vacuum ultraviolet spectroscopy. *Separation Science Plus* **2018,** *1* (1), 37-42.

73. Roberson, Z. R.; Gordon, H. C.; Goodpaster, J. V., Instrumental and chemometric analysis of opiates via gas chromatography-vacuum ultraviolet spectrophotometry (GC-VUV). *Anal Bioanal Chem* **2020,** *412* (5), 1123-1128.

74. Gruber, B.; Groeger, T.; Harrison, D.; Zimmermann, R., Vacuum ultraviolet absorption spectroscopy in combination with comprehensive two-dimensional gas chromatography for the monitoring of volatile organic compounds in breath gas: A feasibility study. *J Chromatogr A* **2016,** *1464*, 141-6.

75. Pechancova, R.; Qiu, C.; Smuts, J.; Lemr, K.; Schug, K. A., Comparative study of ink photoinitiators in food packages using gas chromatography with vacuum ultraviolet detection and gas chromatography with mass spectrometry. *J Sep Sci* **2019,** *42* (2), 556-565.

76. Bezerra, M. A.; Santelli, R. E.; Oliveira, E. P.; Villar, L. S.; Escaleira, L. A., Response surface methodology (RSM) as a tool for optimization in analytical chemistry. *Talanta* **2008,** *76* (5), 965-77.

77. Montgomery, D. C., Introduction to Response Surface Methodology. In *Design and Analysis of Experiments*, 6th ed.; John Wiley & Sons: 2005; pp 405-407.

78. Rainey, C. L.; Bors, D. E.; Goodpaster, J. V., Design and optimization of a total vaporization technique coupled to solid-phase microextraction. *Anal Chem* **2014,** *86* (22), 11319-25.

79. Siegel, J., Forensic Identification of Illicit Drugs. In *Forensic Science Handbook*, Second ed.; Saferstein, R., Ed. Prentice Hall: 2005; Vol. II, pp 135-138.

80. Spiller, H. A.; Ryan, M. L.; Weston, R. G.; Jansen, J., Clinical experience with and analytical confirmation of "bath salts" and "legal highs" (synthetic cathinones) in the United States. *Clin Toxicol (Phila)* **2011,** *49* (6), 499-505.

81. Oyler, J.; Darwin, W. D.; Cone, E. J., Cocaine contamination of United States paper currency. *J. Anal. Toxicol.* **1996,** *20* (4), 213-6.

82. Strano-Rossi, S.; Alvarez, I.; Tabernero, M. J.; Cabarcos, P.; Fernandez, P.; Bermejo, A. M., Determination of fentanyl, metabolite and analogs in urine by GC/MS. *J Appl Toxicol* **2011,** *31* (7), 649-54.

83. Casale, J. F.; Corbeil, E. M.; Hayes, P. A., Identification of levamisole impurities found in illicit cocaine exhibits. *Microgram J* **2008,** *6*, 82-89.

84. Broseus, J.; Gentile, N.; Esseiva, P., The cutting of cocaine and heroin: A critical review. *Forensic Sci Int* **2016,** *262*, 73-83.

85. Anthony, I. G. M.; Brantley, M. R.; Floyd, A. R.; Gaw, C. A.; Solouki, T., Improving Accuracy and Confidence of Chemical Identification by Gas Chromatography/Vacuum Ultraviolet Spectroscopy-Mass Spectrometry: Parallel Gas Chromatography, Vacuum Ultraviolet, and Mass Spectrometry Library Searches. *Anal Chem* **2018,** *90* (20), 12307-12313.

86. Bai, L.; Smuts, J.; Walsh, P.; Fan, H.; Hildenbrand, Z.; Wong, D.; Wetz, D.; Schug, K. A., Permanent gas analysis using gas chromatography with vacuum ultraviolet detection. *J Chromatogr A* **2015,** *1388*, 244-50.

87. Smith, F. P.; Athanaselis, S. A., *Handbook of Forensic Drug Analysis*. Elsevier Academic Press: 2005.

88. Wall, L. A.; Pummer, W. J.; Fearn, J. E.; Antonucci, J. M., Reactions of Polyfluorobenzenes With Nucleophilic Reagents. *J Res Natl Bur Stand A Phys Chem* **1963,** *67A* (5), 481-497.

89. Plotka-Wasylka, J. M.; Morrison, C.; Biziuk, M.; Namiesnik, J., Chemical derivatization processes applied to amine determination in samples of different matrix composition. *Chem Rev* **2015,** *115* (11), 4693-718.

90. Ash, J.; Hickey, L.; Goodpaster, J., Formation and identification of novel derivatives of primary amine and zwitterionic drugs. *Forensic Chemistry* **2018,** *10*, 37-47.

91. Lagesson, V.; Lagesson-Andrasko, L.; Andrasko, J.; Baco, F., Identification of compounds and specific functional groups in the wavelength region 168–330 nm using gas chromatography with UV detection. *Journal of Chromatography A* **2000,** *867* (1-2), 187-206.

92. Bowden, J. A.; Ford, D. A., An examination of pentafluorobenzoyl derivatization strategies for the analysis of fatty alcohols using gas chromatography/electron capture negative ion chemical ionization-mass spectrometry. *J Chromatogr B Analyt Technol Biomed Life Sci* **2011,** *879* (17-18), 1375-83.

93. Dobos, A.; Hidvegi, E.; Somogyi, G. P., Comparison of five derivatizing agents for the determination of amphetamine-type stimulants in human urine by extractive acylation and gas chromatography-mass spectrometry. *J Anal Toxicol* **2012,** *36* (5), 340-4.

94. Mohamed, K. M.; Bakdash, A., Comparison of 3 Derivatization Methods for the Analysis of Amphetamine-Related Drugs in Oral Fluid by Gas Chromatography-Mass Spectrometry. *Anal Chem Insights* **2017,** *12*, 1177390117727533.

95. Mohamed, K., One-Step Derivatization-Extraction Method for Rapid Analysis of Eleven Amphetamines and Cathinones in Oral Fluid by GC-MS. *J Anal Toxicol* **2017,** *41* (7), 639-645.

96. Administration, D. E., Fentanyl Remains the Most Significant Synthetic Opioid Threat and Poses the Greatest Threat to the Opioid User Market in the United States. **2018,** *DEA-DCT-DIB-003-18*.

97. Armenian, P.; Vo, K. T.; Barr-Walker, J.; Lynch, K. L., Fentanyl, fentanyl analogs and novel synthetic opioids: A comprehensive review. *Neuropharmacology* **2018,** *134* (Pt A), 121-132.

98. Martin, T. L.; Woodall, K. L.; McLellan, B. A., Fentanyl-related deaths in Ontario, Canada: toxicological findings and circumstances of death in 112 cases (2002-2004). *J Anal Toxicol* **2006,** *30* (8), 603-10.

99.   Riches, J. R.; Read, R. W.; Black, R. M.; Cooper, N. J.; Timperley, C. M., Analysis of clothing and urine from Moscow theatre siege casualties reveals carfentanil and remifentanil use. *J Anal Toxicol* **2012,** *36* (9), 647-56.

100.   Tanen, J. L.; Lurie, I. S.; Marginean, I., Gas chromatography with dual cold electron ionization mass spectrometry and vacuum ultraviolet detection for the analysis of phenylethylamine analogues. *Forensic Chemistry* **2020,** *21*.

101.   Roberson, Z. R.; Goodpaster, J. V., Optimization of the qualitative and quantitative analysis of cocaine and other drugs of abuse via gas chromatography – Vacuum ultraviolet spectrophotometry (GC – VUV). *Talanta* **2021,** *222*, 121461.

102.   Diekmann, J. A., 3rd; Cochran, J.; Hodgson, J. A.; Smuts, D. J., Quantitation and identification of ethanol and inhalant compounds in whole blood using static headspace gas chromatography vacuum ultraviolet spectroscopy. *J Chromatogr A* **2020,** *1611*, 460607.

103.   Kearney, T.; Carson, W.; Zhou, M., Analysis of Synthetic Controlled Substances by Solid Phase GC-IR, Cannabinoids, Methamphetamine, Cathinones and Related Isomers. Spectra Analysis Instruments Inc.: 2013.

VITA

Zackery R. Roberson

Education:

Indiana University Purdue University Indianapolis

Indianapolis, IN

2016-2020, Ph.D., Analytical Chemistry

GPA: 3.7/4.0

Indiana University Purdue University Indianapolis

Indianapolis, IN

2012-2016, B.S., Chemistry (Certified by the American Chemical Society)

2012-2016, B.S., Forensic and Investigative Sciences (Forensic Chemistry Concentration)

GPA: 3.25/4.0

Honors and Awards:

2020 Think Like a Molecule ACS Chair's Award

2019 FIS Outstanding Capstone TA Award

2016 FIS Student Leadership Award

Spring 2015 Dean's List

2012-2016 Academic Honors Scholarship

Publications:

"Optimization of the qualitative and quantitative analysis of cocaine and other drugs of abuse via gas chromatography – vacuum ultraviolet spectrophotometry (GC-VUV)", Z.R. Roberson, J.V. Goodpaster, Talanta, 222 (2021), 121461. DOI: 10.1016/j.talanta.2020.121461

"Instrumental and Chemometric Analysis of Opiates via Gas Chromatography – Vacuum Ultraviolet Spectrophotometry (GC – VUV)", Z.R. Roberson, H.C. Gordon, J.V. Goodpaster, Analytical and Bioanalytical Chemistry, 412, 5 (2020), 1123-1128. DOI: 10.1007/s00216-019-02337-5

"Preparation and characterization of micro-bore wall-coated open-tubular capillaries with low phase ratios for fast-gas chromatography–mass spectrometry: Application to ignitable liquids and fire debris", Z.R. Roberson, J.V. Goodpaster, Science & Justice, 59, 6 (2019), 630-634. DOI: 10.1016/j.scijus.2019.06.009

"Differentiation of structurally similar phenethylamines via gas chromatography–vacuum ultraviolet spectroscopy (GC–VUV)", Z.R. Roberson, J.V. Goodpaster, Forensic Chemistry, 15 (2019), 100172. DOI: 10.1016/j.forc.2019.100172

Presentations:

"Detection and Differentiation of Derivatized Controlled Substances by Gas Chromatography-Vacuum Ultraviolet (GC-VUV) Spectrophotometry" Zackery R. Roberson, Heather C. Gordon, and John V. Goodpaster, AAFS 72nd Annual Scientific Meeting, February 21, 2020. Oral presentation.

"Detection and Differentiation of Controlled Substances by GC-VUV and Chemometrics" Zackery R. Roberson and John V. Goodpaster, AAFS 71st Annual Scientific Meeting, February 22, 2019. Oral presentation.

"Identification of Prohibited Treatments on Racing Tires by Solid Phase Microextraction (SPME)" Zackery R. Roberson and John V. Goodpaster, AAFS 70th Annual Scientific Meeting, February 23, 2018. Oral presentation.

"Gas Chromatography – Vacuum Ultraviolet Spectroscopy for Analyzing Drugs of Abuse" Zackery R. Roberson and John V. Goodpaster, ACS Think Like a Molecule 2020 Virtual Poster Session, April 18, 2020. Poster presentation.

"Optimizing GC-VUV for Drug Detection through Response Surface Methodology" Zackery R. Roberson and John V. Goodpaster, 2020 PittCon Analytical Chemistry Conference, March 3, 2020. Poster presentation.

"Optimizing GC-VUV Parameters for Drugs of Abuse Detection" Zackery R. Roberson and John V. Goodpaster, 2019 Midwestern Universities Analytical Chemistry Conference, November 11, 2019. Poster presentation.

"Optimizing GC-VUV Parameters for Drug Detection" Zackery R. Roberson and John V. Goodpaster, Turkey Run Analytical Chemistry Conference, September 27, 2019. Poster presentation.

"Performance of a Vacuum Ultraviolet Spectrophotometer as a Gas Chromatography detector applied to controlled substances detection" Zackery R. Roberson and John V. Goodpaster, 2019 PittCon Analytical Chemistry Conference, March 19, 2019. Poster presentation.

"Differentiating Vacuum Ultraviolet Spectra Through Chemometrics" Zackery R. Roberson and John V. Goodpaster, Turkey Run Analytical Chemistry Conference, November 2, 2018. Poster presentation.

"Gas Chromatography – Vacuum Ultraviolet (VUV) spectrophotometry for the detection and discrimination of phenethylamines" Zackery R. Roberson and John V. Goodpaster, Midwestern Association of Forensic Scientists 47th Annual Scientific Meeting, September 19, 2018. Poster presentation.

"Micro-Bore Capillary Gas Chromatography for Alcohol and Fire Debris Analysis" Zackery R. Roberson and John V. Goodpaster, IUPUI Department of Chemistry and Chemical Biology Poster Session 2018, May 4, 2018. Poster presentation.

Peer Review:

Assisted Dr. John Goodpaster with peer reviews for Journal of Chromatography A, Journal of Forensic Sciences, Science & Justice, and Rapid Communications in Mass Spectrometry.

Areas of Academic Interest:

Analytical Chemistry with a focus on applications to forensically relevant analytes.

Gas chromatography – vacuum ultraviolet spectroscopy and its application to forensically relevant samples, i.e. drugs of abuse, adulterants, and ignitable liquids.

Separation Science particularly in the areas of GC, LC, and LCxGC.

Spectroscopy applied to analytes of forensic interest.

Experience:

August 2016-Present, Research Assistant, Goodpaster Research Group, IUPUI

Conducted research on gas chromatography – vacuum ultraviolet (VUV) spectroscopy to validate the instrumental performance of a VUV detector, performed GC-VUV analysis of controlled substances, designed and performed experiments using Response Surface Methodology, performed chemometric analyses (Principal component analysis and discriminant analysis) of obtained data, performed derivatization reactions on controlled substances, and analyzed de-identified seized drug exhibits.

Mentored an undergraduate student on research involving GC-VUV analysis of controlled substances, adulterants, and derivatization products of drugs of abuse.

Performed maintenance on gas chromatographs, Agilent single quadrupole mass spectrometers, Agilent ALS and Gerstel MPS autosamplers, and Edwards two stage rotary vane pumps.

Conducted research in the area of fast gas chromatography, prepared micro-bore wall coated open tubular columns using static coating methods, performed GC/MS analysis of samples from United States Auto Club.

Fall 2018, Subject Mentor/TA, FIS Capstone, IUPUI

Mentored students in researching and preparing a poster presentation.

Fall 2016-Spring 2017, Teaching Assistant, Experimental Chemistry I, IUPUI

Supervised lab experiments, graded student reports, followed/enforced lab safety guidelines, and provided tutoring at the Chemistry Resource Center at IUPUI.

May 2012 - August 2016, General Laborer, Roberson Construction LLC.

General carpentry, electrical, and finishing work.

Fall 2013, Peer Leader, Organic Chemistry I, IUPUI

Facilitated discussion among peers to stimulate cooperative learning, provided guidance and correction on assigned worksheets.

Professional Memberships:

American Academy of Forensic Sciences (AAFS), Student Affiliate

American Chemical Society (ACS), Student Member

Volunteer Experience:

Spring 2015-Spring 2019, Assistant instructor for Self-Defense, IUPUI

Taught class in absence of the main instructor, provided instruction and guidance, and performed demonstrations for students.

Fall 2015-Spring 2016, Vice-President, Forensic Science Club at IUPUI

Coordinated events and oversaw club proceedings to maintain compliance with club constitution.

PUBLICATIONS

"Differentiation of structurally similar phenethylamines via gas chromatography–vacuum ultraviolet spectroscopy (GC–VUV)", Z.R. Roberson, J.V. Goodpaster, Forensic Chemistry, 15 (2019), 100172. https://doi.org/10.1016/j.forc.2019.100172

"Preparation and characterization of micro-bore wall-coated open-tubular capillaries with low phase ratios for fast-gas chromatography–mass spectrometry: Application to ignitable liquids and fire debris", Z.R. Roberson, J.V. Goodpaster, Science & Justice 59, 6, (2019), 630-634. https://doi.org/10.1016/j.scijus.2019.06.009

"Instrumental and chemometric analysis of opiates via gas chromatography-vacuum ultraviolet spectrophotometry (GC-VUV)", Z.R. Roberson, H.C. Gordon, J.V. Goodpaster, Analytical and Bioanalytical Chemistry, 412, 5, (2020), 1123-1128. https://doi.org/10.1007/s00216-019-02337-5

"Optimization of the qualitative and quantitative analysis of cocaine and other drugs of abuse via gas chromatography – vacuum ultraviolet spectrophotometry (GC – VUV)", Z.R. Roberson, J.V. Goodpaster, Talanta, 222, (2021), 121461. https://doi.org/10.1016/j.talanta.2020.121461